(4)

Special Report 88-9

July 1988

**US Army Corps
of Engineers**

Cold Regions Research &
Engineering Laboratory

*Behavior of materials
at cold regions temperatures*

Part 1: Program rationale and test plan

Piyush K. Dutta

AD-A199 566

DTIC
ELECT
SEP 0 6 1988
D

88 9   6 106

REPORT DOCUMENTATION PAGE

Form Approved
OMB No 0704 0188
Exp Date Jun 30 1986

1a REPORT SECURITY CLASSIFICATION	1b RESTRICTIVE MARKINGS
Unclassified	

2a SECURITY CLASSIFICATION AUTHORITY	3 DISTRIBUTION/AVAILABILITY OF REPORT
	Approved for public release;
2b DECLASSIFICATION/DOWNGRADING SCHEDULE	distribution is unlimited.

4 PERFORMING ORGANIZATION REPORT NUMBER(S)	5 MONITORING ORGANIZATION REPORT NUMBER(S)
Special Report 88-9	

6a NAME OF PERFORMING ORGANIZATION	6b OFFICE SYMBOL (If applicable)	7a NAME OF MONITORING ORGANIZATION
U.S. Army Cold Regions Research and Engineering Laboratory	CECRL	Office of the Chief of Engineers

6c ADDRESS (City, State, and ZIP Code)	7b ADDRESS (City, State, and ZIP Code)
Hanover, New Hampshire 03755-1290	Washington, D.C. 20314-1000

8a NAME OF FUNDING/SPONSORING ORGANIZATION	8b OFFICE SYMBOL (If applicable)	9 PROCUREMENT INSTRUMENT IDENTIFICATION NUMBER

8c ADDRESS (City, State, and ZIP Code)	10 SOURCE OF FUNDING NUMBERS			
	PROGRAM ELEMENT NO.	PROJECT NO.	TASK NO	WORK UNIT ACCESSION NO
	6.27.30A	4A7627 30AT42	SS	019

11 TITLE (Include Security Classification)
Behavior of Materials at Cold Regions Temperatures
Part 1: Program Rationale and Test Plan

12 PERSONAL AUTHOR(S)
Piyush K. Dutta

13a TYPE OF REPORT	13b TIME COVERED	14 DATE OF REPORT (Year, Month, Day)	15 PAGE COUNT
	FROM _____ TO _____	July 1988	72

16 SUPPLEMENTARY NOTATION

17	COSATI CODES		18 SUBJECT TERMS (Continue on reverse if necessary and identify by block number)
FIELD	GROUP	SUB-GROUP	Cold regions Low temperatures
			Compression, tension testing Materials testing

19 ABSTRACT (Continue on reverse if necessary and identify by block number)

Newer materials and products are being constantly added to the Army's inventory. Cold regions climatic conditions should not impair the reliability and durability of these new systems. This report discusses the rationale of the test program being undertaken at CRREL to evaluate material behavior at low temperatures.

20 DISTRIBUTION/AVAILABILITY OF ABSTRACT	21 ABSTRACT SECURITY CLASSIFICATION
☒ UNCLASSIFIED/UNLIMITED ☐ SAME AS RPT ☐ DTIC USERS	Unclassified

22a NAME OF RESPONSIBLE INDIVIDUAL	22b TELEPHONE (Include Area Code)	22c OFFICE SYMBOL
Piyush K. Dutta	603-646-4100	CECRL-EA

DD FORM 1473, 84 MAR

83 APR edition may be used until exhausted
All other editions are obsolete

PREFACE

The contents of this report are not to be used for advertising or promotional purposes. Citation of brand names does not constitute an official endorsement or approval of the use of such commercial products.

A-1

CONTENTS

ILLUSTRATIONS

TABLES

Behavior of Materials at Cold Regions Temperatures

Part 1: Program Rationale and Test Plan

PIYUSH K. DUTTA

INTRODUCTION

Cold regions engineering has a general need for the evaluation of materials at low temperatures. Performance of many structures and components is seriously affected when the weather becomes very cold. At low temperatures materials tend to become hard and brittle; as a result, legitimate concerns are raised about their reliability and safety in such cold weather. The disastrous accident of space shuttle *Challenger* because of low-temperature-induced failure of O-ring seals is a grim reminder of such problems. Moreover, newer and lighter materials and products for engineering structures and systems are rapidly replacing the older and heavier materials and components. There is a growing need to evaluate these materials at low temperatures. In particular, the U.S. Army needs to evaluate new metal-substitute polymers and polymeric composites in cold climates for its new High-Technology Light Division.

Because of these needs, a low temperature (down to –60°C) material testing program is being established at CRREL. The testing program includes a variety of tests ranging from ordinary compression-tension testing of specimens to loading at very high strain rates in a Hopkinson split-bar system. Destructive, non-destructive and fracture mechanics tests are also planned to be performed at low temperatures. This report discusses the rationale for this program and outlines the test plan.

Cold regions material problems are many. Brittle-fractures initiated by low temperature or high strain rate (or both) have at times caused large-scale damage. In cold weather (0° to 5°C) merchant vessels have broken in two while in harbor (Fig. 1), bridges have collapsed, and pipelines and gas storage tanks have ripped open (Parker 1957). Exploration and production of oil and gas have begun to take place in colder climates (down to –60°C), and in deeper and rougher water; these rigorous conditions aggravate the brittle fracture hazard. At present, the knowledge necessary to prevent brittle fracture is far from complete.

Polymeric composites also have the potential for catastrophic failure at cold regions temperatures. These materials tend to develop brittle failure characteristics, depending on their composition and manufacturing processes. The development of brittle failure in these materials accelerates with lower temperature, material defects (notches or cracks), fatigue, and high-strain-rate loading.

In steel, a small reduction within a narrow temperature range called the transition temperature can cause a sharp decrease in fracture toughness. A preexisting crack that has become arrested at normal temperature and is thus tolerated can become self-propagating at low temperature and may cause catastrophic structural failure.

CRREL's low temperature material testing program will perform both quasi-static and high-strain-rate loading fracture toughness tests on selected materials. Tests will be done on a variety of materials, including plastics, composites, and metals. Some materials will be subjected to cyclic loading at lower temperatures
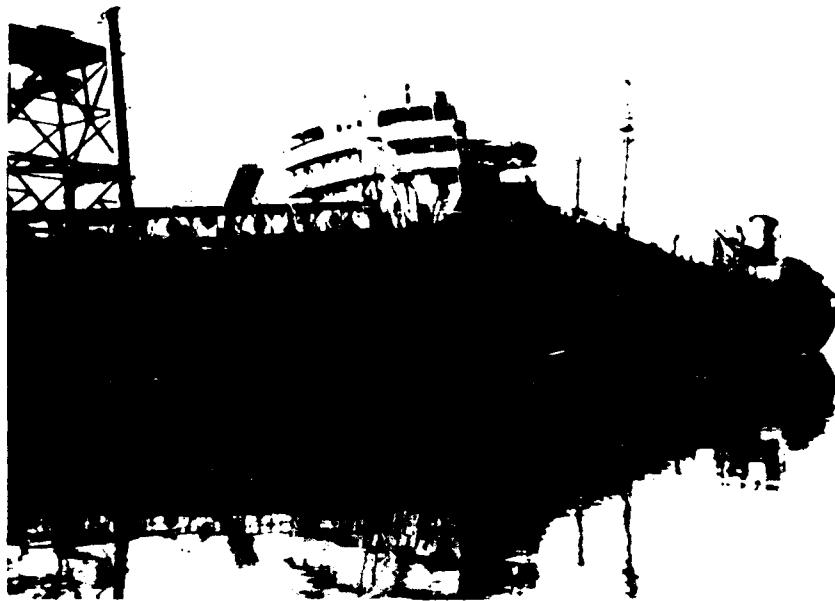
Figure 1. Photograph of a T-2 tanker that failed at pier.

before the fracture mechanics tests are performed in order to evaluate property degradation (fatigue) in service.

Quasi-static tests will be performed using the MTS and INSTRON material testing machines now available at CRREL. A high-strain-rate loading facility using the Hopkinson split-bar system has been installed and suitably instrumented to record and analyze the high-speed stress waveform data.

In the following sections the general background of low temperature material behavior and critical physical and engineering property data are reviewed and discussed. An outline of the proposed program for investigating the critical physical properties of a few selected materials at low temperature is also presented.

LOW TEMPERATURE PROPERTIES OF MANUFACTURED MATERIALS—BACKGROUND

Most manufactured materials exposed to low temperatures show a substantial loss of useful structural properties. Generally speaking, as the temperature is lowered, the hardness, yield strength and modulus of elasticity increase, but fracture toughness/impact strength, fatigue strength, Poisson's ratio, thermal expansion coefficient and specific heat decrease.

Metals

At low temperature the most significant property change in metals is the increase in brittleness. A metallic object or structure will shatter or fracture when subjected to stresses (especially from impact) that are allowable at normal temperatures (Fig. 2). The metals that have face-centered-cubic lattice structure, e.g. nickel, copper, aluminum, lead and silver, show some ductility at low temperature. But a larger group of body-centered-cubic class metals, e.g. iron, chromium, molybdenum and tungsten, show a marked decrease in ductility.

2
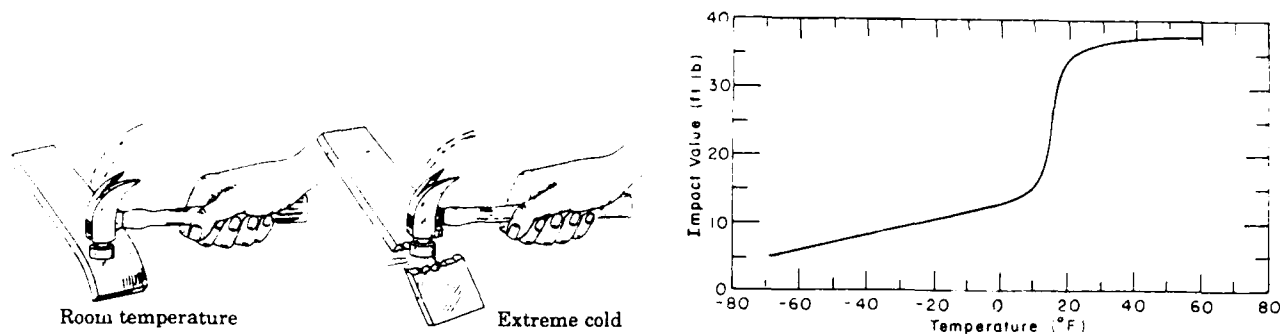
Figure 2. Impact test results for a steel pipe material.
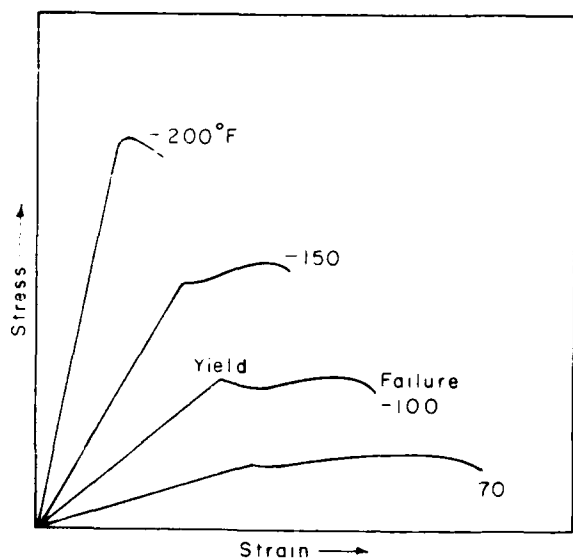
Figure 3. Typical stress-strain curve of a body centered cubic class metal at decreasing temperatures.

Loss of ductility in a metal can be observed by examining its low temperature stress-strain relationship. As the temperature is lowered, both the yield point (where ductility begins) and the ultimate strength point (where failure occurs) may shift to a higher stress value, but fracture may begin at a much lower strain value (Fig. 3).

Figure 4 shows the general aspects of temperature-dependent mechanical behavior of both face-centered-cubic (FCC) and body-centered-cubic (BCC) metals. Note that at the lowest stresses a specimen deforms elastically; increasing stress eventually brings the specimen to the limit of the elastic region where plastic strain (permanent deformation) or brittle fracture occurs. Figure 4a shows the behavior of FCC materials. Note that the yield strength increases with decreasing temperature, but the increase in ultimate strength is larger at lower temperatures. Figure 4b illustrates the BCC behavior. This figure shows a brittle region where the specimen fails before any significant plastic deformation occurs. This brittle region is extended to higher temperatures by several factors, namely (1) sharp cracks or other stress concentrators, (2) higher strain rate, and (3) impurities, e.g. higher carbon contents in steel.

3
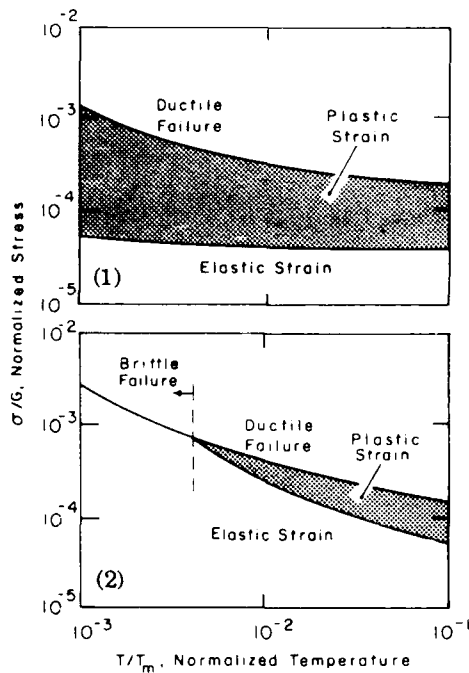
Figure 4. Simplified deformation behavior maps of (1) FCC material and (2) BCC-material.
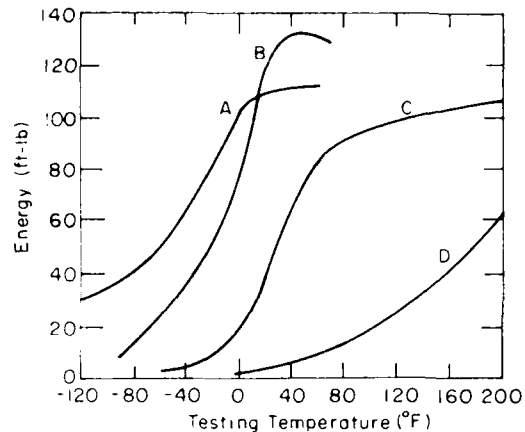
	Composition						
Steel	C	Mn	Si	P	S	Ni	Cr
A	0.17	0.53	0.25	0.011	0.02	3.39	0.06
B	0.18	0.82	0.15	0.012	0.03	0.04	0.03
C	0.18	0.73	0.07	0.008	0.03	0.05	0.03
D	0.20	0.33	0.01	0.013	0.02	0.15	0.09

Figure 5. Energy-temperature curves obtained by Charpy V-notch tests of steels.

The fracture mode transition from relatively ductile to relatively brittle is believed to occur because of the very rapid rise in viscosity with decreasing temperature. In most materials the flow stress is low at high temperatures. The stress concentrations around a dislocation can always be relieved by local plastic deformation and there is no brittle fracture. At low temperatures, the yield stress for slip is high so that deformation will start by microcrack production and subsequent brittle fracture (McClintock and Ali 1966).

Because of the onset of brittle fracture, most standard constructional carbon steels cannot be depended upon at the temperatures encountered in cold regions. Figure 5 shows energy-temperature curves obtained by Charpy V-notch tests of a few steels having different chemical compositions. The curves clearly show the temperatures where transition in the fracture mode occurs (McClintock and Ali 1966). However, continued research in steel development and processing has resulted in a new class of high strength, low alloy steels that can be used in low temperature environments (Baldy 1976).

The low temperature properties of a number of metals have been summarized in Appendix A. These properties indicate that stainless steel is probably the best-suited ferrous metal for cold use. Unlike other steels, stainless steel has no transition from tough to brittle in a cold environment. The properties of aluminum do not degrade at low temperature, and it is a preferred material for many cold weather ap-

4

plications. The ductility of cold-worked copper actually increases at low temperature, which makes it a very good metal for use in the cold regions.

Plastics/polymers

Plastic materials generally become more brittle at low temperatures, but they are not as consistent as metals. The tensile strength of plastics increases very markedly at lower temperatures. For example, a nylon material increases in tensile strength from 7400 psi at 21°C to 13,000 psi at –57°C, but its impact strength decreases from 16 ft-lb at 21°C to 0.9 ft-lb at –40°C (Hansen 1960). Some plastics, for example polyethylene, a thermoplastic polymer, remain tough at temperatures as low as –73°C. However, serviceability of rubber components, e.g. tires, inner tubes, cable, hose, bushings and seals, is seriously affected by low temperature. Rubber develops brittleness and loses flexibility; its loss of resilience is associated with changes in hardness, volume and coefficient of thermal expansion.

Both time and temperature influence the behavior of polymers. Figure 6 shows the typical thermomechanical behavior of a simple polymer. At low temperature it behaves as a glass. As the temperature is raised, it becomes less brittle. The upper limit of the glassy region is called the glass transition temperature, T_g. Commonly observed values of T_g are in the range of –53°C to –97°C (Read 1983). In the glassy region, polymers typically have a modulus of elasticity of 10^5 to 10^6 psi if organic and up to 10^7 psi if inorganic. Poisson's ratios are 0.25 to 0.4. In the rubbery region the modulus drops to 10^2 to 10^3 psi (McClintock 1966).

The stress-strain behavior of polymers can be represented by a system of dashpots and springs as shown in Figure 7. At low temperatures the dashpots become more and more frozen, resulting in very little flow. Near the glass transition temperature the flow is established and the material behaves viscoelastically (Fig. 8). During viscoelastic deformation, the stress-strain relation is strongly dependent on the strain rate $\dot{\varepsilon}$. A high strain rate leaves the polymer little time for plastic flow. The higher the strain rate, the more elastic and stiff a material becomes. At lower strain rates dissipative effects connected with viscous flow result in hysteresis of
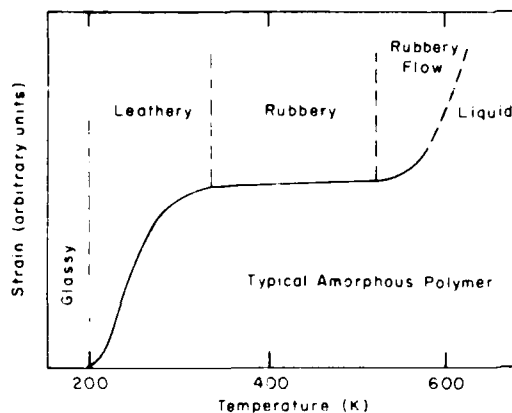

*Figure 6. Thermomechanical curve of a simple polymer.*
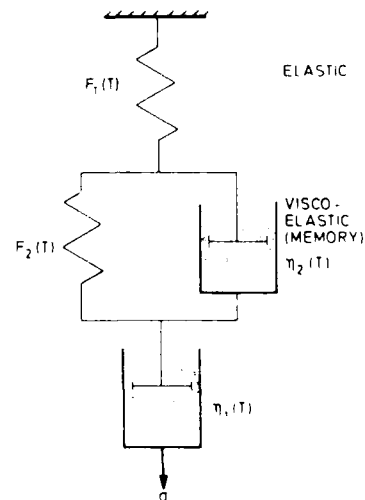
Figure 7. Schematic presentation of viscoelastic properties of polymers.

5
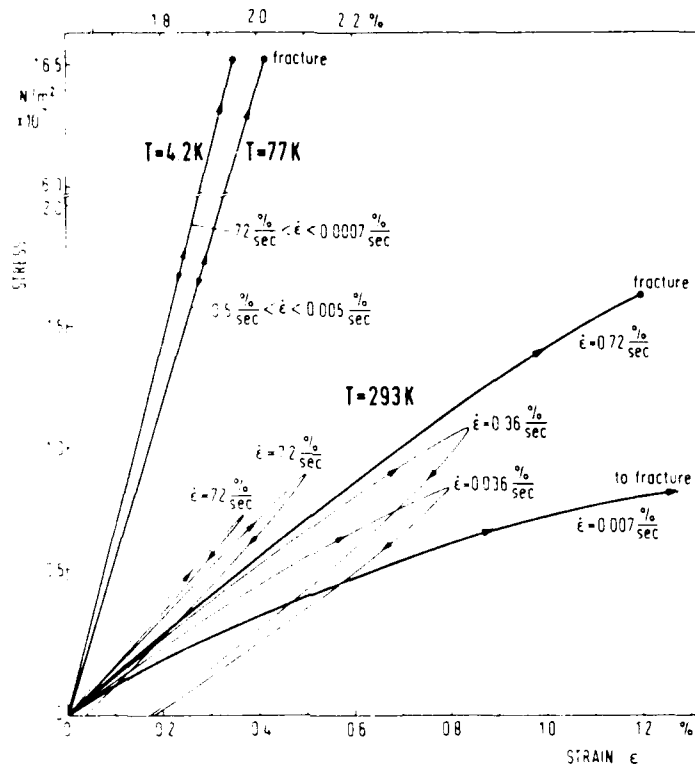
Figure 8. Stress-strain behavior of epoxy resins at different strain rates, $\dot{\varepsilon}$, and temperatures, T (after Hartwig 1979).

the loading and unloading curves. Figure 8 also shows that at low temperatures epoxy resins exhibit a linear elastic behavior up to the fracture point; there is no hysteresis effect and no strain rate dependence (Hartwig 1979).

The behavior of polymers is exceedingly complex. The molecular structures that influence this behavior are (1) branching, (2) chain length (molecular weight), and (3) crystallinity. The influence of low temperature on these parameters and the resulting change in behavior have been studied extensively in recent years (Hartwig 1979, Frank 1979). Appendix B summarizes the low temperature behavior of a number of polymers.

Composites

The term "composite" refers to materials having overall properties that are some average of the properties of several distinct components. One of these components is contiguous and forms a matrix interfacing with the reinforcing elements. In low temperature design, composites are particularly attractive because of their low ratio of thermal conductivity to elastic modulus or strength and their high ratio of elastic modulus to density and strength to density.

Theoretically, both filamentary-reinforced materials, such as fiberglass-epoxy, and aggregates, such as concrete, fall within this definition. Figure 9 gives a simple classification of composite systems. Discussion in this section will primarily relate to polymeric composites.

The material properties of fiber-reinforced composites depend on (1) matrix type, (2) fiber type, (3) fiber fraction, (4) fiber orientation, (5) fiber distribution, (6) fiber

COMPOSITES

Fiber-reinforced | Particulate-reinforced | Aggregate-reinforced

High-pressure reinforced plastic | Low-pressure reinforced plastic | Reinforced metals

Large volume mill products — e.g. rod, pipes, angles, etc. This product will need machining to fabricate components

Permits in-situ fabrication as per component design

Low-modulus reinforcement, e.g. fibers of glass, cotton, etc.

High-modulus reinforcement, advanced composites e.g. fibers of graph'te, boron, alumina

Figure 9. Simple classification of composite system.

strength and (7) temperature. Most of the properties are anisotropic and follow the general trend of increase in elastic modulus, tensile strength, flexural strength, and compressive strength with decrease in temperature. The properties of composites can be controlled by construction techniques, and customized material development is possible. Because composites are relatively new structural materials, their use was initially restricted to selective replacement of specific metal components, but this conservative approach is gradually being abandoned.

Low temperature (to the cryogenic level) behavior of composites has been extensively reviewed by Kasen (1975, 1983). He has observed that there is no systematic data base for lower temperatures. Existing data show extreme variability in strength properties as a result of embrittlement of matrix resins. Efforts to develop matrices with improved low temperature toughness continue; however, achieving this objective remains elusive (Hartwig and Evans 1982). The majority of the current data on polymeric composite strength are for room temperature and for the boiling points of cryogens.

The large variability in composite strength data is due to embrittling of the polymer matrix in cooling. Variability is also a strong function of the quality of laminate manufacture, for example, percentage of void- and resin-rich areas. Quality control during manufacture can therefore largely control the strength properties of composites (Kasen 1983).

The anisotropy of the reinforcement results in anisotropy in the properties of the composite (Fig. 10). Therefore, composite data are customarily related to fiber orientation. Figure 11 shows the temperature dependence of two glass-fabric-reinforced epoxy composites in two different orientations (Ledbetter 1979).

7

WARP. GPa (y-axis) / **FILL. GPa** (x-axis)

(Figure 11 axes: y-axis top value 1 6, 1 4, 2, 0; x-axis TEMPERATURE, K: 0, 100, 200, 300; legend: G 11CR, L 2CR; labels: Normal Direction, Warp Direction)
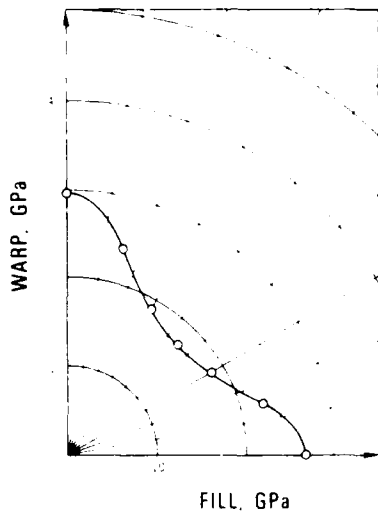
*Figure 10. Orientation dependence of composite property.*
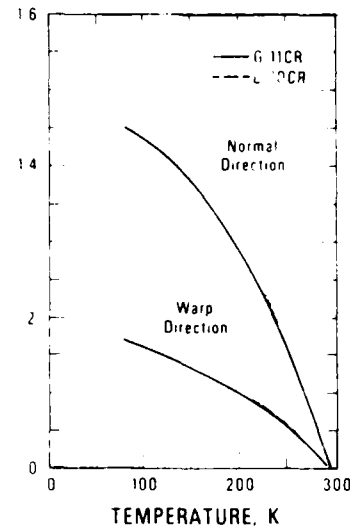
Figure 11. Temperature dependence of composite property.

FRACTURE PROPERTY TESTS FOR
LOW TEMPERATURE APPLICATION OF MATERIALS

Because of economic competition, weight premiums, and the availability of materials with high yield strength, structural engineering designs are tending to incorporate higher nominal stresses. However, this trend has also increased the probability of catastrophic failure. Safe operation of structures at high stresses requires an accurate definition of the fracture resistance of materials to ensure that an adequate safety margin is maintained in material performance to balance the effects of design refinements, fabrication, quality and reliability of inspection.

Fracture resistance depends highly on the conditions related to environment, constraint and strain rate. Fractures can occur at stress levels below yield stress or above yield stress, depending on flaw size, section thickness and strain rate.

In order to discuss the effect of temperature on fracture let us recall Figure 4b and show it schematically in Figure 12. It will be seen from Figure 12 that a material, when stressed at temperature T_i, will deform first by plastic yielding. If it were to strain-harden to the curve σ_F, it would then undergo brittle failure at stress σ_F. If the temperature T_i is below T_A, the nil ductility temperature (NDT) the material will simply fail without any plastic strain when the stress reaches σ_F. We have already mentioned that BCC materials are far more sensitive to temperature than FCC materials. Strain rate tends to increase the yield stress σ_y, displacing the σ_y curve upward as shown by the dashed line in Figure 12. This will lead to brittle failure at higher temperature since T_A will have increased.

Early fracture test approaches

The foregoing discussion shows that the fracture properties of a material depend on test conditions (temperature, strain rate) and specimen conditions (flaws). Early test methods like Charpy impact testing (ASTM 1966, Standard E-23) were therefore designed to introduce a given flaw into a specimen and to test that speci-

8
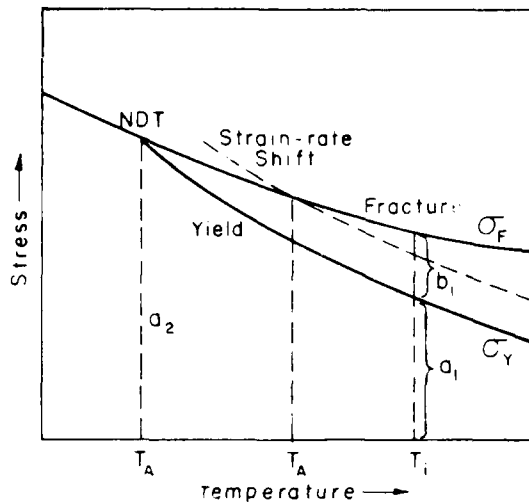
*Figure 12. Temperature effect on the fracture stress.*
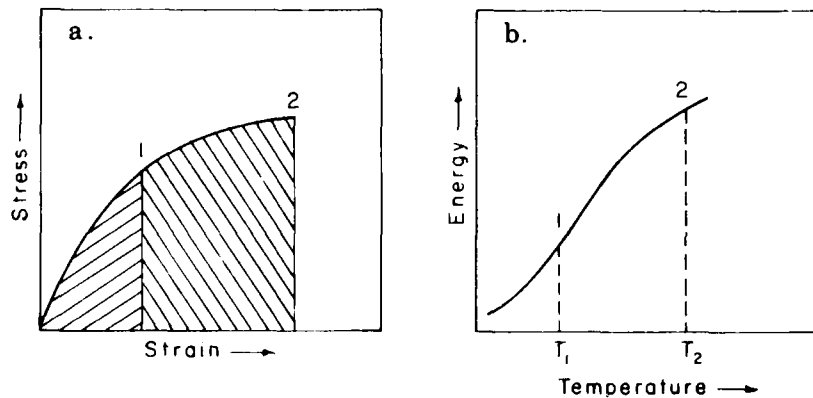
Figure 13. Temperature effect on ductility.

men at a high strain rate. Both the flaw and the high strain rate increase the nil ductility temperature, and the test therefore gives an NDT that tends to be conservative. The energy under the stress-strain curve is used as a measure that can be related to ductility. A low energy is indicative of low ductility, as shown in Figure 13a. The energy measured is really the amount of energy used in causing plastic flow. Figure 13b shows the difference of energy at two different temperature levels, T_1 and T_2 ($T_1 < T_2$). The Charpy impact test is a simple and inexpensive test that is easy to carry out in acceptance testing at the steel works.

The most common specimens employed with the Charpy test in recent years have been of the V-notch or keyhole type. A specimen is machined from the plate or other piece of material being tested, cooled to the desired temperature, and placed in the testing machine in such a way that it is supported on both ends as a beam (Fig. 14). A single blow is applied to the middle of the specimen, opposite the notch; as the impactor swings through, the specimen breaks and a recording dial indicates the absorbed energy. Normally, three specimens are tested at a given temperature and additional tests are made at selected temperatures. A curve showing the mean values of absorbed energy versus temperature is plotted as shown in Figure 13b.

9
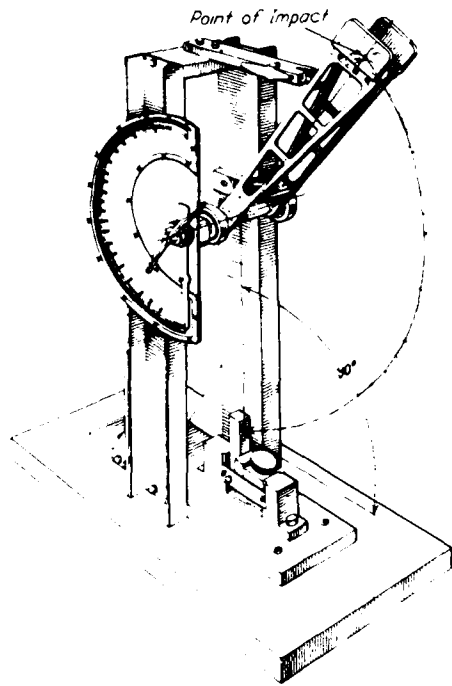
Figure 14. Simple beam Charpy impact machine.

The Charpy test is used primarily to establish acceptance specifications based on fixed energy levels (say 15 ft-lb of energy at 25°F). It usually shows wide scatter when specimens are taken from different areas of the same stock, and there are great variations in the transition ranges. Also, the test has not been very conducive to formulating stress analysis theories (Witzel and Adsit 1969, Harsem 1969, Hall 1969). However, to date it has remained one of the most common methods of tests to evaluate impact resistance properties of materials.

Another test that has increased in usage is the Naval Research Laboratory (NRL) drop weight test (Pellini and Puzak 1963). This test can be carried out with comparatively simple equipment at various temperatures and produces very little scattering in the results (Harsem 1969).

The drop weight test employs special beam specimens in which a crack is created in the tensile surface. The test specimen is generally about 14 in. long, 3.5 in. wide, and between 0.5 and 1 in. thick. A weld deposit is placed at the center of the specimen and notched to provide the initiation source. The test is conducted by subjecting a series of specimens of a given material to a single impact load at selected temperatures to determine the maximum temperature at which there is a break (go) or no-break (no-go) condition. The impact load is provided by a guided free-falling weight with an energy between 250 and 1200 ft-lb, depending on the yield strength of the steel to be tested and the size of the specimen. The specimens are not allowed to deflect more than a few tenths of an inch before they reach a stop.

ASTM (1966) specification E208 describes in detail the provisions for conducting and interpreting these tests. The nil ductility transition (NDT) temperature is determined as the maximum temperature at which a standard drop weight specimen breaks when tested in accordance with the provisions of the drop weight test.

Around 1969, the Naval Research Laboratory developed what was called the dynamic tear (DT) method of testing with the aim of overcoming the limitations of the

10

Charpy V(C_v) test and providing information of engineering design significance in the form of a "stress intensity factor" (Lange and Loss 1969). The test method was considered successful in that for very brittle material, where linear elastic fracture mechanics is applicable, direct correlation has been established between NDT energy and static stress intensity factors, K_{Ic} (discussed later).

Many other test methods have been used in practice and research during the last two decades. A review of all these tests can be found in Hall's (1969) paper on the evaluation of fracture tests.

Fracture mechanics tests

In recent years tremendous interest has been generated in fracture toughness testing based on linear elastic fracture mechanics. The theory of fracture toughness is based on the concepts of Griffith (1920) concerning fracture in brittle material. Because of much interest and extensive research, the theory of fracture toughness will be summarized here to clarify later discussion.

Theory of fracture toughness

According to Griffith's theory, when a centrally cracked panel (Fig. 15) is subjected to a uniform axial stress σ (psi), the elastic energy loss U (in.-lb) of the plate due to the growth of a crack of 2a (in.) length is given (Nadai 1950) by

$$U = \pi \sigma^2 a^2 \, t/E \tag{1}$$

where t is the thickness of the plate (in.) and E Young's modulus (psi). If S is the surface energy (in.-lb) of the two new surfaces created by the crack, then

$$S = 4\gamma a t \tag{2}$$

where t is the surface tension of the material (in.-lb/in.²).
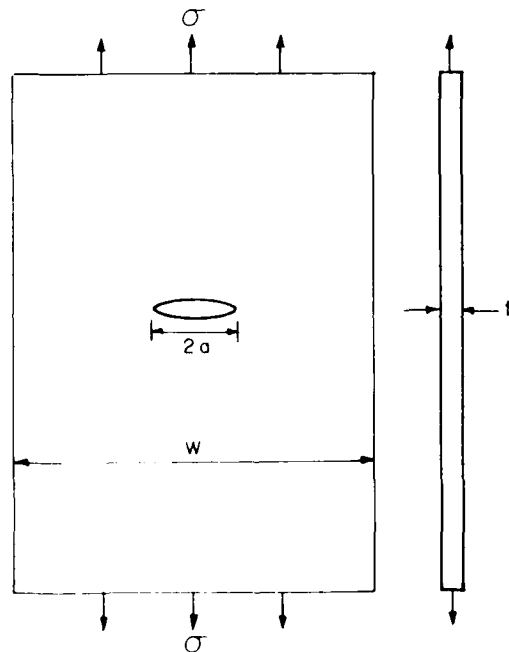
Figure 15. Centrally cracked panel under uniform axial stress σ.

11

Equation 1 shows that if σ is increased, more stored elastic strain energy will be available to propagate the crack. Obviously, this crack-driving force is opposed by an equilibrium resistance of the material. When the rate of increase of the crack-driving force with respect to crack length equals the rate of increase of the resistance, the crack becomes self-propagating. This type of critical condition occurs without additional external work only when the elastic strain energy released by a minute extension of crack length ∂a is sufficient to develop a new ∂a of crack length. This unstable or critical condition can be defined as

$$\frac{\partial(U\text{-}S)}{\partial a} = 0$$

and the stress at which this unstable condition develops is called the critical stress σ_c.

By use of the expressions for U and S from eq 1 and 2 and differentiating, the critical stress σ_c is given by

$$\sigma_c = \left[\frac{2E\gamma}{\pi a}\right]^{1/2}. \tag{3}$$

Although the above argument is true for brittle materials like glass or ceramics, the case of metals is different. For metals a much greater energy is required to plastically deform the grains surrounding the crack tip. However, if a plastic strain energy term P is added to the expression, the new critical stress for metals can be represented (Orowan 1955, Zinkham et al. 1969) by

$$\sigma_c = \left[E\left(2\gamma + P\right)/\pi a\right]^{1/2} \tag{4}$$

For metals, the value of P is normally several orders of magnitude larger than the surface tension of the cracks, so that γ can be disregarded.

Irwin (1958) used linear elastic stress analysis theory to show that in an infinite plate the strain-energy release rate G_c, equivalent to P in eq 4, is related to the critical stress intensity K_c at the crack tip. Thus disregarding γ and substituting G_c for P in eq 4, we have

$$EG_c = K_c^2 = \pi a_c \sigma_c^2 \tag{5}$$

where G_c = critical strain energy release rate (in.-lb/in.)
K_c = critical stress intensity factor (psi/in.)
σ_c = cross-section stress at crack onset (psi)
a_c = half crack length at crack onset (in.).

Equation 5 is true for an infinite plate. For a plate with finite width W the expression for the correction factor α (Irwin 1958) is

$$\alpha = \left[\left(W/\pi\, a_c\right)\tan\left(\pi a_c/W\right)\right]^{1/2} \tag{6}$$

12

According to Irwin (1958), eq 5 for a finite-width panel can be written as

$$EG_c = K_c^2 = \pi a_c \sigma_c^2 \alpha^2 \tag{7}$$

Since from eq 6

$$\alpha^2 = \frac{W}{\pi a_c} \tan \frac{\pi a_c}{W}$$

eq 7 can be simplified to give

$$EG_c = K_c^2 = \sigma_c^2 W \tan \frac{\pi a_c}{W} . \tag{8}$$

The a_c term, a critical crack length, generally includes a correction for the size of the plastic zone r_{Iy} at the tip of the crack, i.e.

$$a_c = a_c' + r_{Iy} = a_c' + \frac{K_c^2}{2\pi\sigma_{ys}^2} \tag{9}$$

where a_c' is physical size of crack and σ_{ys} tensile yield strength of material.

Note that if a calibration is made of the specimen's compliance with crack length, the plastic zone is reflected in the compliance measurement in an actual test, and therefore it is taken into account. If a calibration is not made, the value of r_{Iy} is estimated through an iterative process by first assuming $a_c = a_c'$ and calculating the first K_c value from eq 8.

Irwin (1958) has shown that G_c or K_c decreases if thickness increases because of transition from a plane stress to a plane strain condition (Fig. 16). In thin speci-
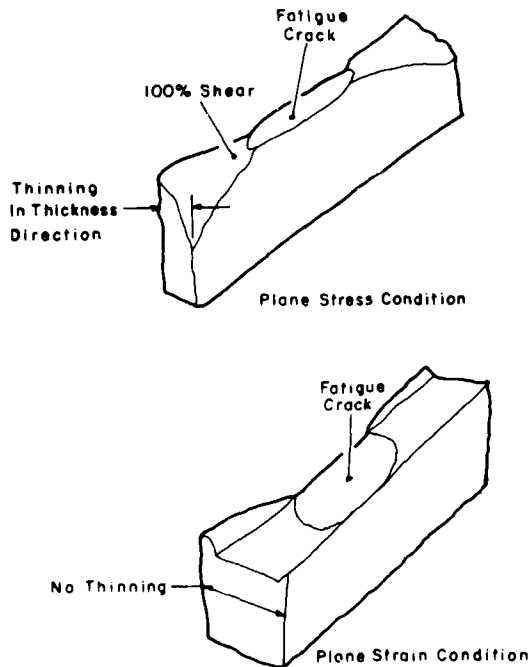
Figure 16. Plane strain and plane stress fractures.

13

mens plane stress situations are associated with a fracture surface which approaches almost 100% shear. Thus stresses are not developed in the thickness direction to resist deformation. The stress intensity factor is associated with plane stress or a mixed mode (normal and shear stress). The material property responsible for developing resistance to deformation is not well defined in this case.

With an increase in thickness the plane strain condition dominates, and the fracture surface becomes flat, with little or no shear lip. The stress in the thickness direction is developed depending on its resistance to deformation.

Now, remembering from eq 7 that for plane stress $EG_c = K_c$, for plane strain we can write

$$EG_c = K_c^2 \left(1 - \mu^2\right)$$

(10)

where μ is Poisson's ratio.

We now need to discuss the distinction between K_I and K_{Ic}. K is termed the general stress concentration factor, and K_I is a mathematical quantity related to the stress intensity factor of the first mode (the opening mode, with no consideration of shear but only of cleavage, i.e. a tensile-stress-related fracture opening). The ability of the material to resist deformation in the cleavage or first mode in the presence of the crack is manifested in the fracture toughness parameter K_{Ic} or G_{Ic}, which may be termed a material constant. The important distinction between K_I and K_{Ic} is similar to the distinction between stress and strength. Several definitions were proposed for K_{Ic} (Strawley and Brown 1965, Strawley 1969). The latest operational definition by Strawley (1969) is somewhat arbitrary. This defines K_{Ic} as the stress intensity at which the crack reaches an effective length 2% greater than at the beginning of the test. This is analogous to definition of yield strength in terms of a specified amount of plastic strain. Defining K_{Ic} in this manner, we can rewrite eq 10 as

$$EG_{Ic} = K_{Ic}^2 \left(1 - \mu^2\right) .$$

(11)

In the plane strain (thick specimen) test condition there are two general points that are relevant in calculating G_{Ic} or K_{Ic} (Strawley and Brown 1965). First, it is assumed that no stable crack occurs and the initial crack length is used in the calculation; and second, the plane strain plastic zone correction term is taken to be one-third of the plane stress term, that is, $r_{Iy} = r_{Iy}/3$ in eq 9, so that

$$a_c = a_c' + \frac{K_{Ic}^2}{6\pi\sigma_{ys}^2} .$$

Equation 8 (after Zinkham and Dedrick 1969) can now be completely modified to show that

$$EG_{Ic} = K_{Ic}^2 \left(1 - \mu^2\right) = \sigma_{Ic}^2 \left(1 - \mu^2\right) W \tan\left(\frac{\pi}{W} a_c + \frac{K_{Ic}^2}{6 W \sigma_{ys}^2}\right)$$

(12)

14

where a_c = half the original crack length (in.)

σ_{Ic} = gross stress at the initiation of slow crack growth (psi)

μ = Poisson's ratio.

In uniaxial tensile tests of an edge-notched or centrally notched specimen, a phenomenon called "pop-in" (a rapid decrease of load and then increase) has been observed. Boyle et al. (1962) have found that the "pop-in" load value coincides with the plane strain parameter K_{Ic}. Figure 17 shows a typical load-crack displacement curve indicating the pop-in point.

The stress σ_{Ic} at pop-in and initial half crack length a_c are used to calculate the G_{Ic} or K_{Ic} values. Even though the stable plane strain crack growth is subsequently arrested by the ability of the material to develop a shear fracture, the K_{Ic} value may be computed from the mixture of the plane strain and plane stress (mixed mode) type fracture that develops as the crack extends to some critical length a_c.

To summarize the above discussion, we find that the crack tip stress field is the driving force for fracture, and the magnitude of this stress field is proportional to the stress intensity factor K. K being a function of crack size, the applied stress and structural geometry, it can be computed using structural stress analysis methods. The resistance to fracture is a material property defined as the fracture toughness K_c. Fracture occurs when $K = K_c$. K_c is also a function of the extent of plastic strain
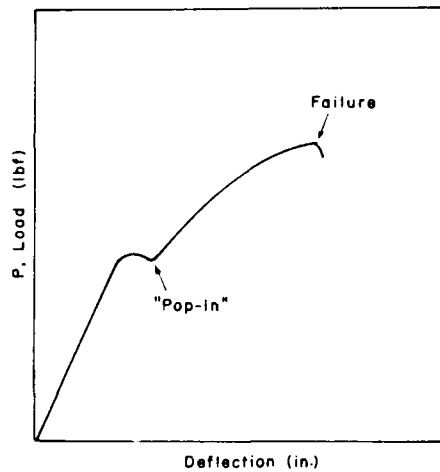
Figure 17. Typical load-crack displacement curve.
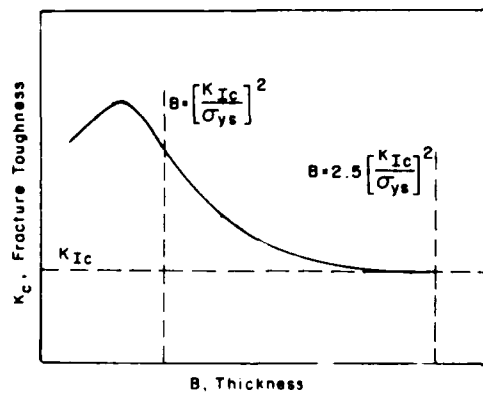
Figure 18. Transition of fracture toughness.

15

at the crack tip. If the plastic zone is small compared to the specimen dimensions, K_c approaches a minimum constant value defined as the plane strain fracture toughness, K_{Ic}. The relation between K_c and K_{Ic} is shown in Figure 18 (Tobler and McHenry 1983).

Fracture toughness test method

A standard test method, ASTM E399 (ASTM 1981), is used to measure plane strain fracture toughness, K_{Ic}. The test is applicable to fatigue-cracked specimens having a thickness of 0.063 in. or greater in tension or a three-point bending load. Load vs displacement across the notch at the specimen edge is recorded graphically. The load corresponding to a 2% increment of crack extension is established. The K_{Ic} value is calculated from this load by equations discussed earlier. The validity of the determination of the K_{Ic} value depends upon the establishment of a "sharp crack" condition at the tip of the fatigue crack.

Fracture toughness tests for polymers and composites

In the past, attempts have been made to characterize the failure of nonmetals like polymers, ceramics, rocks and composites using established fracture mechanics parameters. However, to date no standard fracture toughness test procedure for these materials has been established.

The complexity of fracture toughness tests of polymer materials arises primarily because of the large plastic zone at the crack tip and strain rate sensitivity (Marshall and Williams 1973). Most work in this area pertains to room temperature conditions, but low temperature studies on thermosetting epoxies (Kneifel 1979) and structural thermoplastics (polycarbonate) are available (Kneifel 1979, Martin and Garberich 1976, Tobler and McHenry 1983). K_{Ic} values for plastics are usually lower than 10 MPa–m $^{1/2}$ at low temperatures.

Composites generally fail because of the development of flaws during fabrication that become enlarged in service. At a microscopic scale this behavior is similar to that of metal because metal crystals are known to be anisotropic, and random aggregates of crystals are obviously heterogeneous. Thus, in a fracture mechanics approach, viewing the composites as statistically homogeneous leads to relations between variables that are useful in engineering description and prediction of behavior. Using this fracture mechanics concept, Corten (1972) has developed a mathematical model for two-material, bonded composite fracture analysis. Although the concept offers a mathematical tool for the future development of composite systems, the complexity of the problem has so far prevented this approach from becoming popular.

Influence of cyclic load on fracture toughness

We have discussed that the basic material property essential to all fracture mechanics consideration is the material's fracture toughness, K_{Ic} , at the temperature of interest. The K_{Ic} value gives an estimate of the critical defect size necessary for fracture with a single application of load. But in real life, few structures are built to withstand only a single application of load. Consequently, the useful life of a structure depends upon the rate at which an existing defect will grow to the critical flaw size as a result of fatigue (and also environmental) crack growth. Therefore, an additional material property basic to fracture mechanics consideration is the rate at which a crack will grow under the loading conditions of interest.

16

Clark and Wessel (1970), using their experimental results, have shown that the rate of crack growth (da/dN) is exponentially related to the crack tip stress intensity per cycle (K), as given by

$$\frac{da}{dN} = C_0 \, \Delta K^{\,n}$$

where a = crack length
N = number of loading cycles
n, C_0 = empirical constants determined from the test data
K = stress intensity factor per cycle.

Because the crack growth is influenced by cyclic loading, the recommended procedure for fracture toughness measurement includes consideration of fatigue cracking at nominal stress less than 25% of yield stress (Rolfe and Novak 1970).

Strain rate effect on fracture

One of the simplest ways to idealize viscoelastic material behavior under uniaxial loading at an imposed strain rate $d\varepsilon/dt$ is to express this behavior in the following differential equation:

$$\frac{1}{E} \cdot \frac{d\sigma}{dt} + \frac{\sigma}{\eta} = \frac{d\varepsilon}{dt} \qquad \text{(Maxwell solid)} \qquad (13)$$

where E = Young's modulus
σ = stress
t = time
ε = strain
η = steady-state tensile viscosity.

For finite increments of strain, stress and time, $\Delta\varepsilon$, $\Delta\sigma$ and Δt, eq 13 can be rewritten as

$$E \; \frac{\Delta\varepsilon}{\Delta t} = \frac{\Delta\sigma}{\eta'E} + \frac{\Delta\sigma}{\Delta t}. \qquad (14)$$

Now if time of loading $\Delta t \ll \eta/E$, the term $\Delta\sigma/(\eta/E)$ can be neglected, giving

$$\frac{\Delta\sigma}{\Delta t} = E \cdot \frac{\Delta\varepsilon}{\Delta t} \qquad (15)$$

which is a pure elastic loading. In this case brittle failure would result at the tip of a crack when the local stress exceeds the ideal tensile strength. Alternatively, if η/E is much smaller than Δt, $\Delta\sigma/\Delta t$ can be neglected, giving the equation of Newtonian viscous flow:

$$\frac{\Delta\sigma}{\eta/E} = E \cdot \frac{\Delta\varepsilon}{\Delta t}. \qquad (16)$$

This equation shows that for small strain rates, there is always enough time for the elastic strains to relax—that is, the viscous deformation will alter the shape and orientation of the cracks, making brittle fracture less possible. Also, it follows that brittle fracture in glassy material (viscoelastic) is governed by the time constant of loading.

Many investigators have examined the effects of strain rate and temperature on material behavior (Duffy 1979, Klepaczko 1979, Nicholas 1981). For materials with strong temperature and strain rate dependence, the fracture toughness usually decreases with decreasing temperature and increasing rate of loading. Fracture toughness should therefore be evaluated in the region where it may show its minimal value and the conditions that reveal the transition from high to low values of fracture toughness should be investigated.

In order to develop a suitable testing technique for high-strain-rate loading, Knott (1973) and Klepaczko (1979) have defined the loading rate parameter $\dot{K}_I$ to express how fast the crack tip region is loaded:

$$\dot{K}_I = K_{Ic}/t_c \qquad (17)$$

where K_{Ic} is the crack tip stress intensity factor in mode I (plane strain fracture toughness) and t_c is the time interval from the start of loading to the point when stable crack propagation starts.

The spectrum of rate of loading as defined by Klepaczko falls into the following categories:

I   Quasi-static loading $1\,\text{MPa}\sqrt{m}\,s^{-1} \leq \dot{K}_I \leq 10^3\,\text{MPa}\sqrt{m}\,s^{-1}$
    (with a closed-loop
    static dynamic testing
    machine)

II Instrumented hammer $10^4\,\text{MPa}\sqrt{m}\,s^{-1} \leq \dot{K}_I \leq 10^5\,\text{MPa}\sqrt{m}\,s^{-1}$
    (for example, instrumented
    Charpy hammer)

III Stress wave loading $10^6\,\text{MPa}\sqrt{m}\,s^{-1} \leq \dot{K}_I \leq 10^9\,\text{MPa}\sqrt{m}\,s^{-1}$

Obviously, the $\dot{K}_I$ spectrum covers about 10 orders of magnitude, and requires a number of experimental techniques to be covered. For a K63 Al-Zn-Mg-Cu alloy, Klepaczko (1979) demonstrated that values of K_{Ic} measured at the stress wave loading are 20 to 36% lower than those for static loading, and for another aluminum alloy (PA6) this value is almost half of that for static loading. However, Klepaczko's tests were all done at room temperature. Further reduction in fracture toughness is expected at lower temperature.

18

TEST PLAN

Rationale

In the past decade, fracture mechanics principles have been used to quantify safety factors in structural design, taking into account crack propagation and/or brittle fracture. Most structural members, components, vessels, and piping are designed according to analysis criteria that guard against failure, but variability in manufacturing processes of materials may introduce defects or flaws. Despite nondestructive testing one must realize that flaws do escape detection on occasion and may grow to critical sizes under cyclic loading and stress corrosion cracking. It becomes important, then, to determine the associated minimum critical stress intensity factors, K_{Ic}, that will lead to unstable growth in these cracks and also to know the minimum stress intensity factor, K_{Ia}, at which these cracks will be arrested in a particular material.

Klepaczko (1979) has shown a significant difference between the static and dynamic determination of K_{Ic} at room temperature; at lower temperatures this difference will possibly be higher, with K_{Ic} showing lower values. In cold regions numerous field conditions may be cited in which dynamic loading on structures assumes critical importance. Wave action, wind action, ice sheet movement and impact, drilling vibration on drill rigs, vehicular motion, blasting and earthquakes are a few examples. The hulls of ice-breaking vessels are subjected to repeated impact loading by ice, resulting in deterioration and the need for frequent repair. Therefore, sound engineering design for cold regions should depend on material property data determined at low temperature and at high strain rate loading. The CRREL test program aims to generate these data. The next section discusses this test plan.

Experimental program

The proposed testing system is summarized in Figure 19. For each material selected to be tested, a number of test specimens will be prepared. The number will depend on the expected variation in test results. Enough specimens will be made so that statistically meaningful representative data can be obtained from each type of test.

It is proposed that static, quasi-static and high-strain-rate tests be conducted to evaluate the fracture toughness property of each material. During its service life at low temperature a component material is subjected to repeated low-stress-level loading and occasional high-strain-rate loading. The testing should reflect a similar loading pattern. Therefore, some specimens will be subjected to initial fatigue loading by (tension-tension) load cycling. A comparison of fracture toughness data between the load-cycled and non-load-cycled specimens will reflect the effect of service life on degradation of material property.

Quasi-static fracture toughness test

The quasi-static fracture toughness test (1 MPa $\sqrt{m}$ s^{-1} to 10^3 MPa $\sqrt{m}$ s^{-1}) is proposed to be carried out using modified ASTM compact tension (CT) specimens as described by Klepaczko (1979). In this method, shown schematically in Figure 20, a compressive force is applied to a wedge-loaded specimen. The vertical displacement of the wedge is measured. Also, the transverse displacement of the specimen opening can be measured by a clip gauge. The measurements can be recorded by

19
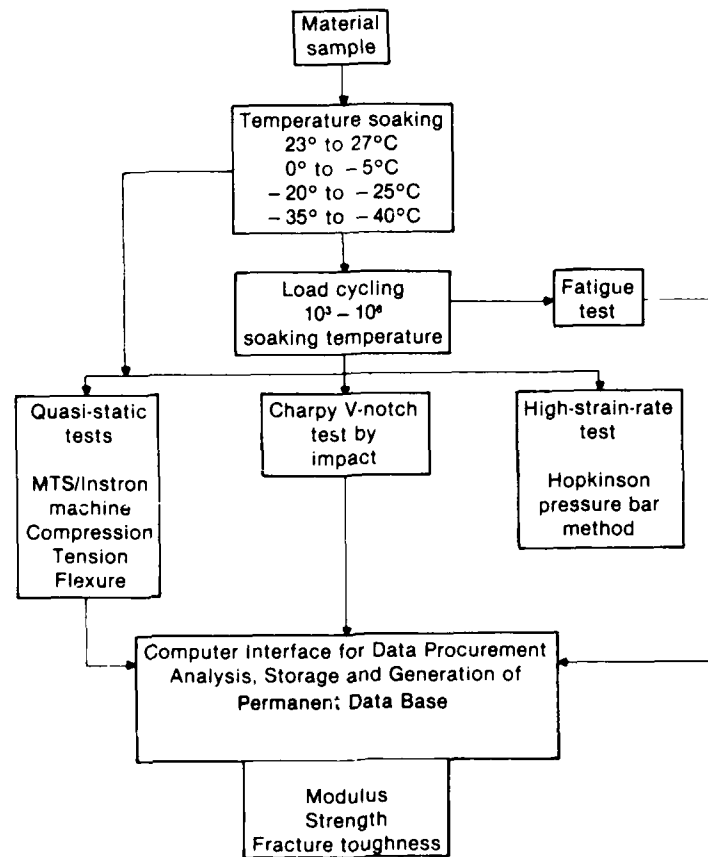
Figure 19. Test program schematic.
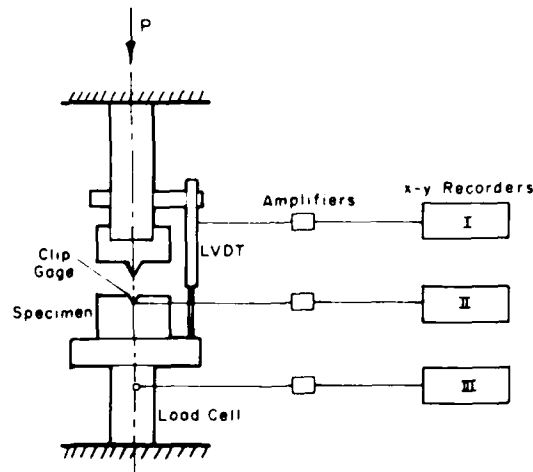
Figure 20. Device for quasi-static slow and fast loading. The force P acting on the wedge is applied by a testing machine.

two x-y recorders. In addition, an oscilloscope can record the force-time curve driving fast crack propagation.

In the configuration of a wedge penetrating the specimen, the tensile force, F_c, acting on the crack is given by

$$F_c = \frac{P_c}{2\tan\left(\frac{\alpha}{2} + \phi\right)} \tag{18}$$

where α = half the wedge angle (degrees)

ϕ = angle of wedge/specimen friction (degrees)

P_c = compressive force acting on the wedge (lbf).

And according to Klepaczko (1979), the fracture toughness K_{Ic} can then be denoted by

$$K_{Ic} = \frac{P_c f(a/W)}{2B\sqrt{W}\tan\left(\frac{\alpha}{2} + \phi\right)} \quad \left(\text{psi}\sqrt{\text{in.}}\right) \tag{19}$$

where α = crack length (in.)

W = width of the specimen (in.)

B = thickness of the specimen (in.),

$f(a/W)$ is given by

$$f(a/w) = 29.6\left(\frac{a}{W}\right)^{1/2} - 185.5\left(\frac{a}{W}\right)^{3/2} + 655.7\left(\frac{a}{W}\right)^{5/2} - 1017\left(\frac{a}{W}\right)^{7/2} + 638.9\left(\frac{a}{W}\right)^{9/2}$$

where $B \geq (K_{Ic}/\sigma_y)^2$ and σ_y denotes the yield limit of the material.

High-strain-rate tests

The high-strain-rate test is proposed to be carried out by using the split Hopkinson bar apparatus (Kolsky 1949). In this technique, a small cylindrical specimen is sandwiched between two long bars. A compression pulse generated by impact from a third bar propagates down one of the bars and through the specimen into the second bar. The bars remain elastic, although the specimen is deformed into the inelastic region because of the impedance mismatch. The equations of one-dimensional elastic wave propagation in long rods along with the recorded strain gauge signals from the two bars are used to determine the time history of both force and displacement at the ends of the rods contacting the specimens.

In Klepaczko's (1979) stress wave loading technique, the geometry of the test specimen is similar to that of an ASTM 399 fracture toughness compact tension (CT) test specimen with the pinholes cut off and an angular incision milled to accommodate a wedge for loading the specimen (Fig. 21). The wedge allows for application of compressive force, whereas the crack tip remains loaded in tension.

The displacement of the wedge, as a rigid body, denoted by u_A is given by
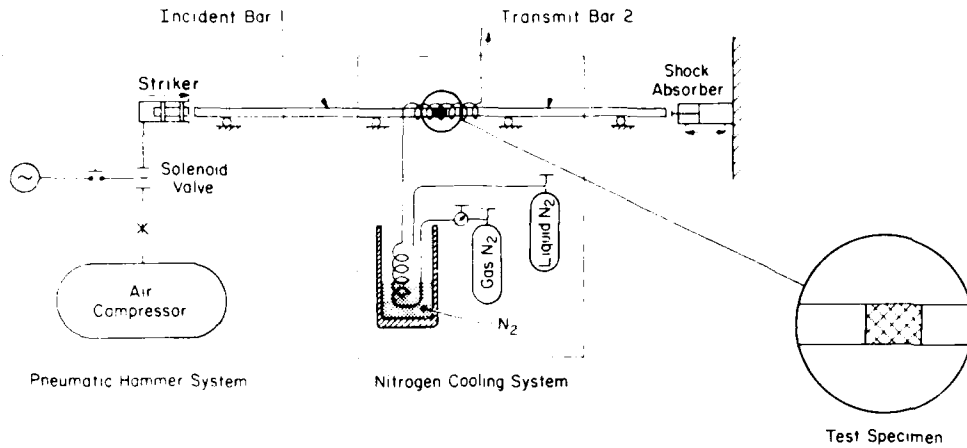
Figure 21. Split Hopkinson pressure bar applied to fracture dynamics.

$$u_A(t) = C_o \int_0^t \left[\varepsilon_I(t) - \varepsilon_R(t)\right] dt \qquad (20)$$

and the displacement of the transmitter bar face, which is backing the specimen (denoted by u_B), is

$$u_B(t) = C_o \int_0^t \varepsilon_T(t)\, dt \qquad (21)$$

where ε_I, ε_R and ε_T are the elastic strains of the incident, reflected and transmitted pulses, respectively, and C_o (in./s) is the elastic strain wave velocity in the bar given by

$$C_o = \left[\frac{Eg}{\rho}\right]^{1/2} \qquad (22)$$

where E denotes Young's modulus (psi), g is the acceleration due to gravity (in./s²) and ρ is the density of the bar material (lb/in.³).

The net displacement of the wedge as a function of time is given by

$$\delta(t) = u_A(t) - u_B(t). \qquad (23)$$

Considering eq 20, 21 and 23, the net displacement $\delta(t)$ (in.) is

$$\delta(t) = C_o \int_0^t \left[\varepsilon_I(t) - \varepsilon_R(t)\right] dt - \int_0^t \varepsilon_T(t)\, dt. \qquad (24)$$

For conditions of equilibrium

$$\varepsilon_I(t) + \varepsilon_R(t) = \varepsilon_T(t).$$

Rewriting,

$$\varepsilon_I(t) - \varepsilon_T(t) = -\varepsilon_R(t) . \tag{25}$$

Substituting the above result in eq 24 above

$$\delta(t) = -2C_o \int_0^t \varepsilon_R(t) dt . \tag{26}$$

If we assume that the bar cross-sectional area is A (in.), $P_A(t)$ = the instantaneous force (lb) at section A, and $P_B(t)$ (lb) = the instantaneous force at section B, the forces acting on the specimen are the following:

$$P_A(t) = EA \left[\varepsilon_I(t) + \varepsilon_R(t) \right] \tag{27}$$

and

$$P_B(t) = EA \left[\varepsilon_T(t) \right] . \tag{28}$$

The average force $P(t)$ on the loading system is

$$\overline{P}(t) = \frac{1}{2} \left[P_A(t) + P_B(t) \right] . \tag{29}$$

From eq 27 and 28

$$\overline{P}(t) = \frac{1}{2} EA \left[\varepsilon_I(t) + \varepsilon_R(t) + \varepsilon_T(t) \right] . \tag{30}$$

Again for equilibrium conditions, eq 25 is satisfied, and using this equation in eq 30 we have

$$\overline{P}(t) = EA \, \varepsilon_T(t) . \tag{31}$$

It will be seen that eq 28 and eq 31 are the same; therefore

$$\overline{P}(t) = P_B(t) . \tag{32}$$

Equation 32 shows that the average force is proportional to the transmitted force, which can now be measured to determine the K_{Ic} value. If the critical point (pop-in) on the $\varepsilon_T(t)$ trace can be detected, the critical force P_c can be calculated:

$$\overline{P}\left(t_c\right) = EA\,\varepsilon_{Tc}\left(t_c\right) \tag{33}$$

where t_c is the time period after which the crack starts to propagate. Once P_c is determined, K_{Ic} can be calculated from

$$K_{Ic} = \frac{EA\,\varepsilon_{Tc}\left(t_c\right)f\left(a/W\right)}{2B\,\sqrt{W}\,\tan\left[\left(\alpha/2\right) + \tan^{-1}\mu\right]}\ \text{psi}\cdot\sqrt{\text{in.}} \tag{34}$$

where α = wedge angle (degrees)
W = width of specimen (in.)
a = half crack length (in.)
μ = coefficient of friction between wedge and material surface
B = thickness of specimen (in.).

Thus, if the coefficient of friction is known, the fracture toughness K_{Ic} may be calculated from the record of $P(t)$ or $P(\delta)$ where δ is the wedge displacement.

Test equipment

The complete range of testing from quasi-static (10^{-3} strain/s) to high (10^3 strain/s) strain rate will require loading equipment, specimen clamping devices in a variety of configurations, transducers, sensors, suitable recording instruments and signal analyzing devices. Table 1 lists this equipment, instrumentation and facilities.

Table 1. Mechanical equipment and instrumentation requirements for low temperature testing of materials.

Type of equipment	Description
Mechanical	1. Universal testing machine with necessary accessories, 200 kips (intermittent use— MTS testing machine available at CRRFL will suffice)
	2. Fracture toughness and fatigue testing machine, 20 kips (continuous use), includes load frame, actuator, hydraulic power supply, load cells, strain transducers, grips and fixtures, environmental chamber and control console
	3. Charpy testing machine
Instrumentation	1. Four-channel, 500-kHz digital oscilloscope with signal storing, analyzing, plotting and computer interface capability
	2. High resolution camera
	3. High resolution microscope
Fabrication material	1. Testing frame angle irons and miscellaneous fasteners
	2. Impactor/gas system
	3. Electronic parts, strain gage and accessories
	4. Pressure bars

A large number of tests to determine primary elastic material properties at room and low temperature will be conducted using test specimens in the MTS universal testing machine currently available at CRREL.

A study of the effect of quasi-static strain rate on fracture toughness will be conducted, both with pre- and post-fatigue conditioning of the specimens. Fatigue-testing, tensile testing and fracture toughness testing will be carried out using the 20-kip machine.

Composites and plastics cannot be tested for brittle fracture/toughness using the 20-kip testing machine. For these tests it is necessary to use a Charpy testing machine that can be remotely operated in a low temperature environment chamber.

High strain rate studies will be conducted in the Hopkinson bar test setup installed at CRREL. The specimen will be jacketed for low temperature testing. The test setup will be designed for use of two 8-ft-long pressure bars, one 1-ft-long impact bar and an impacting mechanism using a gas gun and associated remote control valving. The instrumentation consists of the following:

1. Impactor velocity: photo-diode-activated timer.
2. Triggering circuit electronics: accelerometer/vibration pickup.
3. Longitudinal, torsional and flexural strain wave pickup strain gauges.
4. Reaction pad instrumentation: dynamic load cell.
5. Digital oscilloscope to record incident, transmitted, and reflected stress wave pulses, and to integrate.
6. Associated electronic parts for connection and interfacing of various equipment.

EXPECTED INFORMATION

Expected information from the tests on each material will include its behavior data, within both elastic and inelastic limits. Within elastic limits, studies will be made of the change of modulus or stiffness with decreasing temperature and increasing strain rate. Conventional uniaxial tension, compression and flexure tests and Charpy V-notch test results will establish the baseline material characteristics at decreasing temperatures. For engineering design input, data will be generated by fracture mechanics tests. Results of these tests will provide a stress concentration factor at the crack tips, K_{Ic} values, and the minimum crack size that can be tolerated at various temperatures and loading rates.

Data from fatigue tests to failure at various low temperatures will be generated to characterize the materials. In order to reflect the conditions of failure of materials in service, fracture mechanics tests will be performed on specimens after subjecting them to a given amount of cyclic loading

The initial emphasis of the testing will be on polymeric composites; standard test methods are not available for these materials. Although testing of steel and other isotropic materials has achieved high sophistication through fracture mechanics tests, fracture mechanics of composites are not well understood. Like the material itself the art of composite material testing is also in a development phase, and the proposed test program will contribute to this evolutionary process.

Low temperature property data will be of great value to composite structure designers. Besides basic stiffness and strength data, several types of ancillary data may be generated during the testing process. For example, acoustic emissions from the sample may be studied during tensile loading of composite beams and re-

lated to its behavior through the fracture process. With infrared imagery techniques crack nucleation spots may be identified and crack growth may be followed. X-ray study may show the filament dislocations developing during testing. Fractography and scanning electron micrography techniques may be employed to develop understanding of the fracture processes of composites. Room temperature data generated by these test methods are available but low temperature data are sparse. The low temperature data will contribute to the basic understanding of low temperature behavior.

At later dates, special steels and other materials for cold application will be included in the test program. Expected results from the tests of structural metals, e.g. steel, will be based on the approach that the standard fracture toughness testing is a complex task in its present form in terms of specimen preparation, instrumentation and recording of the data. This complexity increases more when the tests are to be done on material at temperatures below or near their nil ductility temperatures. As a result, Charpy-V-notch impact testing (CV) is still the most frequently used test method, despite large scatter in the data. We plan to evaluate simple-geometry specimens in dynamic tests such as the Hopkinson pressure bar test to obtain room and low temperature fracture toughness data as a conservative estimate of this property. The Hopkinson pressure bar method is simple and less time-consuming, and through proper data processing equipment, results are obtained quickly. Specimens can be cooled to their nil ductility temperatures by a refrigerant inside a jacketing around the specimen, and the test is finished in a short time because of impact loading. It is expected that a large volume of low temperature data can be generated at much less cost by this method than by standard fracture mechanics tests.

Material specimens for tests will be obtained by contacting the Army research and materials development communities that have the real need for such materials data. For example, a need for low temperature composite behavior data has already been identified by the U.S. Army Materials Technology Laboratory, Watertown, Massachusetts, and it has provided the first batch of composite materials for testing. Results of the study will be published as CRREL reports and will be made available to primary users (AMC, TRADOC) and other users (TACOM, MERADCOM, ARDC) through OCE (DAEN-ZCM). The results will also have a high potential for non-mission-related technology transfer to local, state, and other federal government agencies as well as to private industry.

SELECTED BIBLIOGRAPHY

Argon, A.S. (1974) Statistical aspects of fracture. In *Composite Materials: Fracture and Fatigue* (L.J. Broutman, Ed.). New York: Academic Press, vol.5.

Ashby, M.F. (1972) A first report on deformation-mechanism maps. *Acta Metall.*, 20: 887–897.

ASTM (1966) *ASTM Standard*, Philadelphia: American Society for Testing and Materials, Part 30.

ASTM (1966) Behavior of materials at cryogenic temperatures. Philadephia: American Society for Testing and Materials, STP 387.

ASTM (1981) *Annual Book of ASTM Standards*. Philadephia: American Society for Testing and Materials, E399, part 10, pp. 588–618.

Baldy, M.F. (1976) The development of large-diameter high strength line pipe for low temperature service. Offshore Technology Conference, Paper no. OTC2667.

Berg, K.R. (1983) Composites components—most likely to succeed in vehicles. In *Proceedings, Sixth Conference on Fibrous Composites in Structural Design,* AMMRC, Watertown, Mass., pp. 67–70.

Boyle, R.W., A.M. Sullivan and J.M. Krafft (1962) *Welding Journal (N.Y.), Research Supplement,* 41:4285–4325.

Clark, W.G. and E.T. Wessel (1970) Application of fracture mechanics technology to medium-strength steel. In *Review of Developments in Plane Strain Fracture Toughness Testing* (W.F. Brown, Ed.). ASTM Special Publication 463, pp.160–190.

Corten, H.T. (1972) Fracture mechanics of composites. In *Fracture: An Advanced Treatise,* (H. Leibowitz, Ed.). New York: Academic Press, vol. VII.

Couch, W.P., J.E. Gagorcik and T.F. White (1983) Structural evaluation of advanced composite application to hydrofoil strut/foil system. In *Proceedings, Sixth Conference on Fibrous Composites in Structural Design,* AMMRC, Watertown, pp. 25–65.

Daziel, D. (1983) High technology test bed: Where we have been, where we are going. In *Proceedings of the Sixth Conference on Fibrous Composites in Structural Design,* AMMRC, Watertown, Mass., pp. 23–24.

Duffy, J. (1979) Testing techniques and material behavior at high rates of strain. In *Proceedings, Conference on Mechanical Properties at High Rates of Strain,* (J. Harding, Ed.). The Institute of Physics (London).

Favor, R.J., D.N. Cidieon, H.J. Grover, J.E. Hayes and G.M. McClure (1961) Investigation of fatigue behavior of certain alloys in the temperature range room to –423°F. WADD Technical Report 61-132, Defense Technical Information Center, Alexandria, Virginia.

Foye, R.L. (1983) Status of the NASA/DOD composite flight service evaluation programs. In *Proceedings, Sixth Conference on Fibrous Composites in Structural Design,* AMMRC, Watertown, Mass.

Frank, W.F.X. (1979) Spectroscopic analysis of high polymers for use at low temperatures. In *Nonmetallic Materials and Composites at Low temperature* (A.F. Clark, R.P. Reed and G. Hartwig, Ed.). New York: Plenum Press.

Griffith, A.A. (1920) *The phenomena of rupture and flow in solids.* Philosophical Transactions, Royal Soc. (London), Series A, **221**: 163–198.

Hall, W.J. (1969) Evaluation of fracture tests and specimen preparation. In *Fracture* (H. Liebowitz, Ed.). New York: Academic Press, IV:1–44.

Hallet, B. (1983) The breakdown of rock due to freezing: A theoretical model. In *Permafrost: Fourth International Conference, Proceedings,* Washington, National Academy Press, pp. 433–438.

Hansen, O.A. (1960) Materials for low temperature use: Short course on process industry corrosion. In *Proceedings, National Association of Corrosion Engineers,* Houston, pp. 273–286.

Harsem, O. and H. Wintermark (1969) An evaluation of the Charpy impact test. In *Proceedings ASTM Annual Meeting, Symposium on Impact Testing of Metals,* Atlantic City, New Jersey, NTIS No. N71-11585.

Hartwig, G. (1979) Mechanical and electrical low temperature properties of high polymers. In *Nonmetallic Materials and Composites at Low Temperature* (A.F. Clark, R.P. Reed and G. Hartwig, Ed.). New York: Plenum Press.

Hartwig, G. and D. Evans (1982) *Fundamentals and Applications of Nonmetallic Materials at Low Temperatures.* New York: Plenum Press.

Irwin, G.R. (1958) Fracture. *Handbuch der Physik VI* (Flügg Ed.). Springer, pp. 551–590.

Irwin, G.R. (1960) Fracture testing of high strength sheet materials under conditions appropriate for stress analysis. U.S. Naval Research Laboratory, Report 5486.

Kasen, M.B. (1975) Properties of filamentary reinforced composites at cryogenic temperatures. In *Composite Reliability*, Philadephia: ASTM STP 580, American Society for Testing and Materials, pp. 586–611.

Kasen, M.B. (1983) Composites. In *Materials at Low Temperatures* (R.P. Reed and A.F. Clark, Ed.). Metals Park, Ohio: American Society for Metals, pp. 413–463.

Klepaczko, J. (1979) Application of the split Hopkinson pressure bar to fracture dynamics. Inst. Phys. Conf., Ser. 47., pp. 201–214.

Kneifel, B. (1979) Fracture properties of epoxy resins at low temperatures. In *Nonmetallic Materials and Composites at Low Temperatures*, New York: Plenum Press, pp. 123–129.

Knott, J.F. (1973) *Fundamentals of Fracture Mechanics*. London: Butterworth.

Kolsky, H. (1949) An investigation of the mechanical properties of materials at very high rates of loading. In *Proceedings, Physics Society* (London), vol. B62, pp. 676–700.

Kreibich, U.T., F. Lohse and R. Schmid (1979) Polymers in low temperature technology. In *Nonmetallic Materials at Low Temperatures* (A.F. Clark, R.P. Reed and G. Hartwig, Ed.). New York: Plenum Press, pp. 1–30.

Lange, E.A. and F.J. Loss (1969) Dynamic tear energy—a practical performance criterion for fracture resistance. Naval Research Laboratory, Washington, D.C., NRL Report 6975.

Ledbetter, H.M. (1979) Dynamic elastic modulus and internal friction in G-10CR and G-11CR fiberglass-cloth-epoxy laminates. NBSIR 79-1609, Boulder, Colorado: National Bureau of Standards.

Marshall, G.P. and J.B. Williams (1973) The correlation of fracture data for PMMA. *Journal of Material Science*, 8: 138–140.

Martin, G.C. and W.W. Gerberich (1976) Temperature effects on fatigue crack growth in polycarbonate. *Journal of Material Science*, 11: 231–238.

Martin, H.L., P.C. Miller, A.G. Ingram and J.E. Campbell (1968) Effects of low temperatures on the mechanical properties of structural metals. NASA Report SP-5012(01), Washington, D.C.

McClintock, F.A. and S.A. Ali (1966) *Mechanical Behavior of Materials*. Reading, Mass.: Addison-Wesley, pp. 546–561.

McHenry, H.I. (1983) Structural alloys. In *Materials at Low Temperatures* (A.F. Clark, R.P. Reed and G. Hartwig, Ed.). New York: Plenum Press, pp. 371–411.

Nadai, A., (1950) *Theory of Flow and Fracture of Solids*. New York: McGraw-Hill.

Nicholas, T. (1981) *Impact Dynamics* (J.A. Zukas et al., Ed.). New York: Wiley, p. 227.

Nichols, R.W. and A. Cowan (1969) Selection of materials and other aspects of design against brittle fracture in large steel structures. In *Fracture: An Advanced Treatise* (H. Liebowitz, Ed.). New York: Academic Press, V: 233–284.

Parker, E.R. (1957) *Brittle Behavior of Engineering Structures*. New York: Wiley, pp. 253–301.

Pellini, W.S. and P.P. Puzak (1963) Report No. 5920, Naval Research Laboratory, Washington, D.C.

Plumer, J.R., N.R. Schott, J.A. McElman and S.B. Driscoll (1983) Design and fabrication of FRP truck trailer side rack. In *Proceedings of the Sixth Conference*

on Fibrous Composites in Structural Design, AMMRC, Watertown, Mass., pp. 23–24.

Read, D.T. (1983) Mechanical properties. In *Materials at Low Temperature* (Reed and Clark, Ed.). Metals Park, Ohio: American Society for Metals, pp. 237–267.

Reed, R.P. and R.P. Mikesell (1967) Low temperature mechanical properties of copper and selected alloys. National Bureau of Standards, Monograph 101.

Rinebolt, J.A. and W.J. Harris, Jr. (1951) Effect of alloying elements on notch toughness of pearlistic steels. *Transactions, ASM*, **43**: 1175–1214.

Rittenhouse, J.B. and J.B. Singletary (1968) *Space Materials Handbook*. Third Edition, Lockheed Missiles and Space Co. Technical Report AFML-TR-68-205. Air Force Systems Command, Wright-Patterson Air Force Base, Ohio.

Rolfe, S.T. and S.R. Novak (1970) Slow bend K_{Ic} testing of medium strength high toughness steel. In *Review of Development in Plane Strain Fracture Toughness Testing* (W.F. Brown, Ed.). ASTM Special Publication 463, pp. 124–159.

Sparks, L.L. (1978) Cryogenic foam insulations: Polyurethane and polystyrene. In *Nonmetallic Materials and Composites at Low Temperatures* (A.F. Clark, R.P. Reed and G. Hartwig, Ed.). New York: Plenum Press, pp. 165–205.

Strawley, J.E. (1969) Plane strain fracture toughness. In *Fracture: An Advanced Treatise* (H. Liebowitz, Ed.). New York: Academic Press, vol. IV.

Strawley, J.E. and W.F. Brown (1965) Fracture toughness testing methods. In *Fracture Toughness Testing and Its Applications*, American Society for Testing and Materials, ASTM Special Technical Publication no. 381, pp. 133–198.

Tetelman, A.S. and A.J. McEvily, Jr. (1967) *Fracture of Structural Materials*. New York: Wiley, p. 268.

Titus, J.B. (1967) Effect of low temperature (0 to 65°F) on the properties of plastics. Plastics Technical Evaluation Center, Picatinny Arsenal, Dover, New Jersey, Plastic Report 30.

Tobler, R.L. and H.I. McHenry (1983) Fracture mechanics. In *Materials at Low Temperatures* (R.P. Reed and A.F. Clark, Ed.). Metals Park, Ohio: American Society for Metals, pp. 269–293.

Tomin, M.J. (1983) Fracture mechanics approach to minimize risk of failure in steels for arctic use. In *Proceedings, Fracture Toughness Evaluation of Steels for Arctic Marine Use* (R. Thomson and C.S. Champion, Ed.). Physical Met. Lab. Canmet., pp. 12-1–12-15.

Witzell, W.E. and N.R. Adsit (1969) Temperature effects on fracture, In *Fracture: An Advanced Treatise* (H. Liebowitz, Ed.). New York: Academic Press, **IV**: 69–112.

Zinkham, R.E. and J.H. Dedrick (1969) Fracture behavior of aluminum alloys. In *Fracture: An Advanced Treatise* (H. Liebowitz, Ed.). New York: Academic Press, **IV**: 299–370.

APPENDIX A: LOW TEMPERATURE BEHAVIOR
OF SOME STRUCTURAL METALS AND ALLOYS.
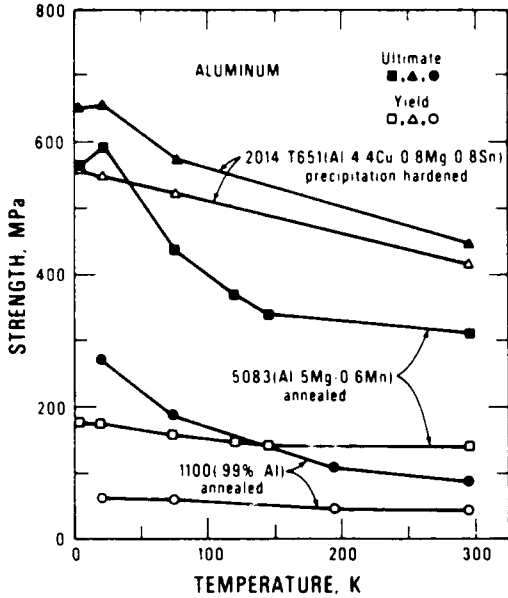
Figure A1. Yield and ultimate tensile
strengths as a function of temperature for
annealed, commercially pure, and solution-
hardened aluminum and a precipitation-
hardened alloy. Open symbols are yield
strengths; closed symbols are ultimate tensile
strengths (in Read 1983).
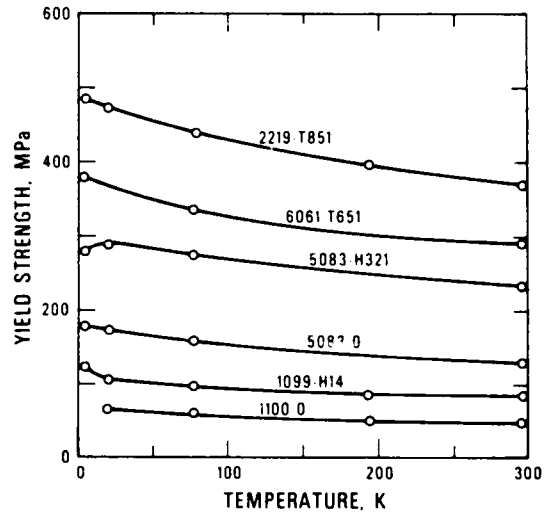
Figure A2. Yield strength of six aluminum
alloys at temperatures between 4 and 300 K
(Kaufman et al. 1968) (in McHenry 1983).
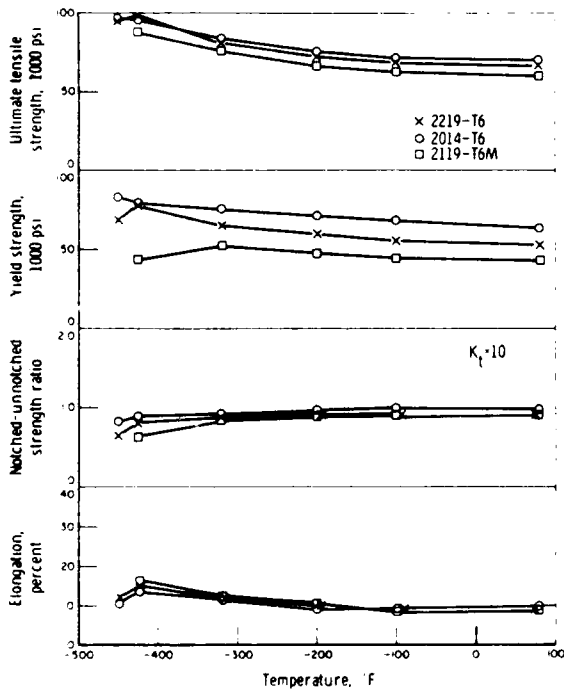
Figure A3. Tensile properties of 2000-series
aluminum alloys in the T6 condition (Martin
et al. 1968).
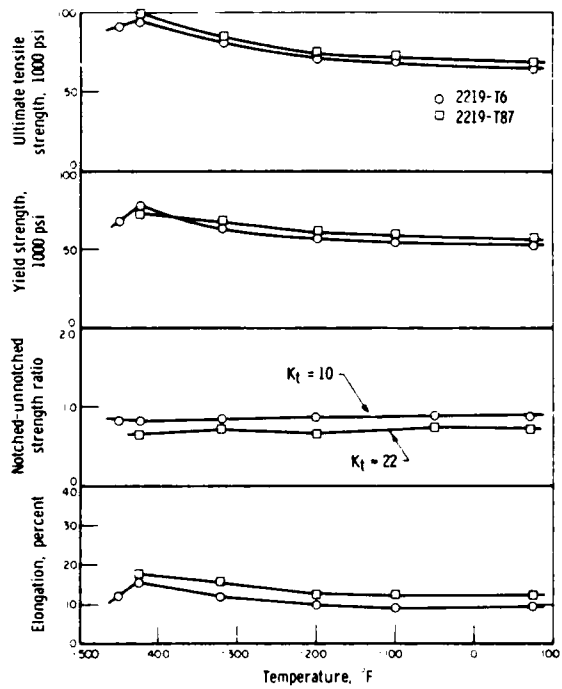
Figure A4. Effect of heat treatment on 2219
aluminum alloy (Martin et al. 1968).
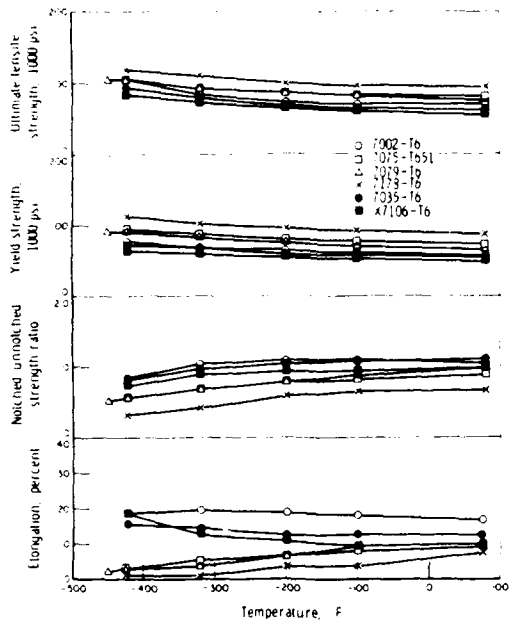
Figure A5. Tensile properties of 7000-series aluminum alloys in the T6 condition (Martin et al. 1968).
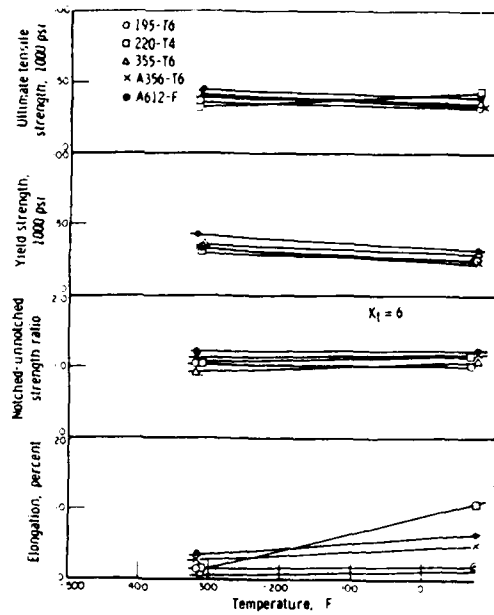
Figure A6. Tensile properties of aluminum casting alloys (Martin et al. 1968).
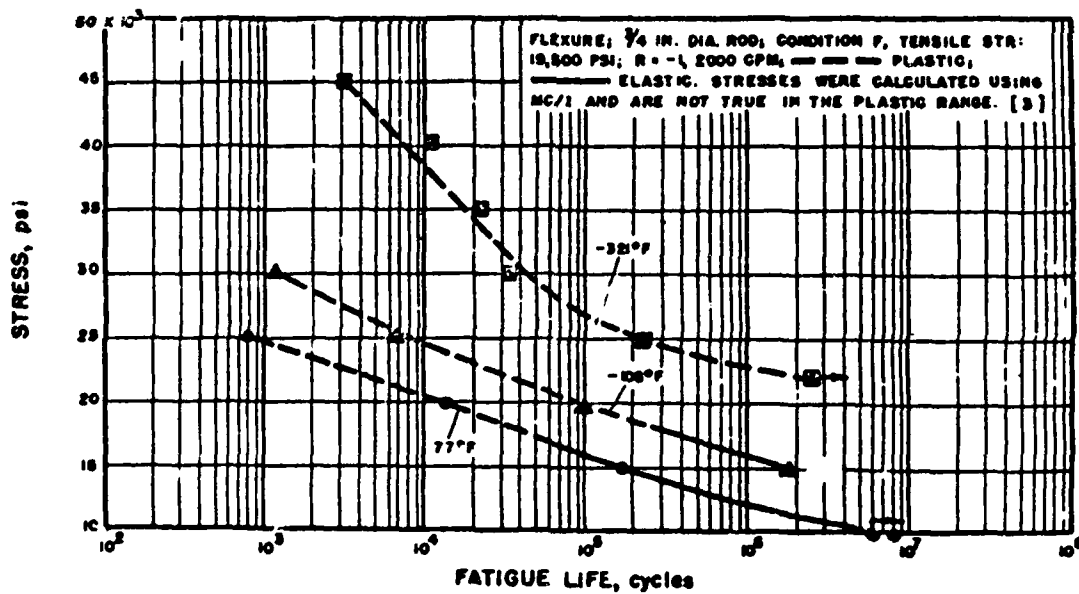
Figure A7. Fatigue behavior of 1100 aluminum (Favor et al. 1961).
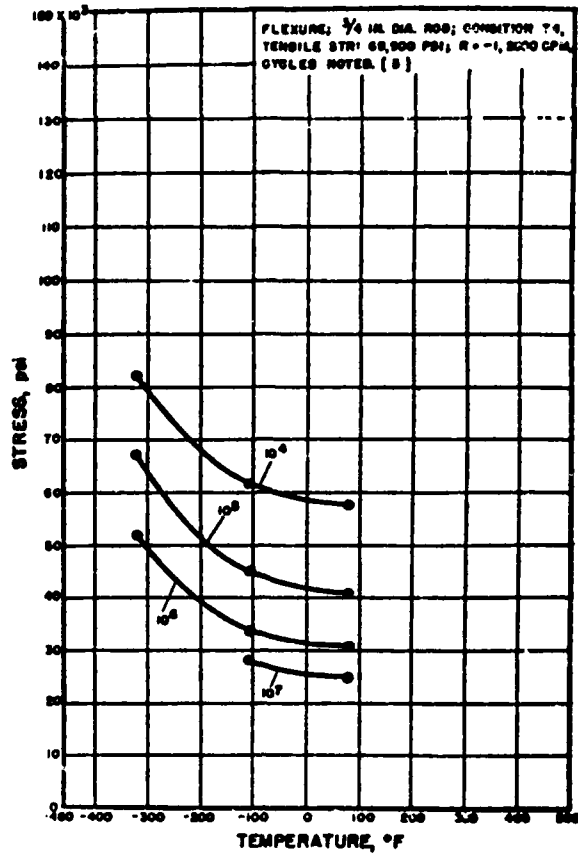
Figure A8. Fatigue strength of 2024 aluminum (Favor et al. 1961)
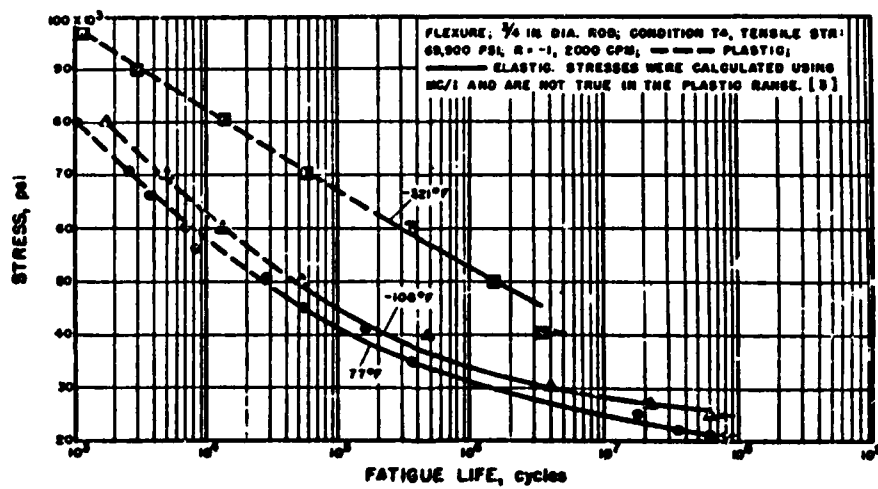
Figure A9. Fatigue failure of 2024 aluminum (Favor et al. 1961)
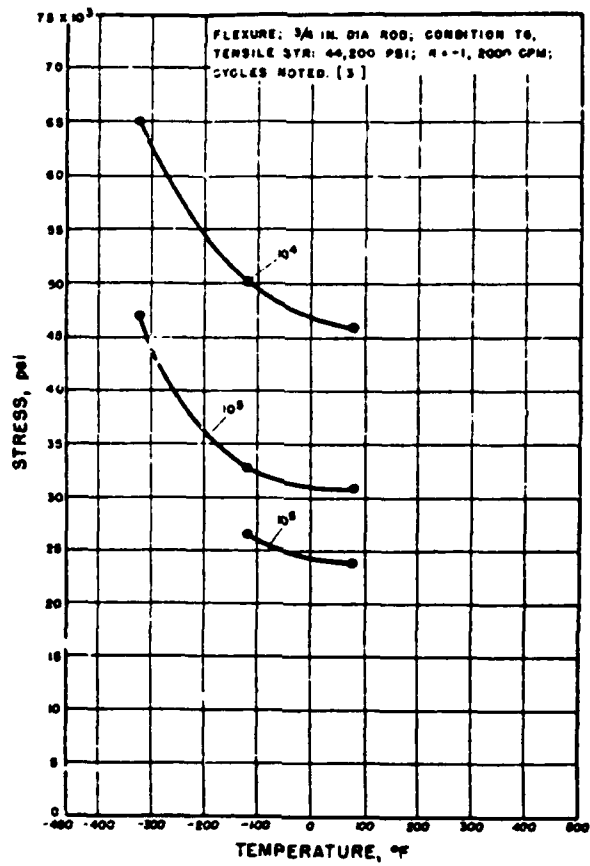
*Figure A10. Fatigue strength of 6061 aluminum
(Favor et al. 1961).*
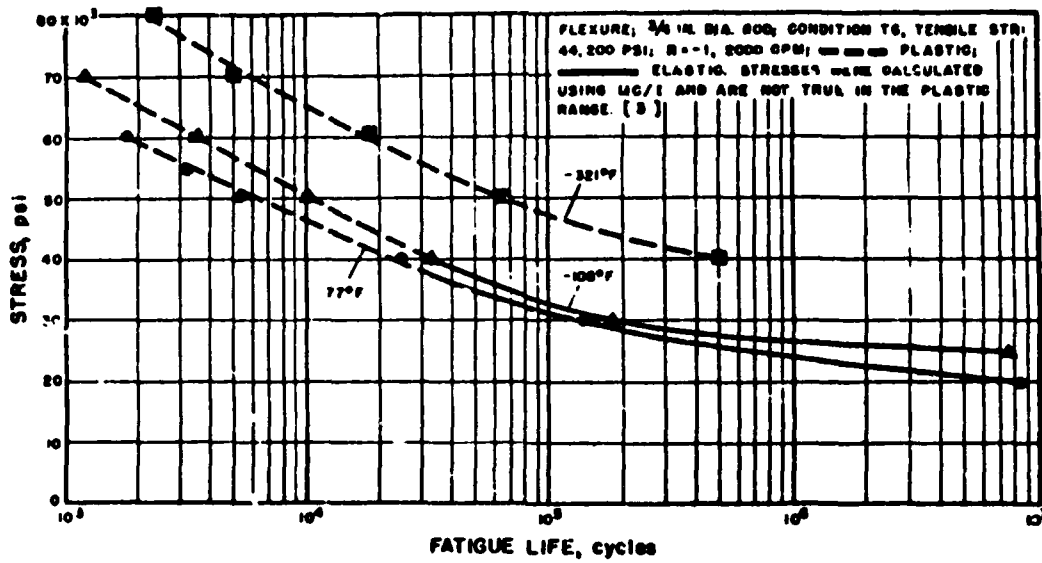
Figure A11. Fatigue behavior of 6061 aluminum (Favor et al. 1961)

34
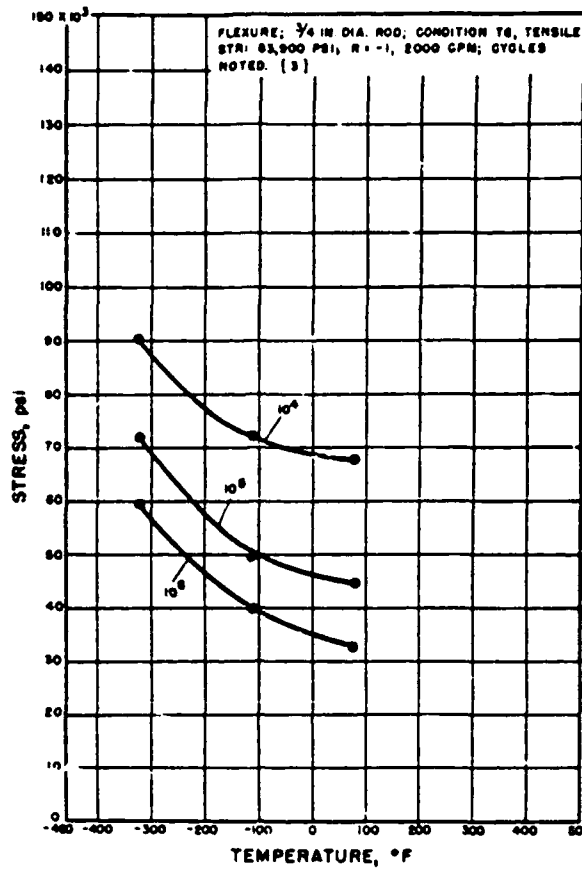
Figure A12 Fatigue strength of 7075 aluminum (Favor et al. 1961).
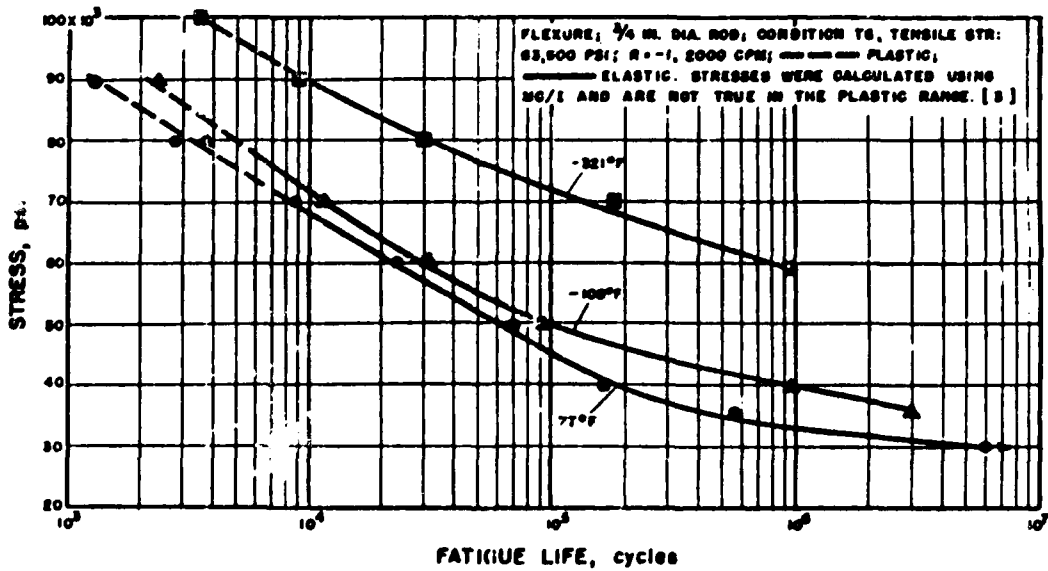
Figure A13. Fatigue behavior of 7075 aluminum (Favor et al. 1961)
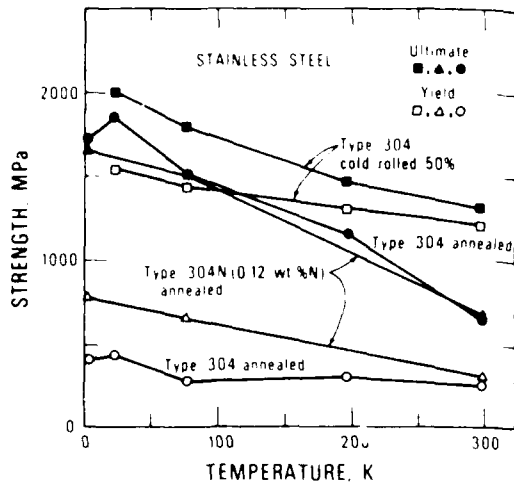
Figure A14. Yield and ultimate tensile strengths as a function of temperature for zone-purified iron, 9-nickel steel, and carbon steel. Open symbols indicate yield strengths; closed symbols indicate ultimate strengths (in Read 1983).
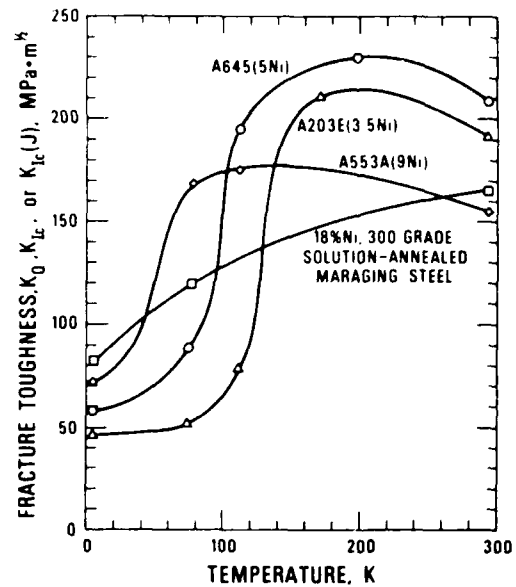
Figure A15. Temperature dependence of fracture toughness for various nonaustenitic steels, showing the beneficial effects of increased nickel content on transition temperature and subtransition range toughness (in Tobler and McHenry 1983).
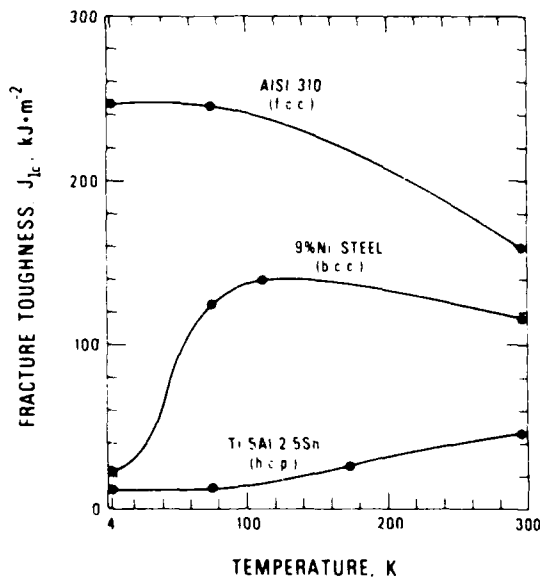
Figure A16. Temperature dependence of fracture toughness for alloys, illustrating characteristic behavior for three different crystal structures (in Tobler and McHenry 1983).
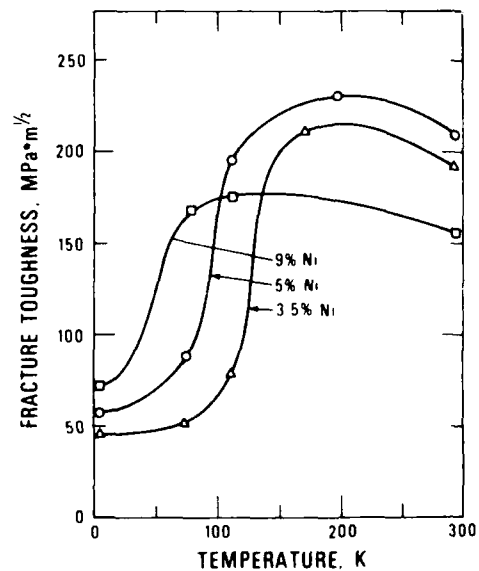
Figure A17. Fracture toughness of 3.5, 5, and 9% N steels at temperatures between 4 and 300 K (Tobler et al. 1976) (in McHenry 1983).

36

ROTATING BEAM; ¾ IN. PLATE; NORMALIZED,
TENSILE STR: 118,500 PSI; R = -1, 1750 RPM;
ROOM TEMP. [13]

UNNOTCHED

V-NOTCH; K = 2.9

STRESS, psi

FATIGUE LIFE, cycles
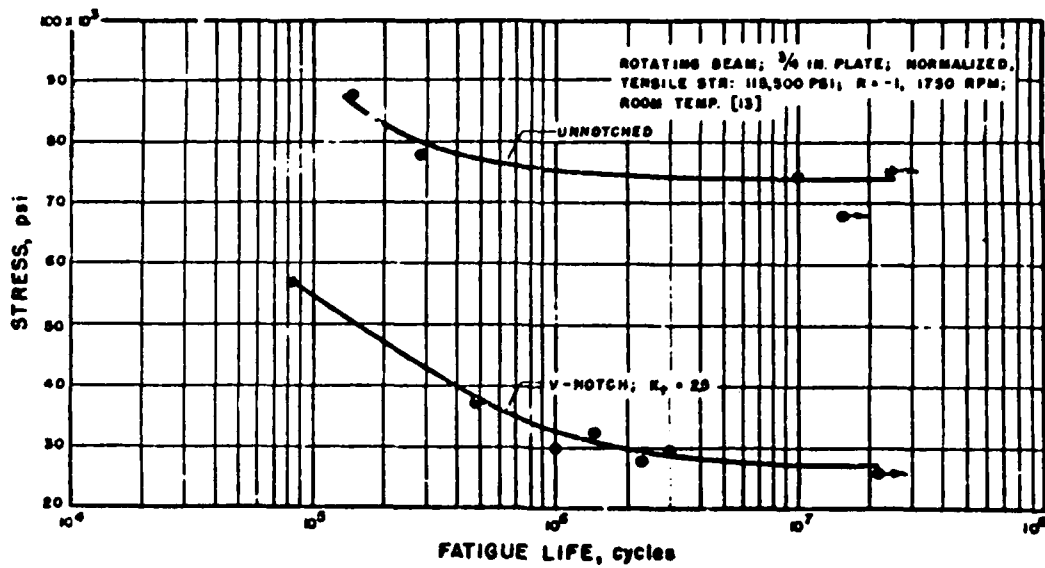
Figure A18. Fatigue behavior of 2800 steel (Favor et al. 1961).

FLEXURE; ¼ IN. DIA. BAR; 1650°F 1 HR. AIR COOL,
1450°F 1 HR. AIR COOL, 1050°F 2 HRS. AIR COOL,
TENSILE STR: 117,500 PSI; R = -1, 2000 CPM;
— — — PLASTIC; ———— ELASTIC
STRESSES WERE CALCULATED USING MC/I AND ARE
NOT TRUE IN THE PLASTIC RANGE. [3]

-321°F

-109°F

77°F

STRESS, psi

FATIGUE LIFE, cycles
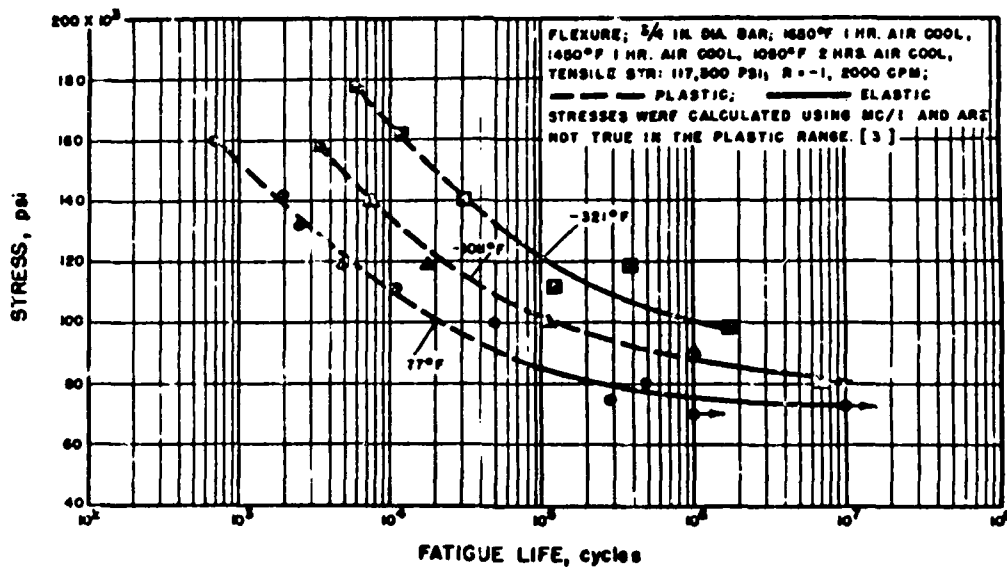
Figure 19. Fatigue behavior of 2800 steel (Favor et al. 1961).

37
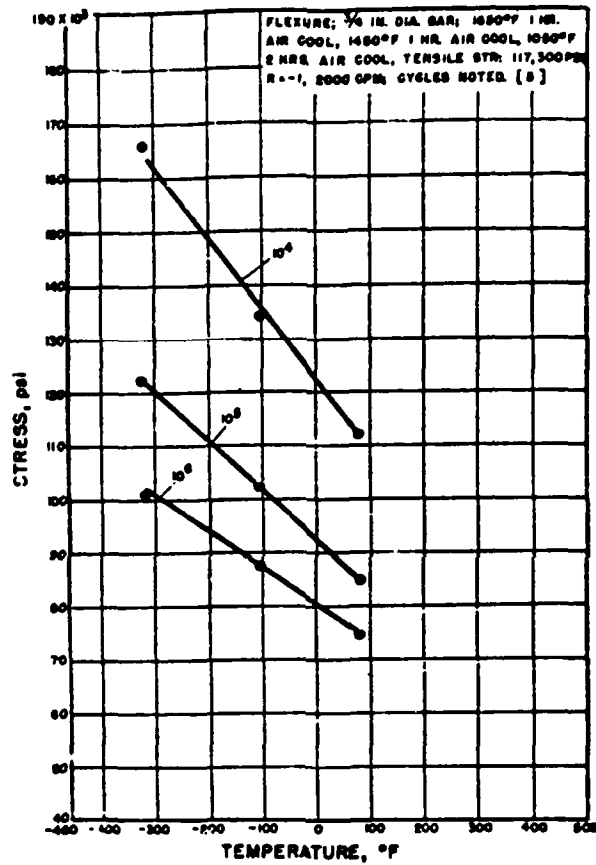
Figure A20. Fatigue strength of 2800 steel (Favor et al. 1961).

38
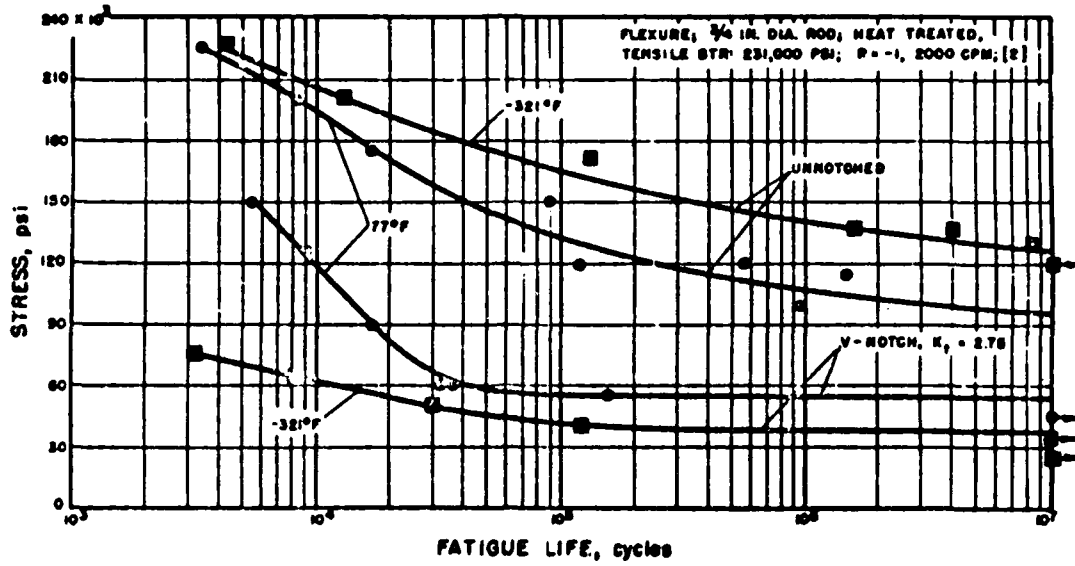
Figure A21. Fatigue behavior of 4340 steel.
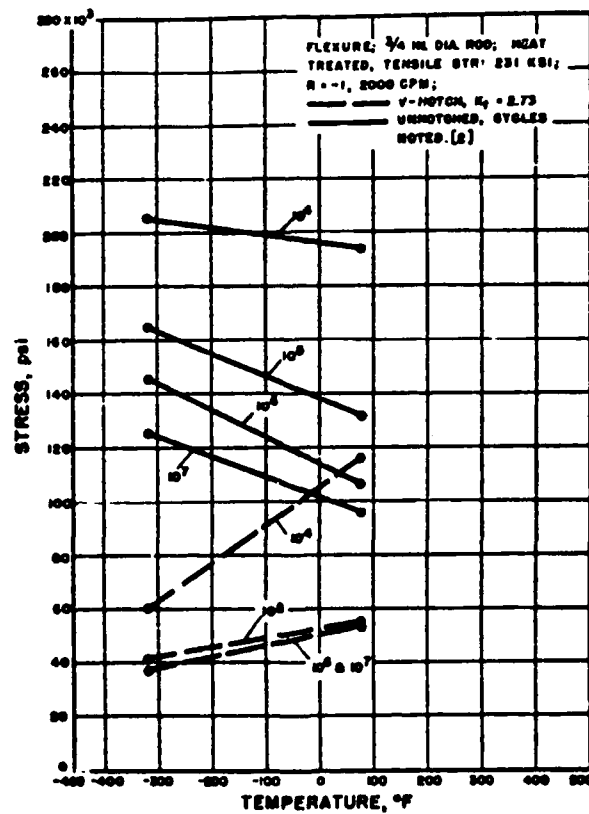
Figure A22. Fatigue strength of 4340 steel (Favor et al. 1961).

39
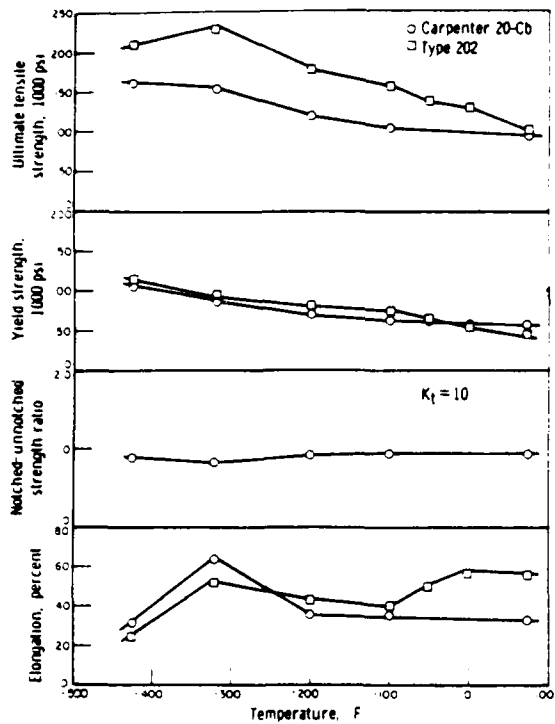
Figure A23. Tensile properties of austenitic stainless steels (Martin et al. 1968).
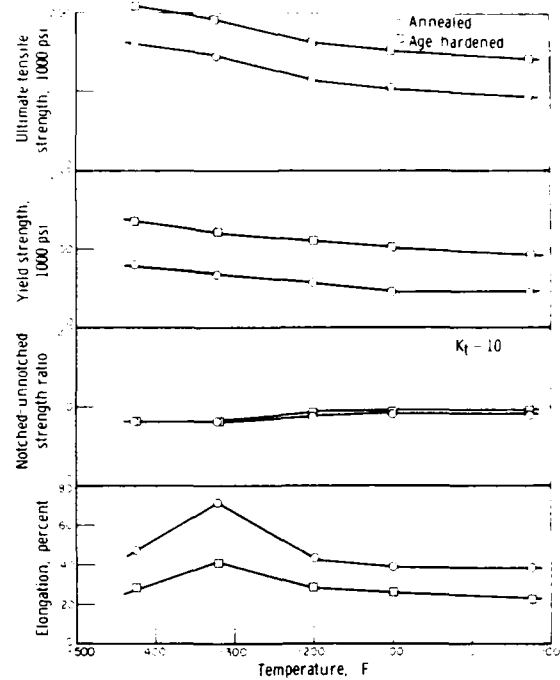
Figure A24. Tensile properties of A286 alloy steel (Martin et al. 1968).
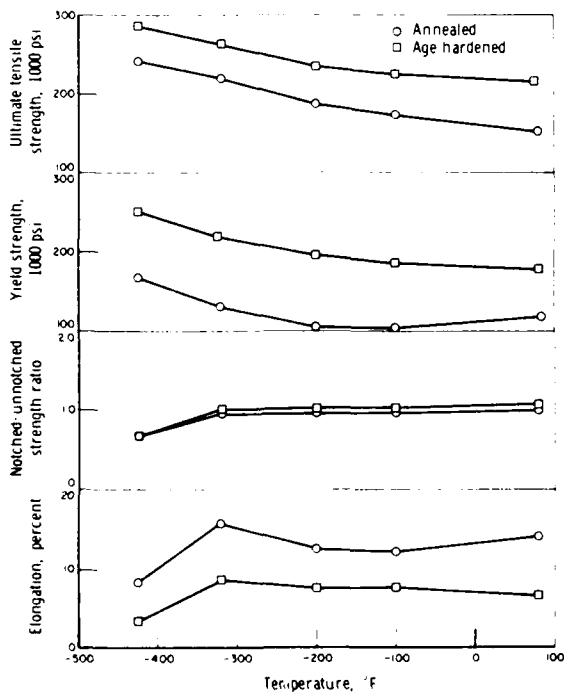
Figure A25. Tensile properties of HP 9-4-25 steel (Martin et al. 1968).
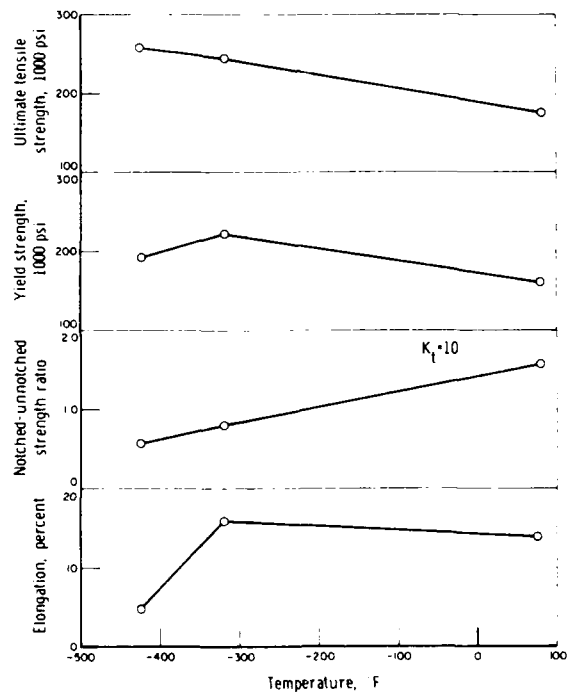
Figure A26. Tensile properties of AM 355 steel (Martin et al. 1968).

40
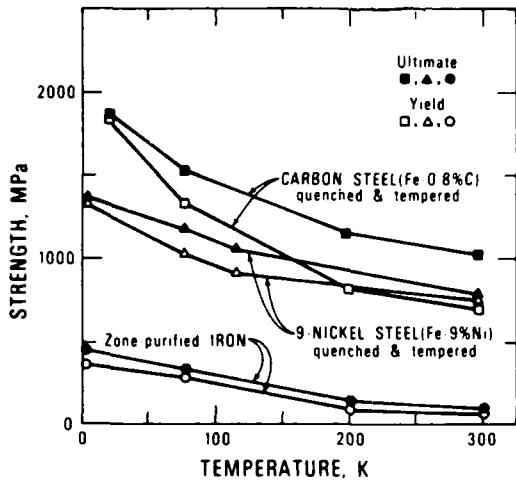
Figure A27. Yield and ultimate tensile strengths as a function of temperature for annealed, nitrogen-strengthened, and cold-drawn stainless steel 304. Open symbols–yield stengths; closed symbols–ultimate tensile strengths (in Read 1983).

Figure A28. Tensile and yield strengths of three austenitic strainless steels (AISI types 304, 310 and 316) at temperatures between 4K and 300K (in McHenry, 1983).

Figure A29. Fatigue test results for stainless steels 304L and 304LN at 300, 78 and 4K (in Read 1983).
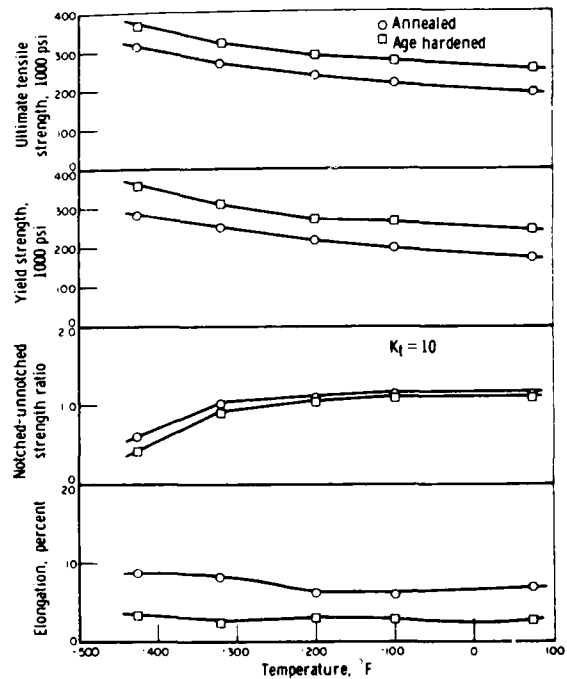
Figure A30. Tensile properties of 18Ni-8Co-5Mo maraging steel (Martin et al 1968).

41
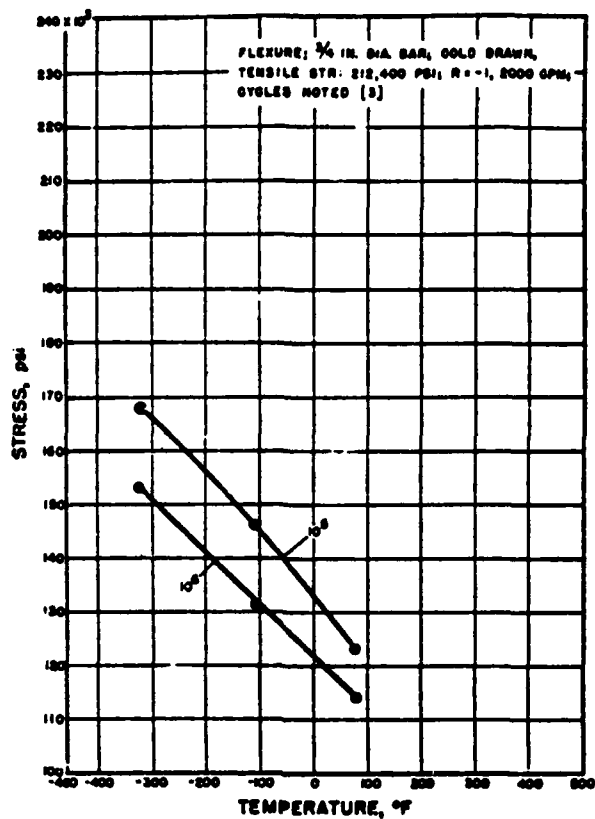
Figure A31. Fatigue strength of AISI 304 stainless steel (Favor et al. 1961).
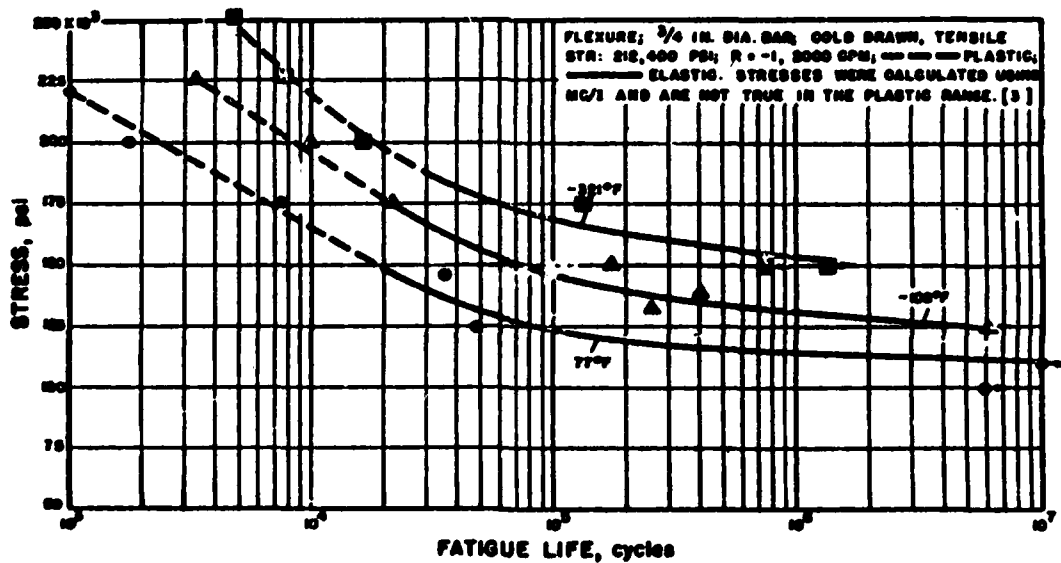
Figure A32. Fatigue behavior of AISI 304 stainless steel (Favor et al. 1961)
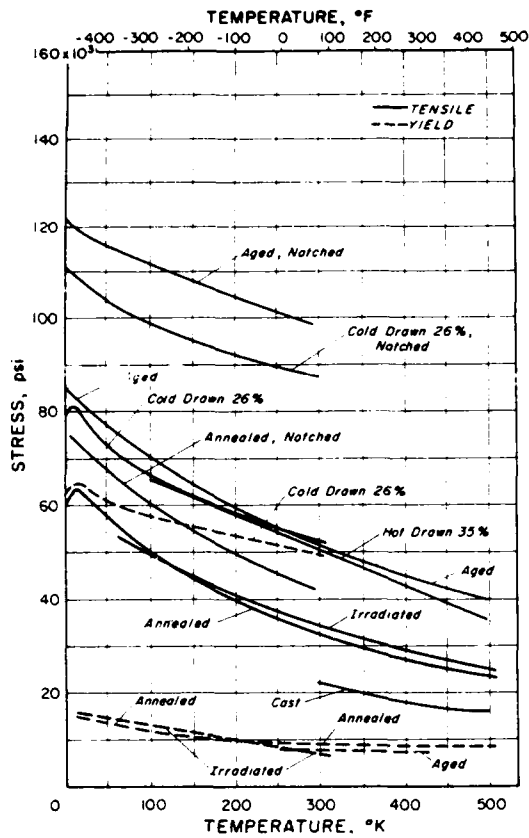
Figure A33. Strength of copper (Reed and Mikesell 1967).
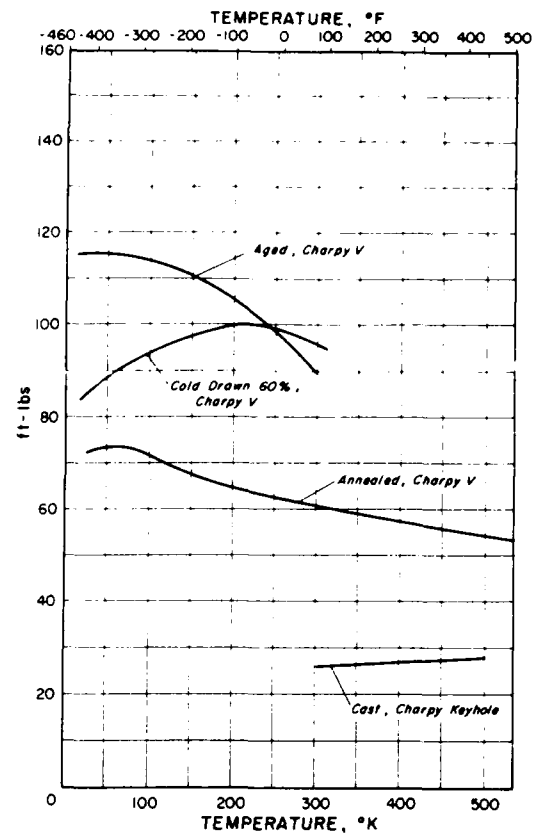
Figure A34. Impact energy of copper (Reed and Mikesell 1967).
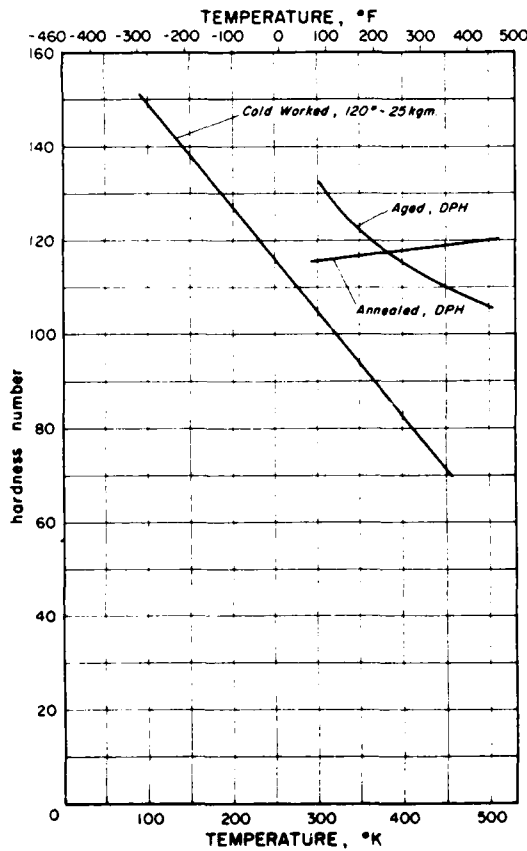
Figure A35. Hardness of copper (Reed and Mikesell 1967).

43
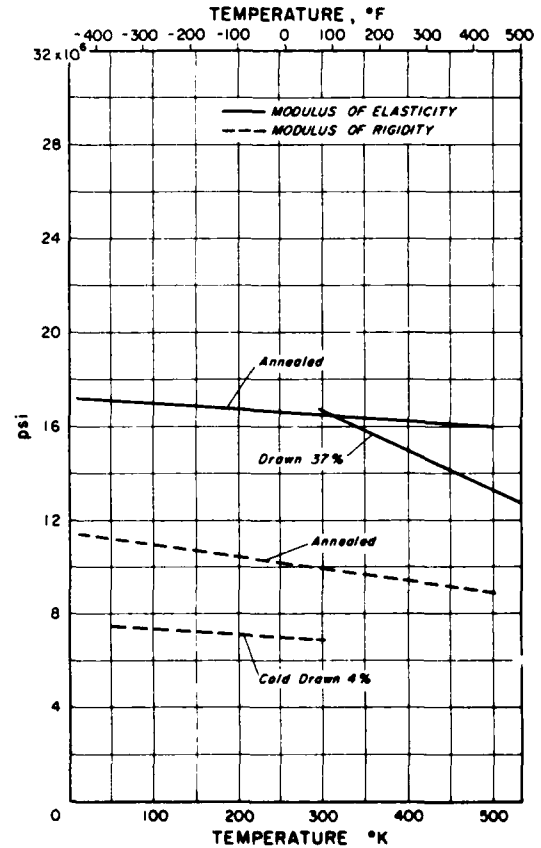
Figure A36. Modulus of copper (Reed and Mikesell 1967).
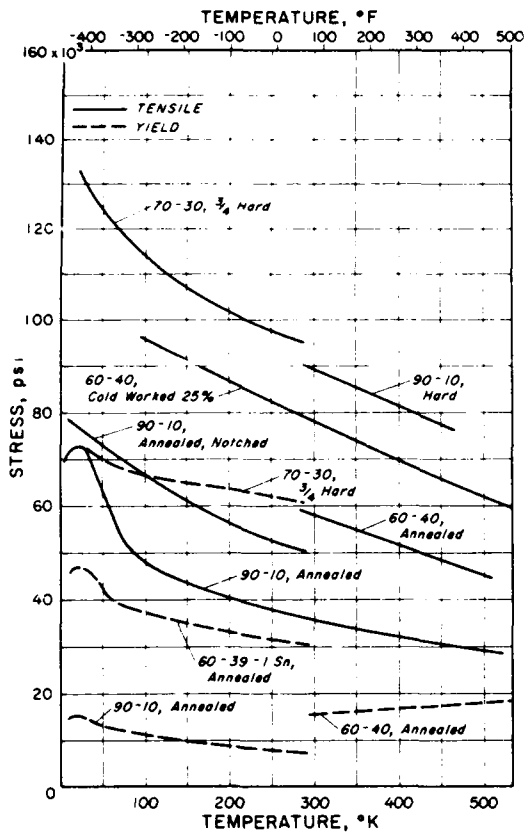
Figure A37. Strength of Cu-Zn (brass) (Read and Mikesell 1967).
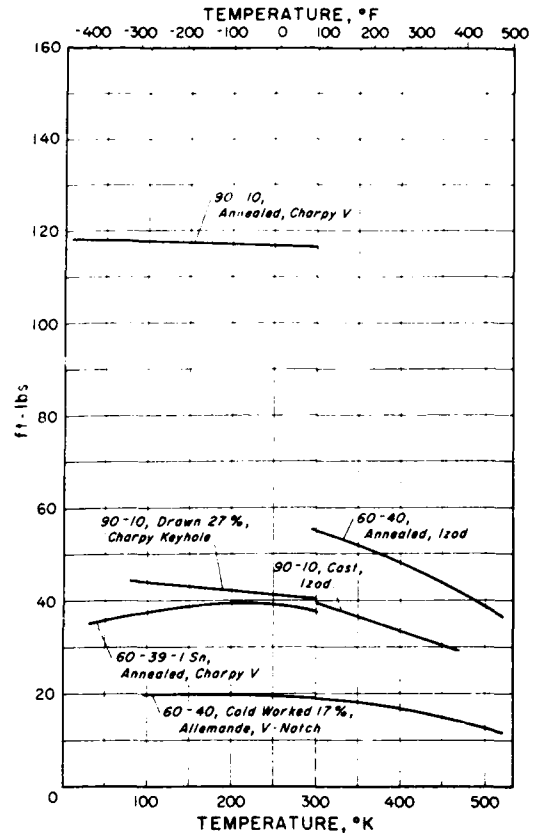
Figure A38. Impact energy of Cu-Zn (brass) (Reed and Mikesell 1967).
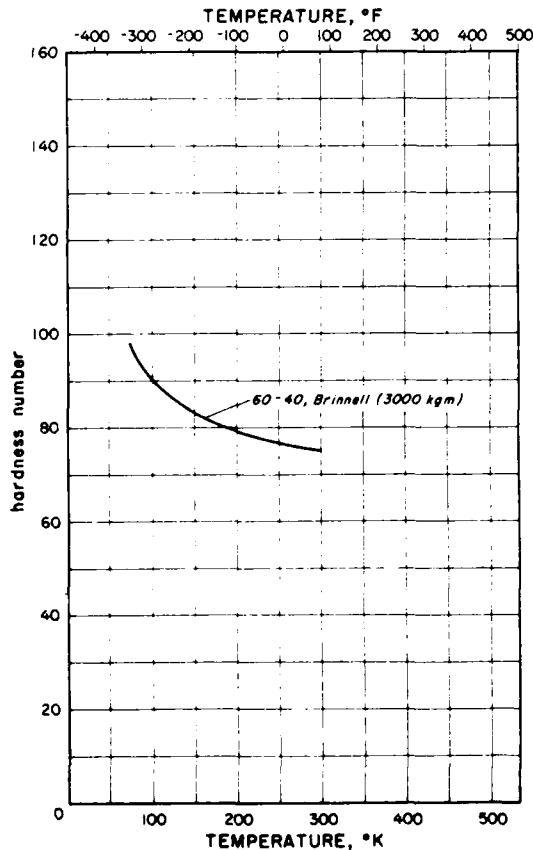
Figure A39. Hardness of Cu-Z (brass) (Reed and Mikesell 1967).
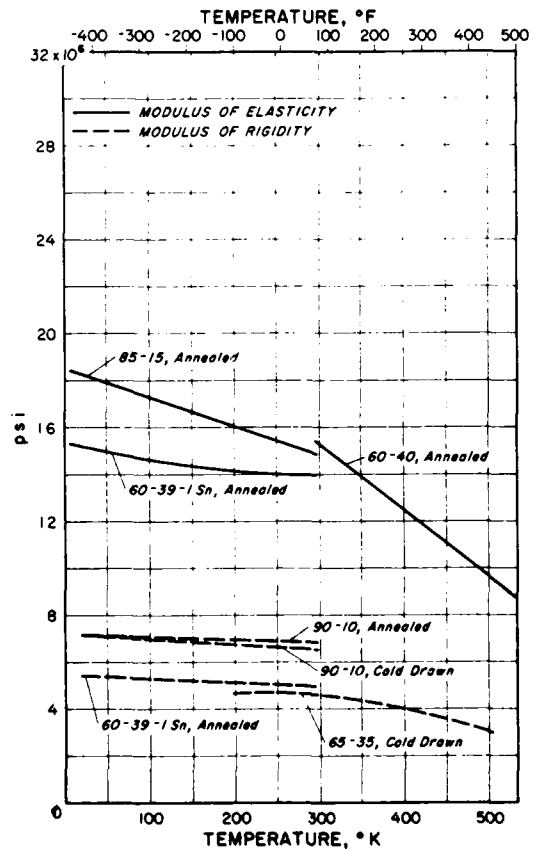
Figure A40. Modulus of Cu-Zn (brass) (Reed and Mikesell 1967).

44

APPENDIX B: LOW TEMPERATURE BEHAVIOR
OF SOME SELECTED POLYMERS
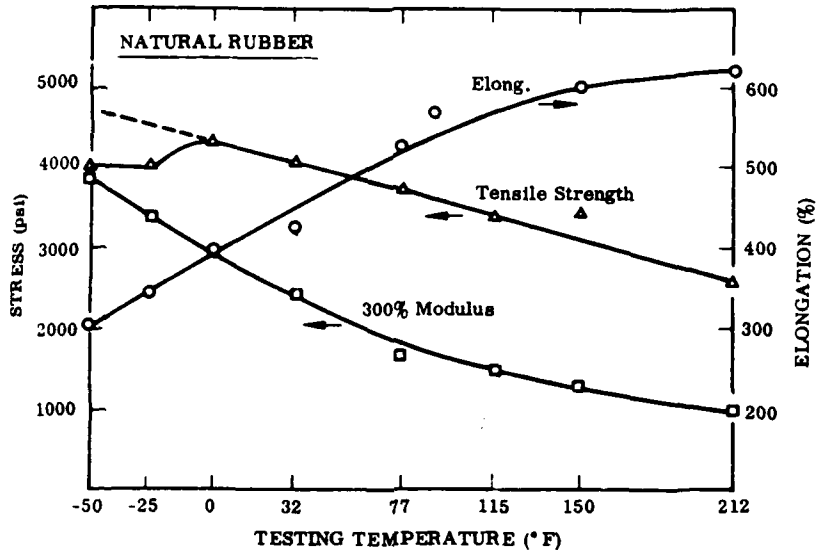
*Figure B1. Effect of testing temperature on stress-strain properties
for natural rubber (Rittenhouse 1968).*
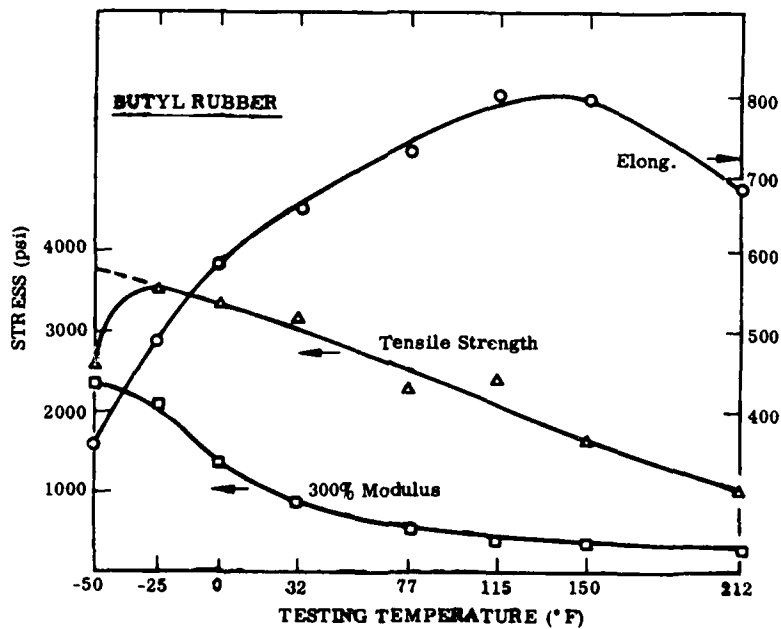
*Figure B2. Effect of testing temperature on stress-strain proper-
ties for butyl rubber (Rittenhouse and Singletary 1968).*
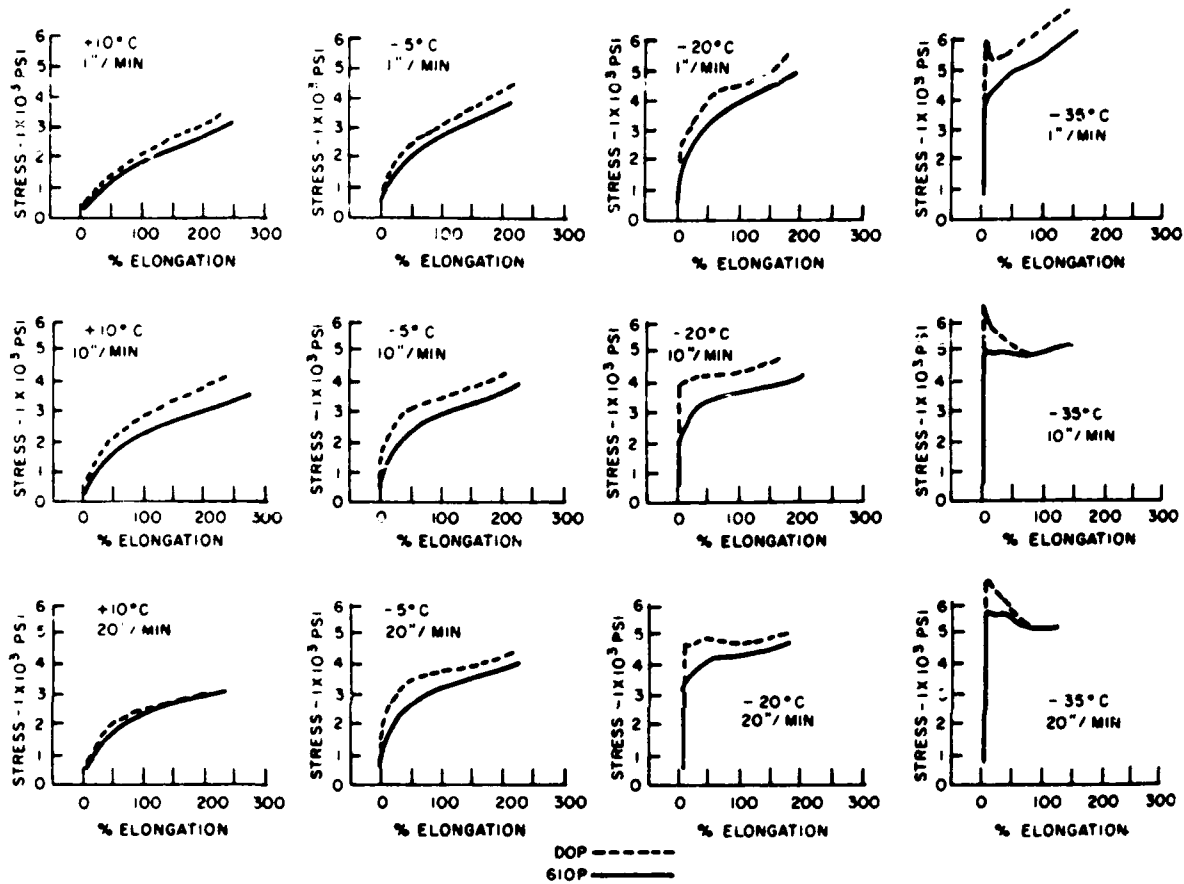
Figure B3. Stress-strain curves of plasticized PVC resin (Titus 1967).

- *Lowering temperature and increasing rate of loading have the same effect. The curve at –5°C and at a loading rate of 20 in./min. is the same as that of –20°C at a loading rate of 1 in./min. Therefore, a 20-fold increase in loading rate is equivalent to a 15°C reduction in temperature on the tensile properties of this material.*

- *Decreasing temperature and increasing the rate of loading changes the curves from soft to weak, to soft and tough, to hard and tough, to hard and strong, to hard and brittle.*

46
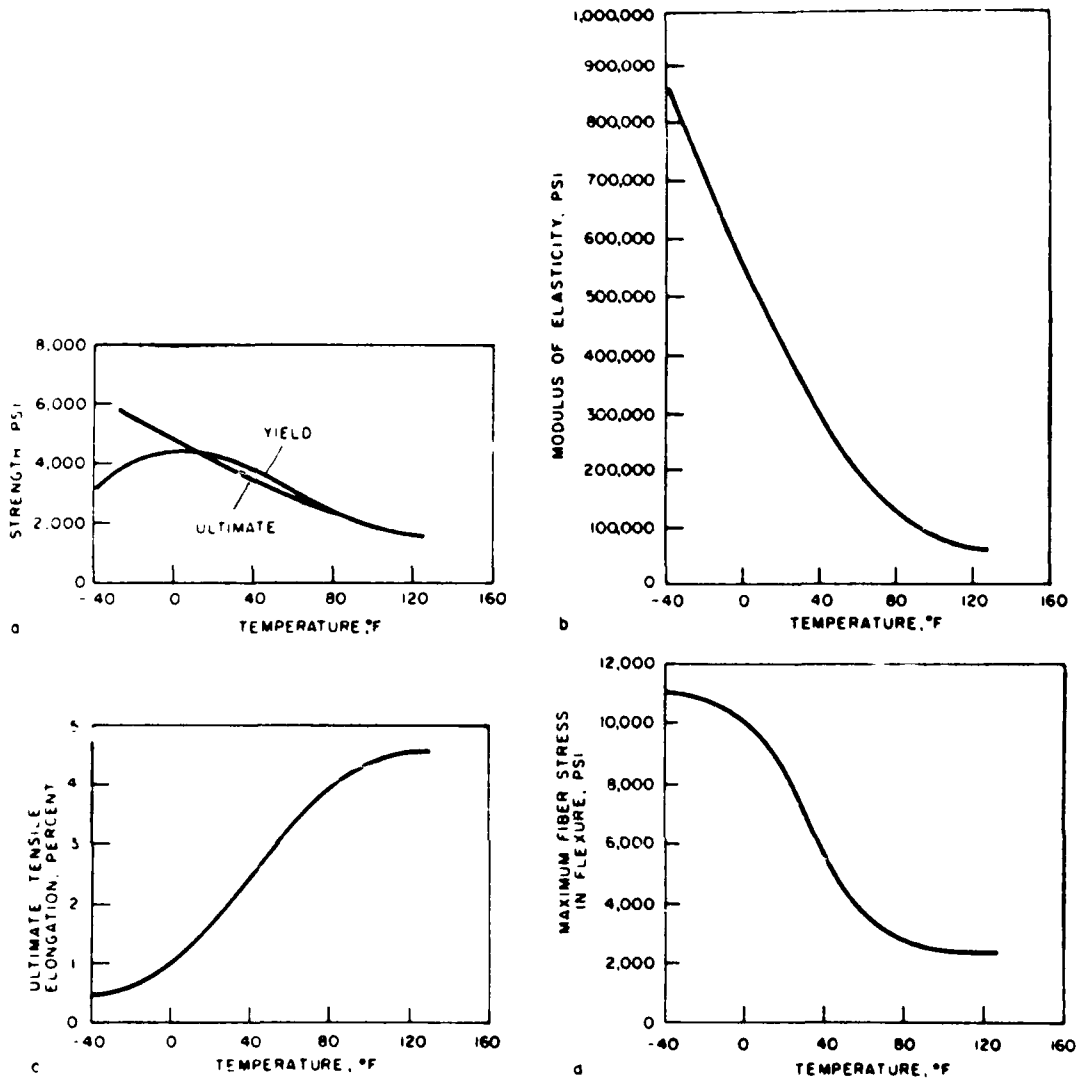
Figure B4. Tensile and flexural properties of vinyl chloride (Saran 909) (Titus 1967).

47
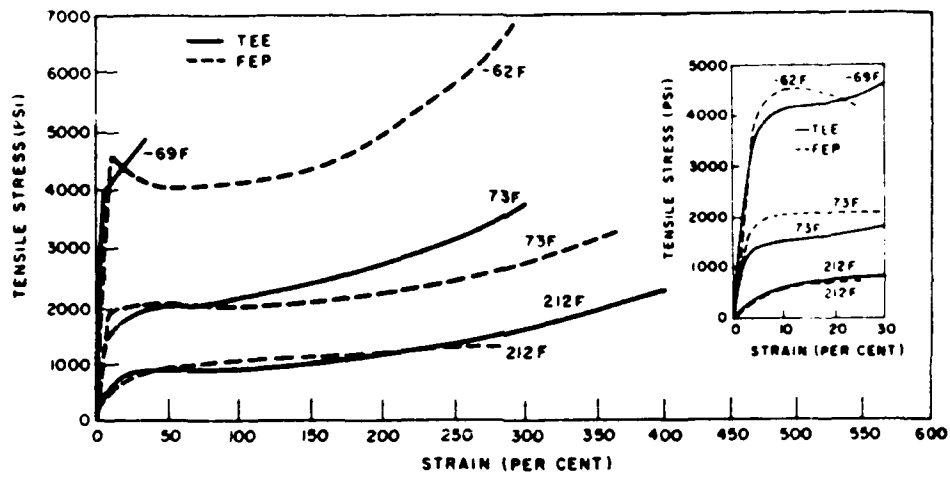
Figure B5. Tensile stress vs strain (to fracture) of TEE and FEP (Titus 1967).
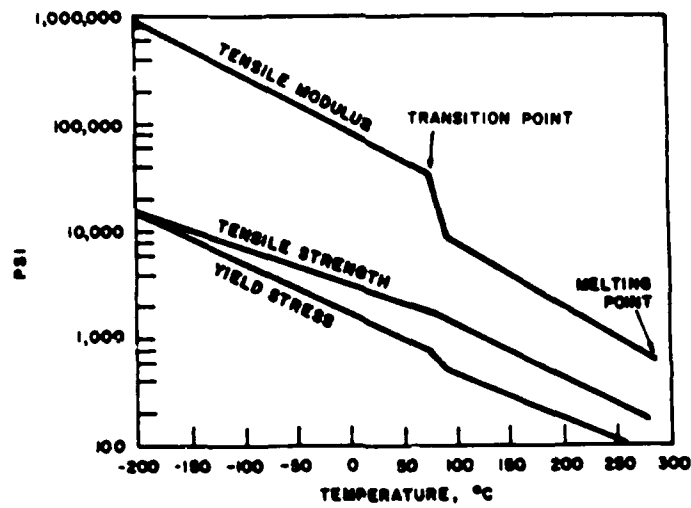
Figure B6. Tensile properties vs temperature of Teflon FEP film (Titus 1967).

48

Table B1. Effect of crystallinity on Teflon TFE fluorocarbon resins (Titus 1967).

Property	°F	Crystallinity, %						
		50	55	60	65	70	75	80
Tensile Yield Strength, Kpsi[1]	212	1.20	1.14	1.08	1.04	0.98	0.92	0.83
	73	1.90	1.80	1.60	1.40	1.30	1.20	1.00
	-40	3.80	3.20	2.80	2.40	2.30	2.10	1.60
Elongation, %[1]	212	—	44	39	33	25	—	—
	72	58	50	40	32	25	14	6
	-40	40	35	30	25	20	10	8
Flexural Modulus[2] Elasticity, Kpsi	212	26	33	41	49	57	64	72
	73	45	67	88	110	132	154	176
	-88	210	240	270	310	340	370	400

(1) ASTM D638-52T modified for test specimens 3/16" x 1/16" x 7/8" for low-and high-temperature tests. Crosshead speeds of 0.02 in./min. (Baldwin) for low temperatures and 0.05 in./min. (Instron) for high temperatures.

(2) ASTM D790

49

Table B2. Mechanical properties of FE 2421.

	Temperature (°F)			
	73	0	-20	-40
Tensile Strength (p.s.i.)	8,320	14,820	16,570	17,990
Yield Strength (p.s.i.)	8,320	14,820	16,570	17,990
Elongation (%)	250	23	15	14
Flexural Modulus (p.s.i.)	66,500	336,000	426,000	463,000

Moisture: 0.19-0.23%
[1]Data obtained in accordance with ASTM D 759.
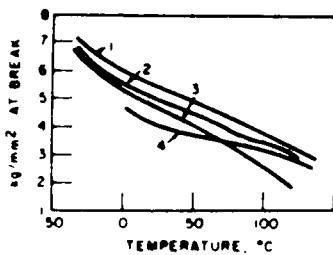
*Figure B7. Maximum
tensile strength of nylon
11 (Titus 1967).*
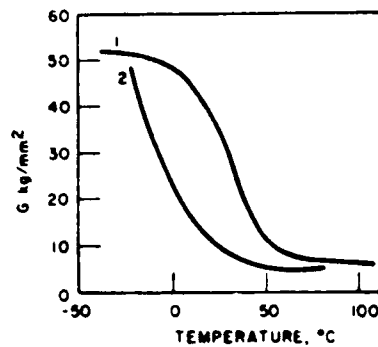
*Figure B8. Variation of modulus
of rigidity in torsion (G) for two
typical grades of nylon 11.*
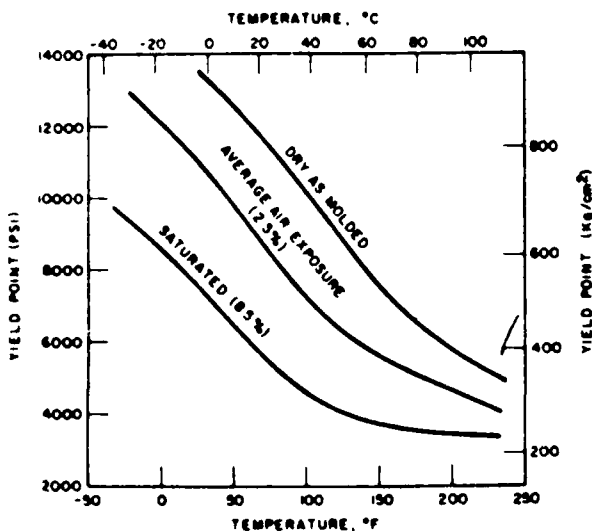
*Figure B9. Yield point of nylon 6/6 (Zytel 101) vs
temperature and moisture content (Titus 1967).*
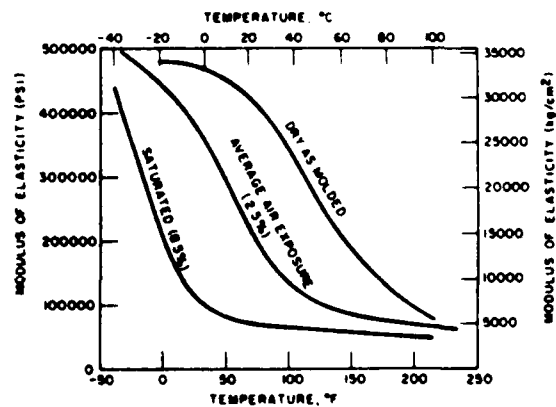
*Figure B10. Modulus of elasticity of ny-
lon 6/6 (Zytel 101) vs temperature at
various moisture contents (Titus
1967).*

50

Table B3. Tensile impact of Zytel nylon resins (Titus 1967).

Property	ZYTEL				
	$101^{(1)}$	$101^{(1)}$ WT07	$31^{(2)}$	$37^{(2)}$	$42^{(1)}$
Tensile impact, ft lb sq in.					
Dry: at 73^0 F	82	74	79	103	155
at 0^0 F	93	80	73	90	105
at -40^0 F	85	88	68	94	107
Conditioned to 50% RH:					
at 73^0 F	156	164	121	135	300
at 0^0 F	113	90	73	96	118
at -40^0 F	79	71	86	88	110

(1) Nylon 66

(2) Nylon 610
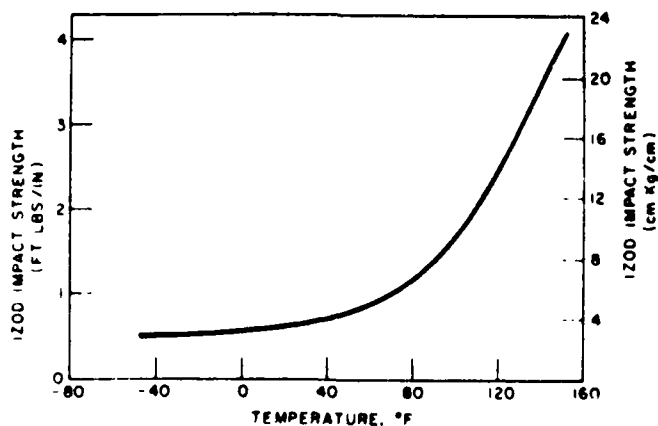
Figure B11. Effect of temperature of nylon 6/6 (Zytel 101) on Izod impact strength at 0.3 percent moisture content (Titus 1967).
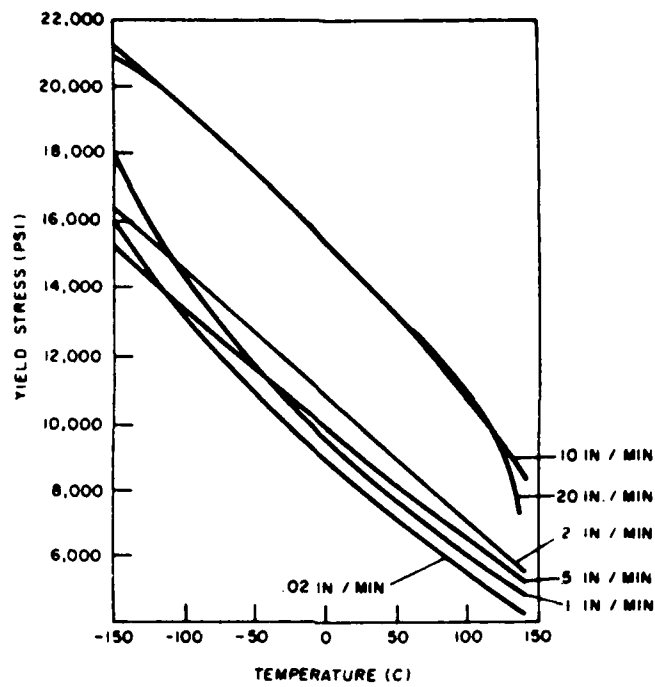
*Figure B12. Yield stress vs temperatures for polysulfone
at various loading rates (Titus 1967).*
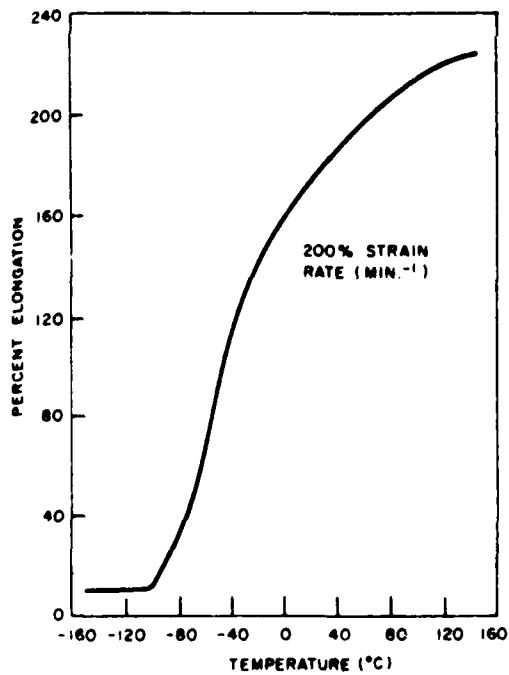
*Figure B13. Percent elongation vs temper-
ature for polysulfone (Titus 1967). The co-
efficient of thermal expansion is 3.1x10⁻⁵ in./in.
—°F over the temperature range -22° to +300°F.*
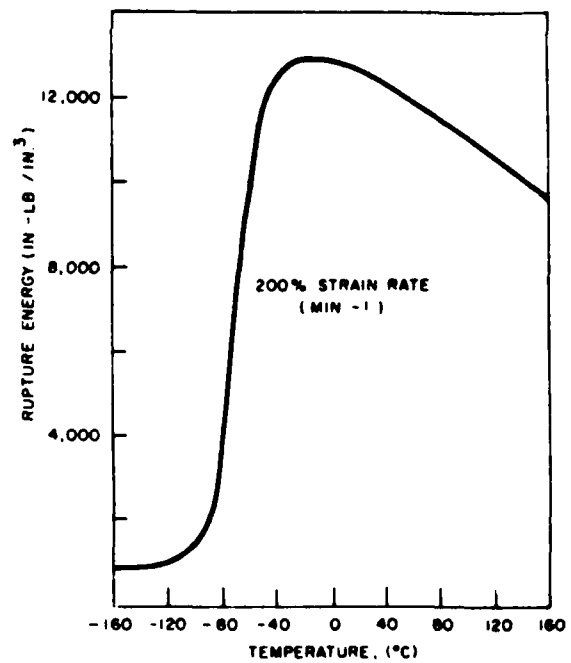
*Figure B14. Rupture energy vs temperature
for polysulfone (Titus 1967).*
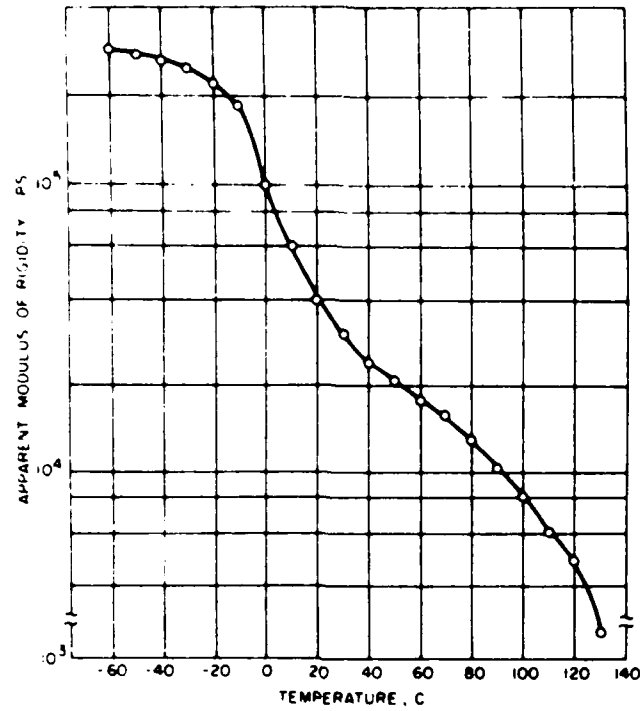
Figure B15. Modulus of rigidity for a typical general polypropylene ASTM D1043 (Titus 1967).
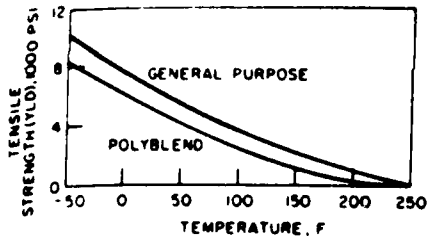
Figure B16. Tensile yield strength of polypropylenes (Titus 1967).
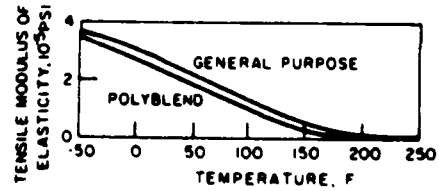
Figure B17. Flexural modulus vs temperature of polypropylenes (Titus 1967).
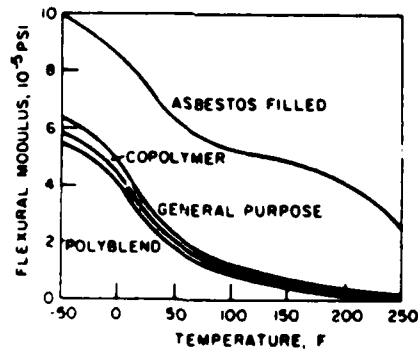
Figure B18. Flexural modulus vs temperature of polypropylenes (Titus 1967).

53
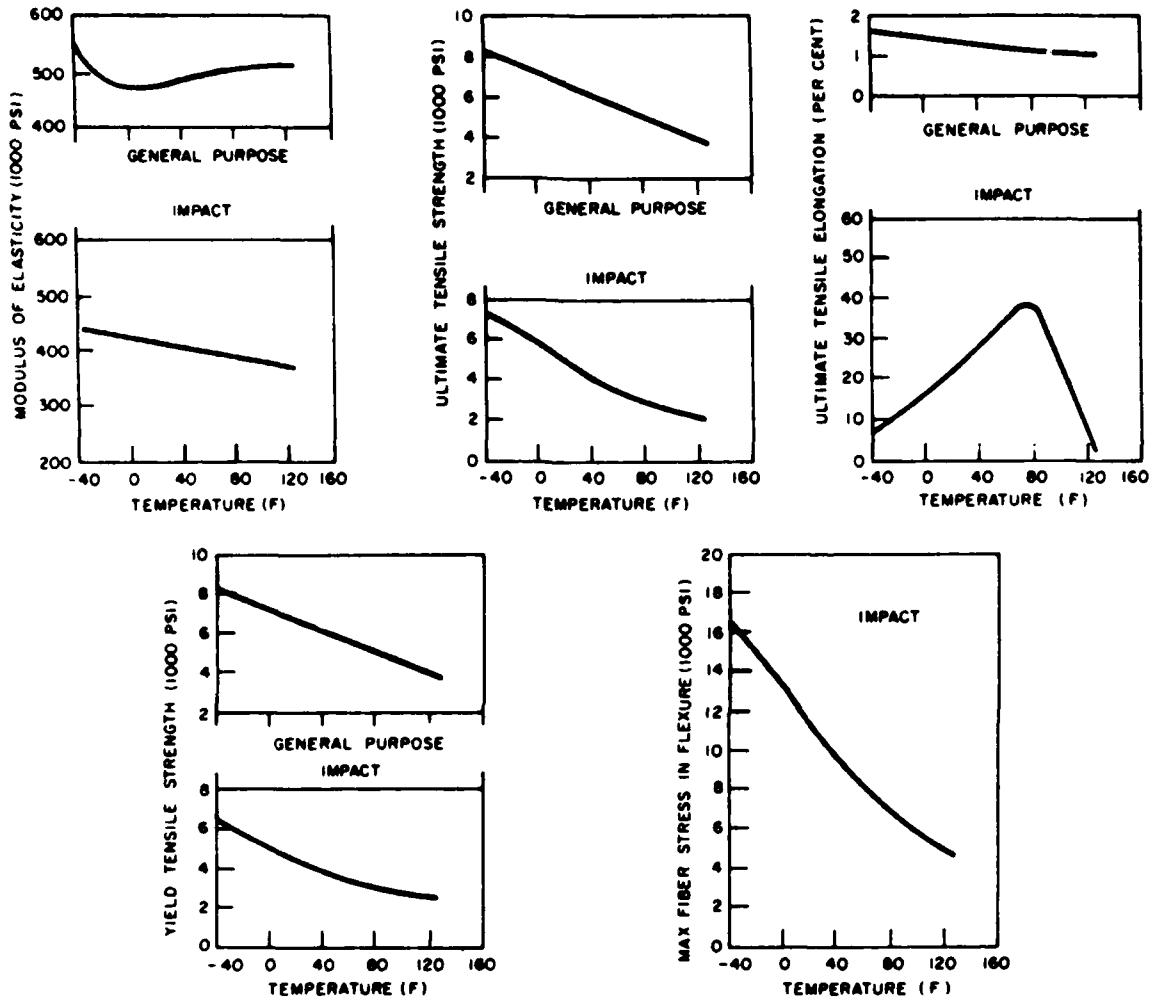
Figure B19. Temperature vs mechanical properties for typical general-purpose and impact grades of compression-molded polystyrenes (Titus 1967).

54
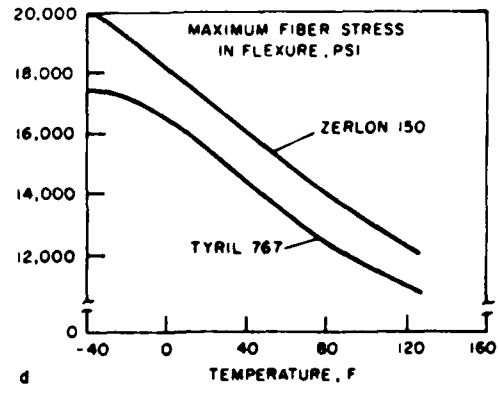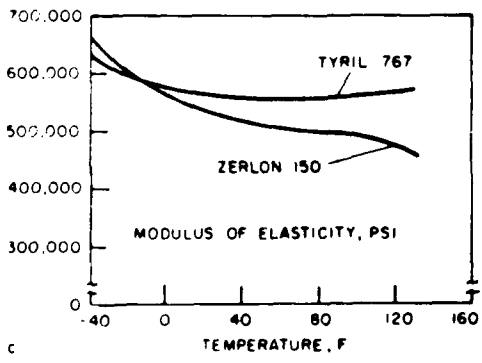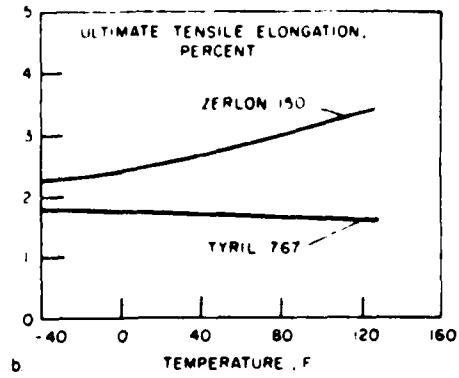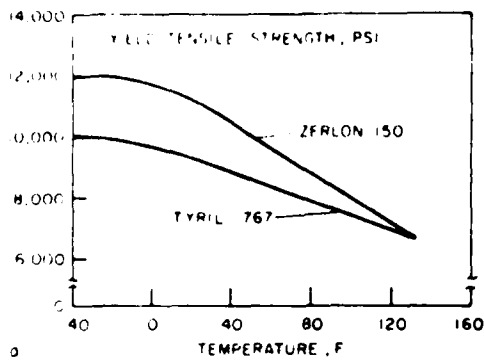
Figure B20. Mechanical properties of polystyrene copolymers as a function of temperature (Titus 1967). Note: Tyril: acrylonitrile–styrene copolymer, Zerlon: methyl methacrylate - styrene copolymer.

55
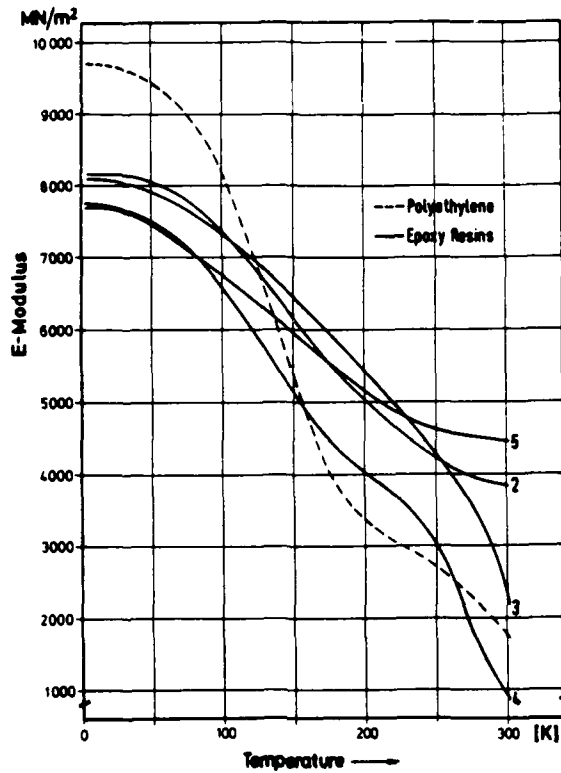
Figure B21. Young's modulus of several epoxy-resins vs temperature (Hardwig 1979).
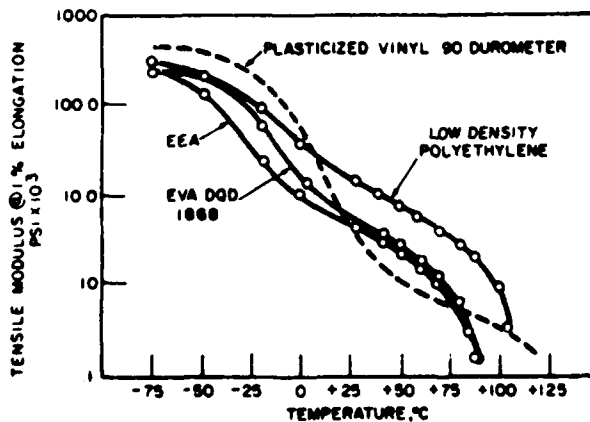
Figure B22. Stiffness modulus vs temperature of polyuethylene, polyethylene copolymers and vinyl (Titus 1967).
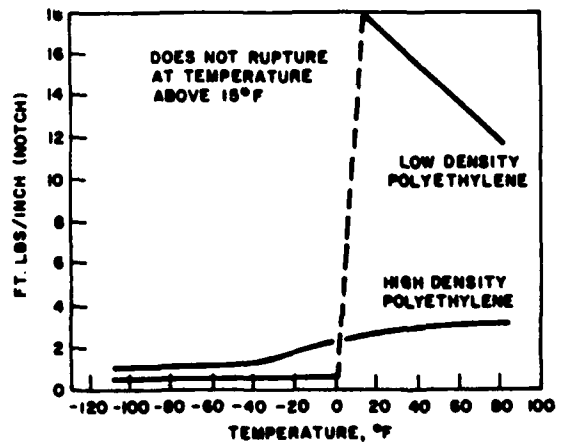
Figure B23. Effect of temperature on Izod impact strengths of (Marlex) polyethylene (Titus 1967).

56
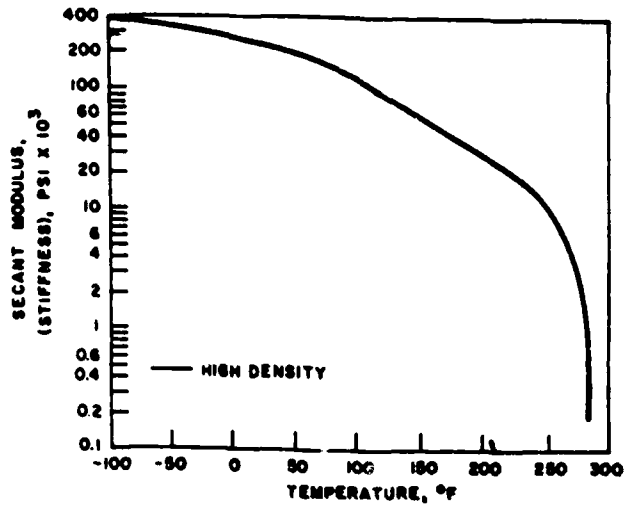
Figure B24. Modulus of polyethylene as a function of temperature (Titus 1967).
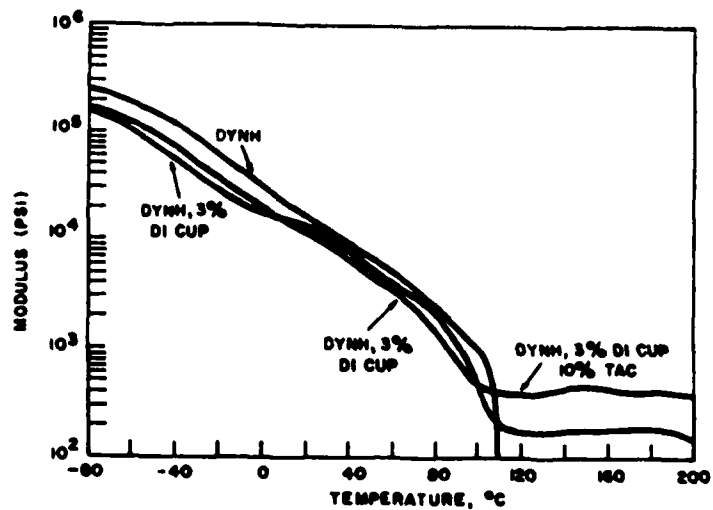
Figure B25. Modulus vs temperature—unfilled cross-linked low density PE (Titus 1967). DYNH–cross-linked 0.919 density polyethylene; DI CUP–dicumyl peroxide; TAC–triallyl cyanurate.
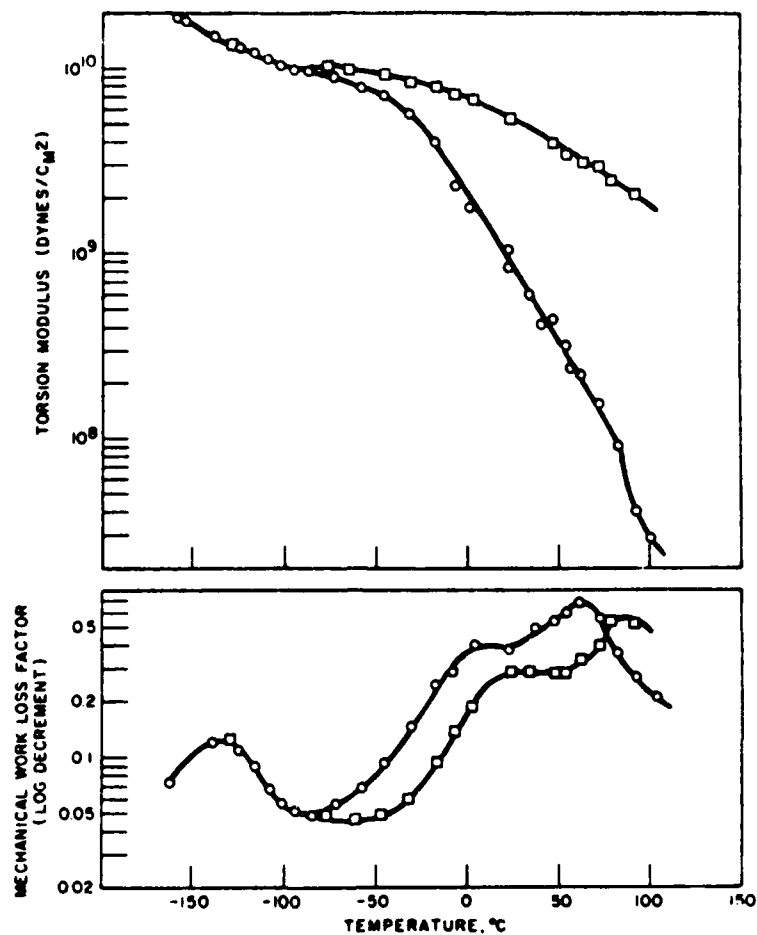
*Figure B26. Dynamic mechanical properties of (Alathon 10)—
(MI = 2.1; density = 0.923; point = 0) free radical polyethylene
and (Alathon 7020) MI = 1.5; density = 0.954; point = □) linear
polyethylene (Titus 1967).*
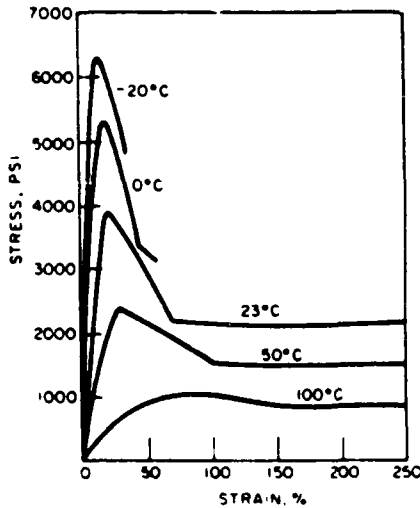
Figure B27. Stress-strain curves at various temperatures for QX-4262.6 high density polyethylene—8% acrylic acid graft copolymer (Titus 1967).
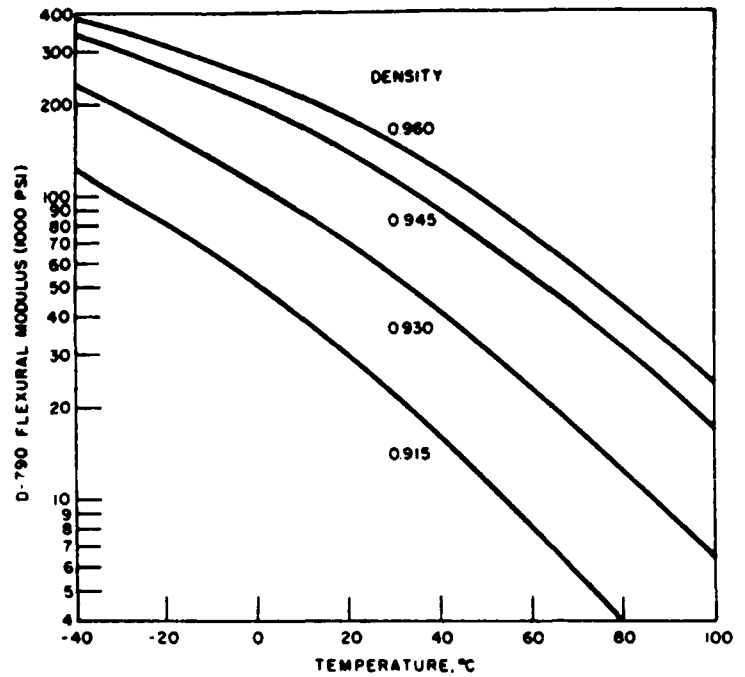
Figure B28. Effect of temperature on D-790 flexural modulus of polyethylenes of various densities (Titus 1967).
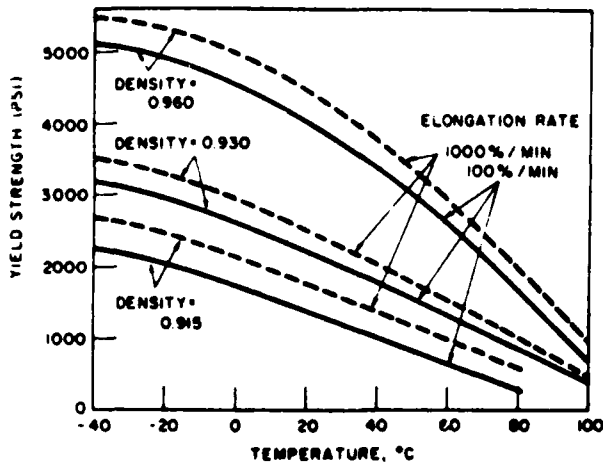
Figure B29. Yield strength and elongations (by ASTM D-412) on compression moldings of polyethylenes having densities of 0.915, 0.930 and 0.960 (and melt indexes of 1.8, 2.1 and 0.5, respectively) at strain rates of 100%/min. and 1000%/min. (Titus 1967).
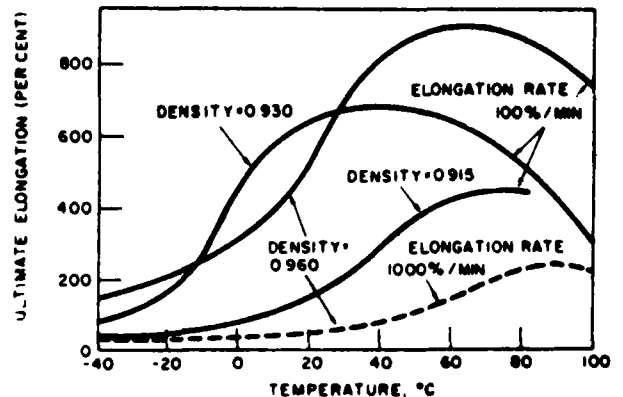
Figure B30. Tensile properties (ASTM D-412) vs temperature for polyethylenes (Titus 1967).
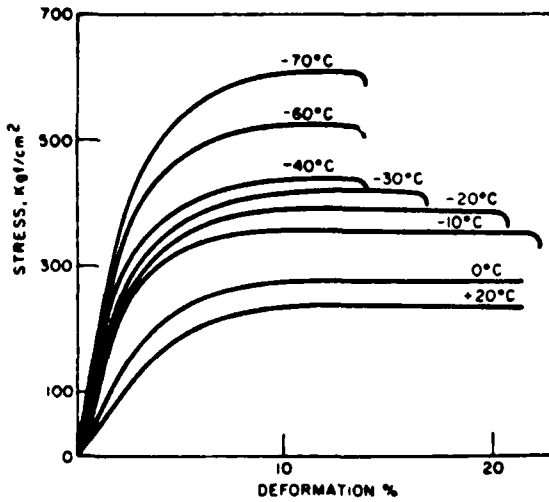
Figure B31. Stres-strain curves at various temperatures of low pressure polyethylene (Titus 1967).
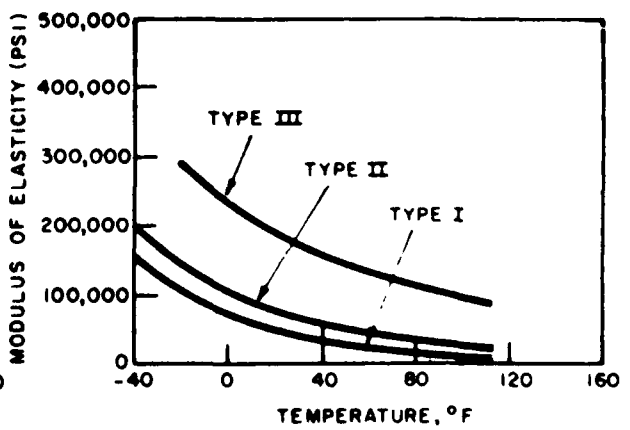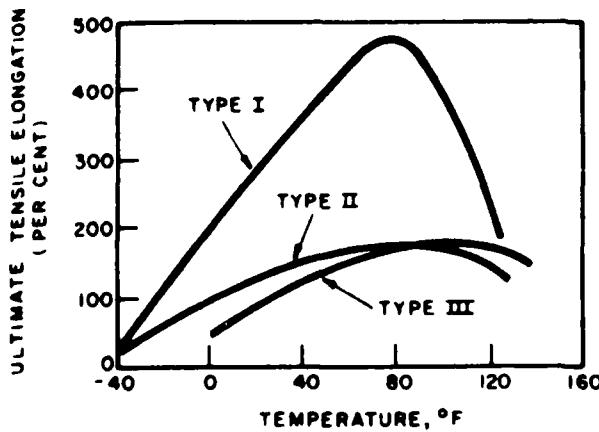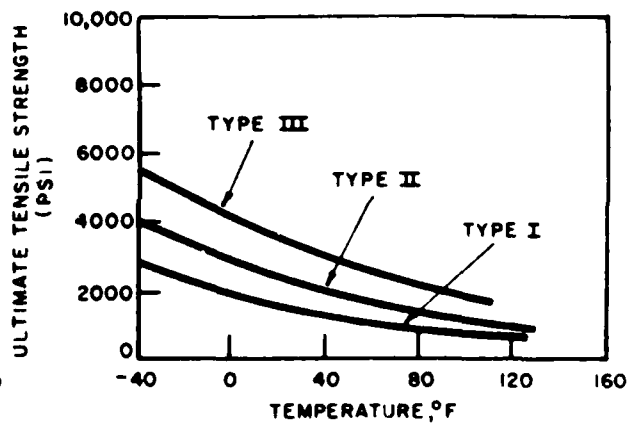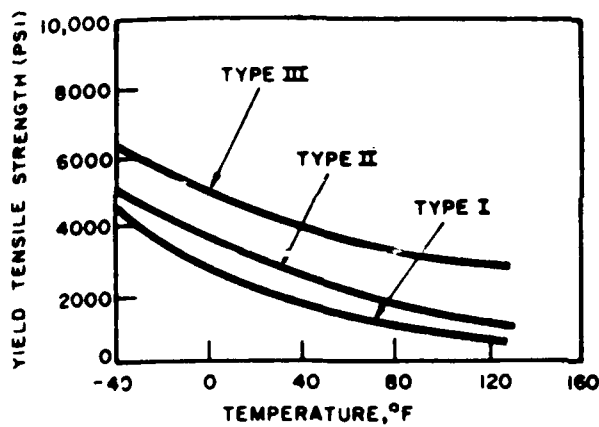
Figure B32. Strength of compression-molded polyethylene at various temperatures (Titus 1967).

60
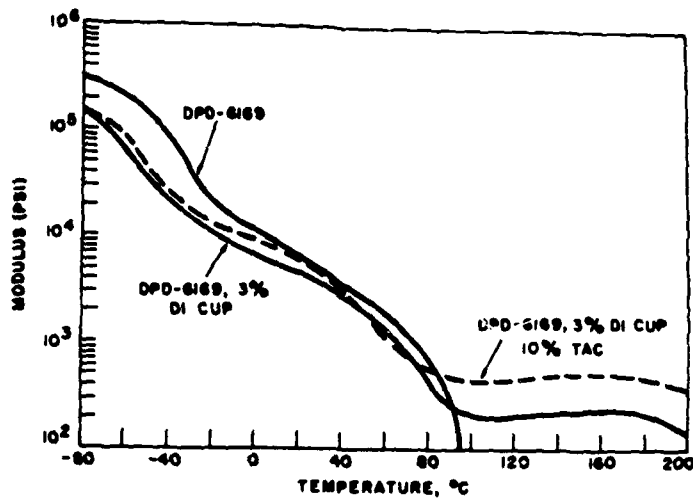
Figure B33. Modulus vs temperature—unfilled cross-linked acrylate copolymer DPD-6169 (Titus 1967). DPD–ethylene ethyl acrylate copolymer; DI CUP–dicumyl peroxide; TAC–triallyl cyanurate.
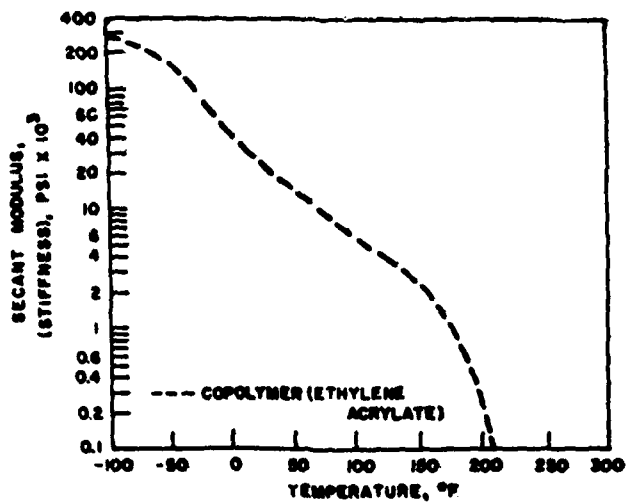
Figure B34. Modulus of ethylene acrylate copolymer as a function of temperature (Titus 1967).
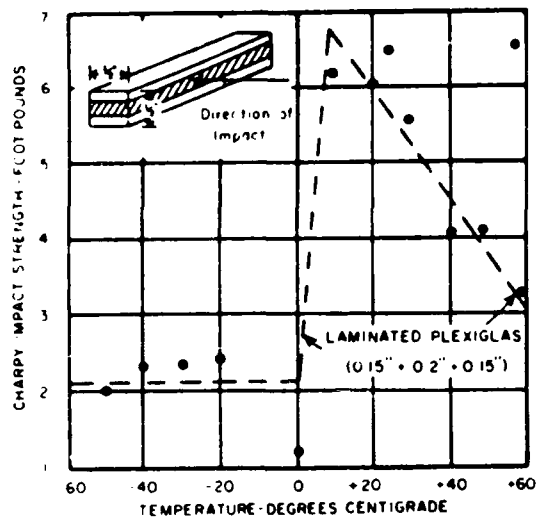
(a)
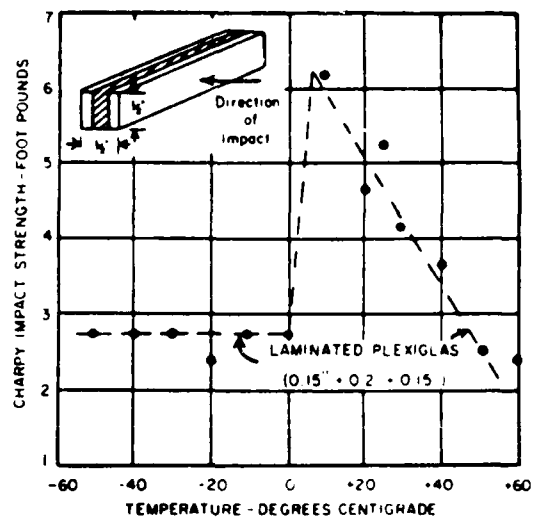
(b)
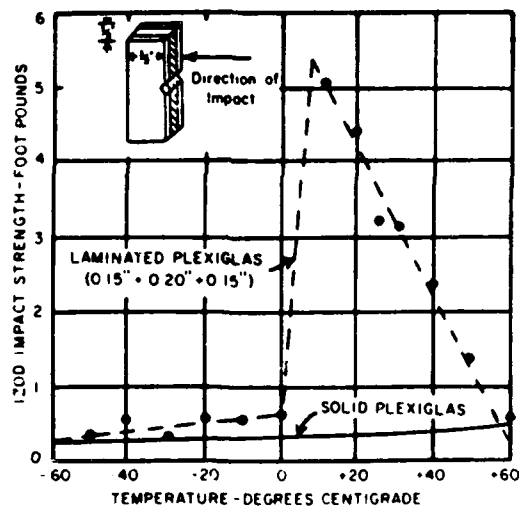
(c)

Figure B35. Impact strength of laminated acrylic (Plexiglas) (Titus 1967).
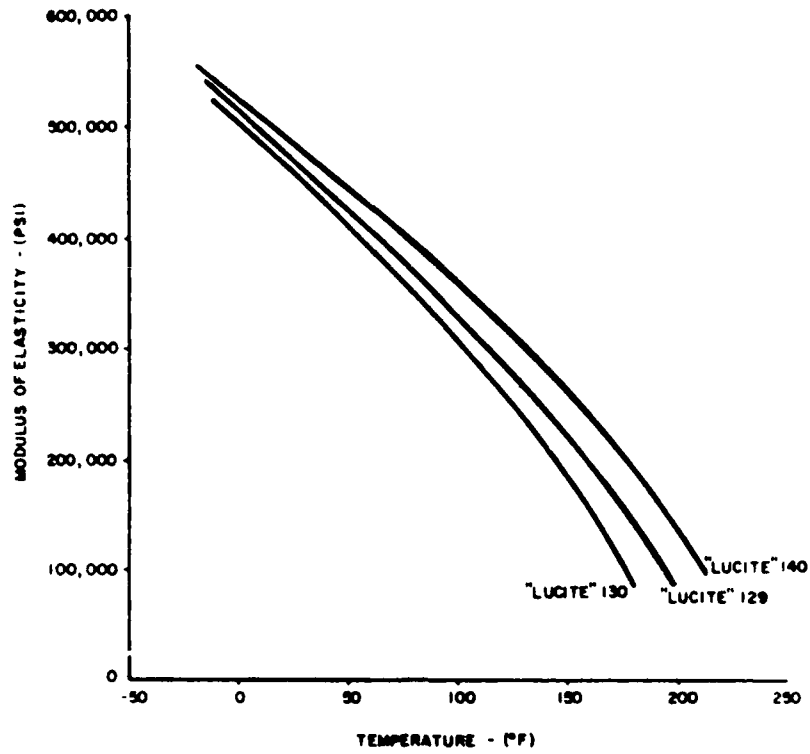
Figure B36. Modulus of elasticity of acrylic (Lucite) vs temperature (ASTM D 638-52T) (Titus 1967).
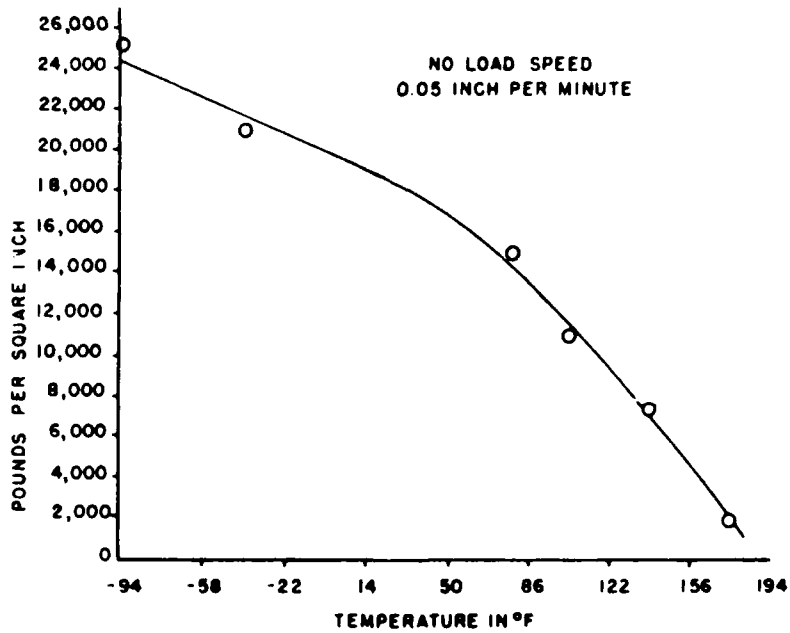
Figure B37. Flexural strength variation with temperature of cast acrylic sheet (Titus 1967).
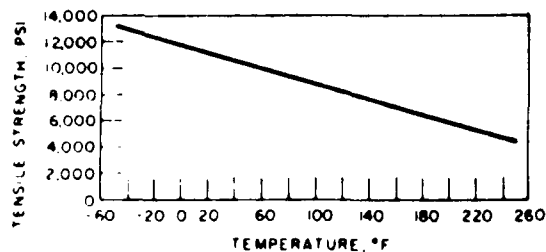
Figure B38. Tensile strength vs temperature of
polycarbonate molding material (Titus 1967).
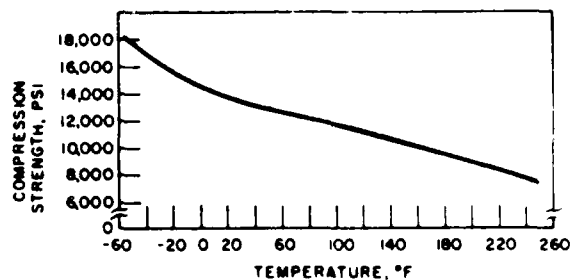
Figure B39. Compression strength vs tempera-
ture of polycarbonate (Merlon) (Titus 1967).
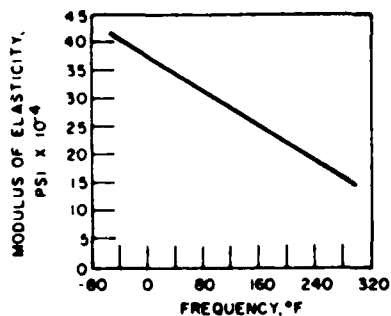
Figure B40. Effect of temperature
on modulus of elasticity of poly-
carbonate resin (Titus 1967).
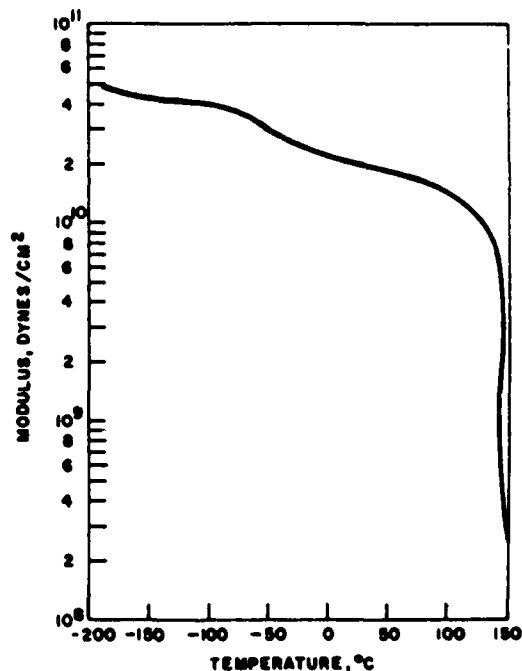
Figure B41. Torsional modulus of polycar-
bonate vs temperature (Titus 1967).

64
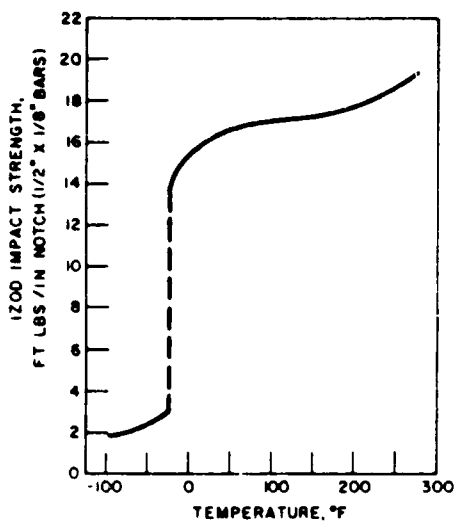
Figure B42. Izod impact strength vs temperature of (Merlon) polycarbonate (ASTM) D-256) (Titus 1967).
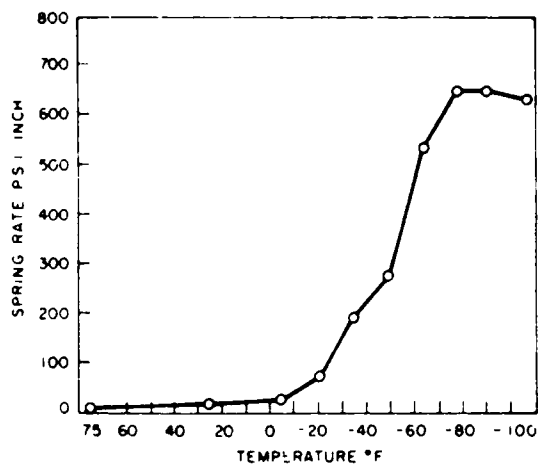

*Figure B43. Urethane foam spring rate vs temperature (Titus 1967).*
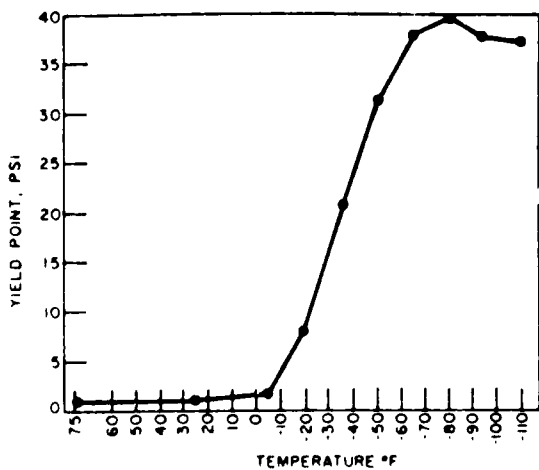
*Figure B44. Urethane foam yield point vs temperature (Titus 1967).*
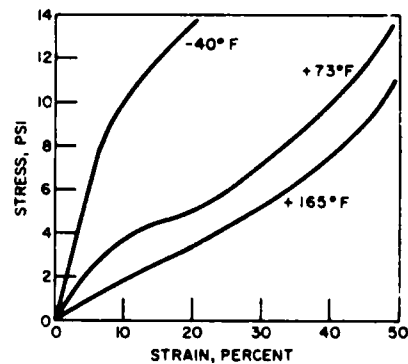
Figure B45. Compressive stress-strain of low density density polyethylene foam at various temperatures (Titus 1967).
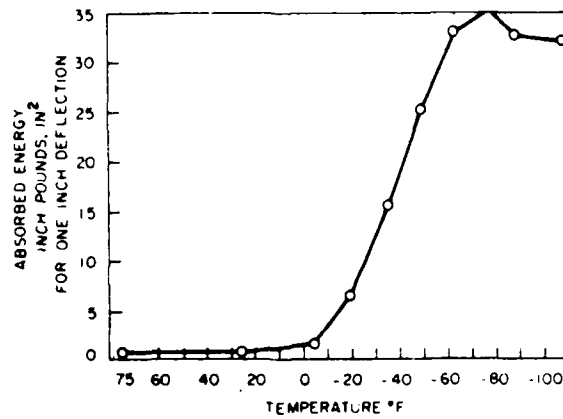
Figure B46. Urethane foam absorbed energy vs
temperature (Titus 1967).
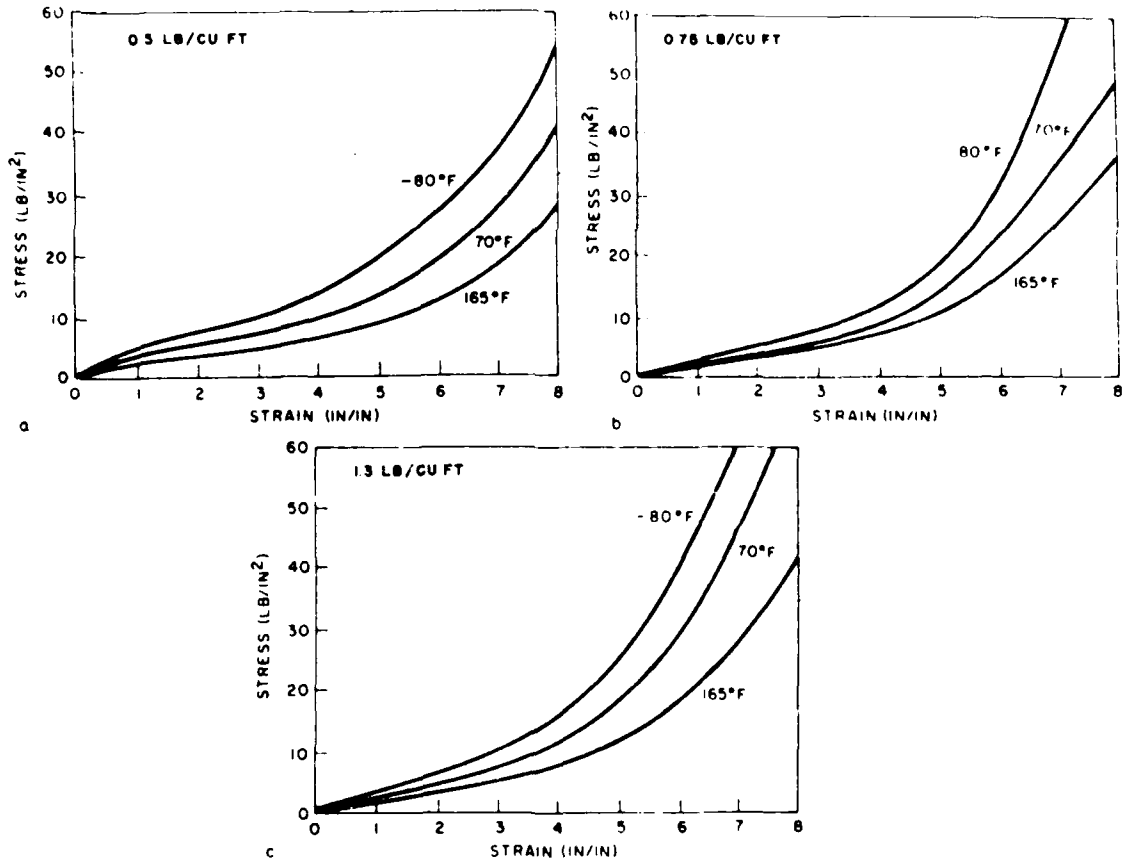
Figure B47. Static stress vs strain curves for resilient expanded polystyrene foam (Resilo-Pak)
at temperature extremes (0.5, 0.75 and 1.3 lb/ft³ densities) (Titus 1967).

66
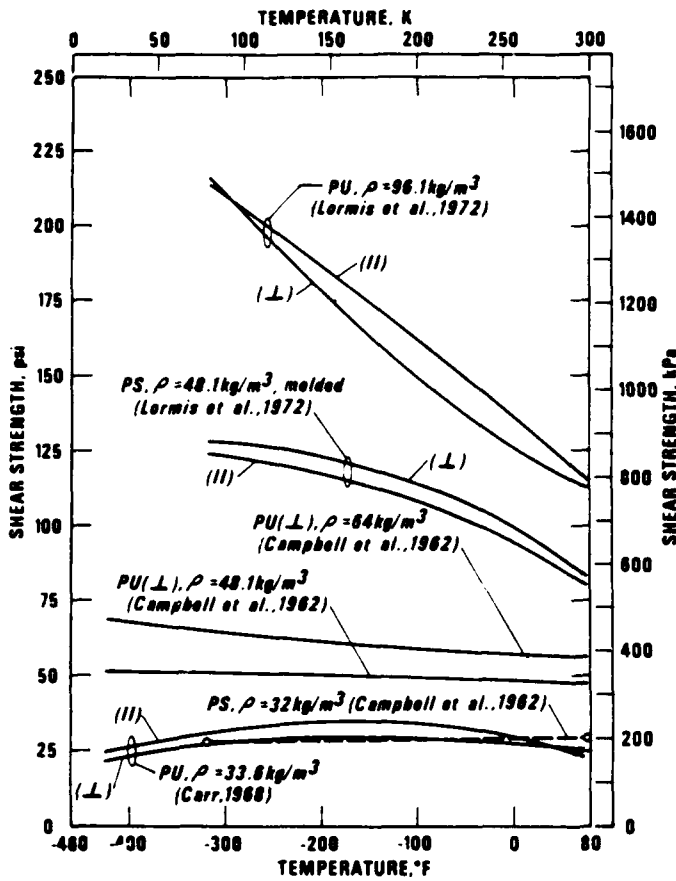
Figure B48. Shear strength as a function of temperature for PU and PS foams with density, process, and orientation as parameters (Sparks, 1978).
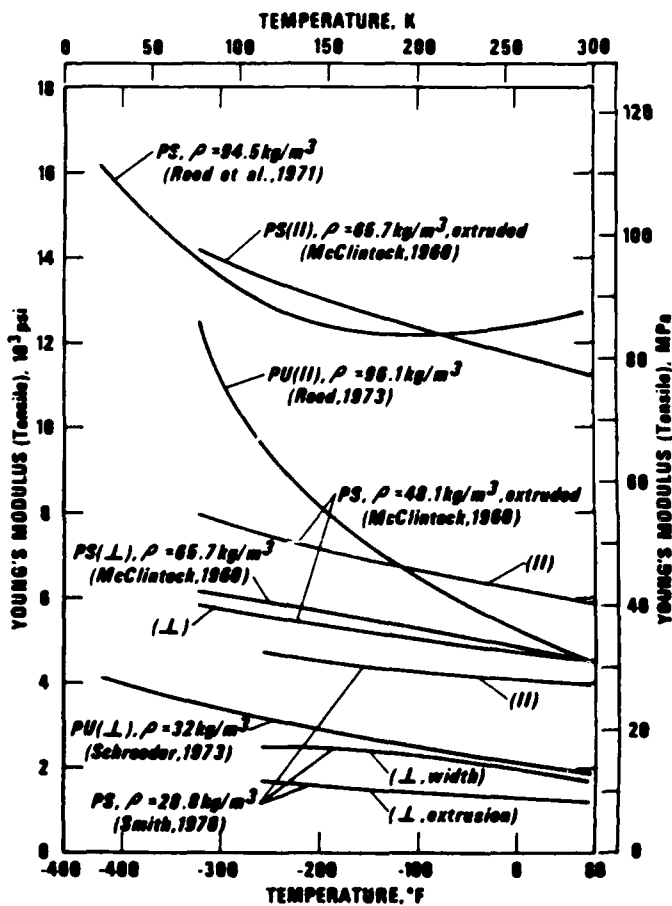

Figure B49. Young's modulus measured in tension as a function of temperature for PU and PS foams with density, process, and orientation as parameters (Sparks 1978).

67

TEMPERATURE, K

0   50   100   150   200   250   300

PS(II), ρ=52.9 kg/m³, extruded
(Bennett,1974)

PU(II), ρ=94.5 kg/m³
(Arvidson et al.,1973)

PU(II), ρ=54.5 kg/m³
(Campbell et al.,1962)

PS, ρ=51.3 kg/m³, molded
(Arvidson et al.,1973)

($\perp$)

PU(II), ρ=33.6 kg/m³
(Carr,1968)

(II)

PS(II), ρ=32 kg/m³, molded
(Stewart et al.,1974)

PU($\perp$), ρ=33.6 kg/m³
(Carr,1968)

COMPRESSIVE STRENGTH, psi
260 240 220 200 180 160 140 120 100 80 60 40 20 0

COMPRESSIVE STRENGTH, kPa
1800 1600 1400 1200 1000 800 600 400 200 0

TEMPERATURE, °F
-460   -400   -300   -200   -100   0   80
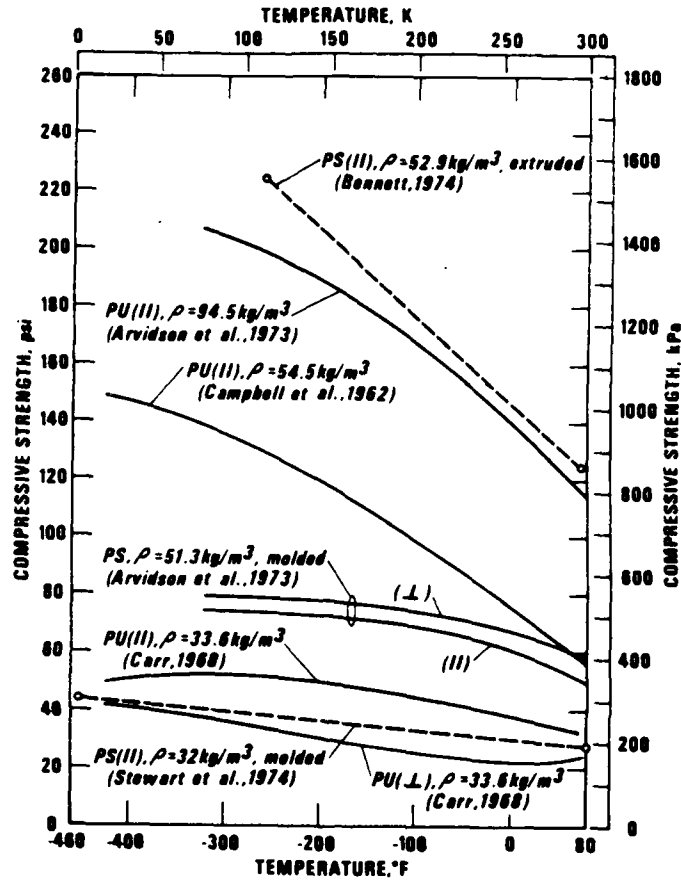
Figure B50. Compressive strength as a function of temperature for PU and PS foams with density, process and orientation as parameters (Sparks 1978).

68